POLITECNICO DI MILANO

Facoltà di Ingegneria Industriale

Corso di Laurea in
Ingegneria Energetica

Fluid Dynamics Study for the Application of a Chemical EOR (Enhanced Oil Recovery) Process

ANALYSIS FOR A POLYMER INJECTION TECHNIQUE

Relatore: Prof. Raffaele ROMAGNOLI

Co-relatore: Dott. Franco MASSERANO

Tesi di Laurea di:

Francesco SILIPRANDI
Matr. 734770

Anno Accademico 2009- 2010

Ringraziamenti

Desidero ringraziare il professor Raffaele Romagnoli, che ha supervisionato e corretto tutto questo lavoro.

Un ringraziamento particolare va al dottor Franco Masserano, per la pazienza con cui ha coordinato, corretto e chiarito i miei dubbi in ogni fase che ha portato al completamento di questa tesi.

Ringrazio anche i miei colleghi, per l'aiuto, i consigli e l'amicizia dimostratami in questi mesi.

Un grazie particolare anche al team di sviluppo del software Kraken, e all'università del Texas di Austin, che mi hanno fornito gli strumenti necessari per portare a compimento lo studio.

Ringrazio infine la mia famiglia, senza il cui supporto difficilmente sarei arrivato a questo punto.

Acknowledgments

I would like to thank professor Raffaele Romagnoli, who supervised and corrected all this work.

Special thanks to doctor Franco Masserano, for the patience with which he coordinated, corrected and clarified my doubts during each stage of this work.

I thank also my colleagues, for the aid, the advices and the friendship they showed me in these months.

A particular thank to the Kraken development team, and to the University of Texas at Austin, who gave me the instruments needed to perform this work.

Finally I thank my family, without whose support I would not have arrived at this point.

INDEX

INDEX OF FIGURES

ABSTRACT

After the primary exploitation of an oil field, a medium percentage around the 70% of the oil initially present in the reservoir remains untapped. Several innovative EOR (Enhanced Oil Recovery) techniques are under study, which may improve oil recovery from fields. The main objective of this work was to study the chances of implementing one of these, polymer flooding, upon an existing reservoir.

Experimental analyses have been performed, together with matches using a numerical simulator, UtChem, which implements an innovative model. A target of this work was to check the consistency of the model and its ability to reproduce experimental data.

The model was found to be accurate and then used to simulate the effects due to the application of the EOR technique on a reservoir scale. After several trials and economic analyses, polymer flooding was found to be a promising and competitive method to produce more oil and increasing the net gain from the exploitation of oil fields.

Key Words: Enhanced Oil Recovery, Reservoir Engineering, Polymer Injection, Reservoir simulation, UtChem

SOMMARIO

Dopo la prima fase di recupero in un giacimento, una percentuale media di circa il 70% del petrolio inizialmente presente rimane non estratto. Diverse tecniche che permettano di aumentare l'efficienza di recupero, dette EOR (Enhanced Oil Recovery, Tecniche di Recupero Avanzato), sono sotto studio. Il principale scopo di questo lavoro è studiare le possibilità di implementare una di queste, in particolare il flussaggio di polimero, in un giacimento reale.

Sono state eseguite analisi sperimentali, riprodotte in seguito da simulazioni effettuate usando un modello innovativo, implementato dal simulatore UtChem.

Uno degli obiettivi è stato quello di verificare la consistenza del modello e la sua abilità di rappresentare i risultati di laboratorio.

Il modello è risultato essere accurato ed è stato poi utilizzato per simulare gli effetti dovuti all'applicazione della tecnica EOR sul reservoir. Dalle simulazioni e dalle analisi economiche, la tecnica di iniezione di polimero è risultata essere promettente, nonché potenzialmente competitiva per aumentare il guadagno netto nello sfruttamento del campo petrolifero.

Parole Chiave: Tecniche di recupero avanzato, Ingegneria di giacimento, Iniezione di polimero, simulazione di giacimento, UtChem

I. COMPENDIO

1.1. Introduzione

Secondo il più probabile scenario di evoluzione del consumo globale di energia, i combustibili fossili sono destinati a rimanere la principale fonte di energia mondiale nel prossimo futuro (IEA, 2009 [1]). Più di tre quarti dell'aumento del consumo consisterà in un aumento del loro utilizzo.

In questo quadro il petrolio rimarrà il combustibile più sfruttato, almeno fino al 2030, con una domanda che crescerà dell'1% annuo.

L'estrazione di idrocarburi è quindi un'attività determinante per venire incontro alla domanda globale di energia. Uno dei suoi principali limiti consiste nel fatto che, mediamente, solo il 30% delle riserve contenute nella maggior parte dei giacimenti è recuperato.

La diminuzione delle riserve e l'incremento dei prezzi del petrolio a valori superiori i 40 dollari al barile hanno reso conveniente la ricerca in nuove metodologie di estrazione, chiamate EOR, "Enhanced Oil Recovery" ("Recupero Avanzato di Petrolio"), che permettono di migliorare l'efficienza di estrazione.

In questo lavoro, dopo un'introduzione sui principi di ingegneria dei giacimenti e sui principali concetti riguardanti l'estrazione e il recupero di olio, è presentato uno stato dell'arte delle principali tecniche di EOR esistenti.

In seguito è studiata la possibilità di implementare una di queste tecniche innovative per la coltivazione di un giacimento situato in Nord Africa.

Lo studio passa attraverso una prima fase di selezione, in cui è scelta la tecnica migliore da applicare tra quelle esistenti, considerando le caratteristiche del campo su cui intervenire.

In seguito lo studio è condotto su campioni sperimentali prelevati direttamente dal campo. Questa fase serve per determinare le principali proprietà della roccia costituente il giacimento, attraverso prove sperimentali, i cui risultati sono poi stati riprodotti con simulazioni numeriche.

E' stato utilizzato un simulatore fluidodinamico a differenze finite, tridimensionale, multifase, multicomponente, chiamato UtChem. Il modello implementato, sviluppato all'università di Austin in Texas, è innovativo ed ha lo scopo di risolvere le equazioni di pressione e di flusso governanti la fluidodinamica all'interno della roccia serbatoio del giacimento. Contiene modelli chimico-fisici avanzati in grado di simulare il flusso di sostanze chimiche e le loro interazioni. Uno degli scopi del lavoro è stato quello di verificare la consistenza del modello e l'accuratezza con cui riproduce i dati sperimentali.

Come ultima fase, è stato simulato il comportamento di un settore reale del giacimento. Il primo scopo è stato quello di testare se le proprietà trovate durante la fase precedente permettono di riprodurre, se implementate nel modello, la simulazione con il reale comportamento passato del campo.

In seguito si verifica la risposta del giacimento in seguito all'attuazione della tecnica EOR, per verificare se determina effettivamente un incremento di olio prodotto, oltre che un maggiore guadagno.

1.2. Principali definizioni di ingegneria dei giacimenti

In una modellazione semplice, un giacimento di petrolio ("reservoir") è composto di uno o più strati di roccia permeabile e porosa. Gli idrocarburi saturano i pori della roccia-serbatoio, che è delimitata da argille impermeabili e da uno strato contente acqua, chiamato "acquifero",

Nella zona occupata dagli idrocarburi è in genere presente anche una fase acquosa, chiamata "*acqua connata*", che ricopre i grani di roccia. Si tratta della parte rimanente dell'acqua che saturava i pori, prima del processo geofisico di accumulo degli idrocarburi.

1.2.1.Proprietà della roccia

Porosità

La porosità di un campione di roccia è il rapporto tra il volume occupato dai pori e il volume totale del campione (Equazione I-1).

$$\Phi = \frac{V_P}{V_t}$$

Equazione I-1 – porosità

Dove:

Φ è la porosità

V_P è il volume totale dei pori comunicanti tra di loro

V_t è il volume totale del campione.

Permeabilità assoluta

La permeabilità assoluta è una proprietà intrinseca della roccia. Esprime l'abilità del mezzo poroso di consentire il flusso attraverso di sé, senza alterare la sua struttura.

E' deducibile dalla legge di Darcy, ottenuta sperimentalmente nel 1856:

$$\frac{q}{A} = v = -\frac{k}{\mu} \cdot \frac{dp}{dx}$$

Equazione I-2 – legge di Darcy

Dove:
q è la portata volumetrica di flusso
A è la sezione del mezzo
υ è la velocità media del fluido
μ è la viscosità dinamica del fluido
p è la pressione
x è la coordinate lungo la direzione del flusso

Permeabilità relative

All'interno dei giacimenti di idrocarburi il mezzo poroso risulta solitamente essere saturo di due o tre fluidi: acqua, olio e gas. Esiste, quindi, la necessità di generalizzare la legge di Darcy per tenere conto del flusso contemporaneo di più fluidi.

Se la saturazione di un fluido è minore di 1 la roccia porosa detiene, rispetto ad esso, un valore di permeabilità minore di quello assoluto. In questo caso ciascun fluido ha rispetto alla roccia la sua permeabilità relativa.

Le permeabilità relative sono dipendenti dalla saturazione di ciascun fluido e la loro somma è sempre minore della permeabilità assoluta.

Considerando l'andamento della permeabilità relativa dell'acqua è possibile determinare due condizioni note: quando la saturazione di acqua è uguale alla saturazione irriducibile (S_{WC}), la permeabilità dell'acqua è uguale a zero e l'acqua non fluisce. Quando, invece, la saturazione d'acqua è unitaria, la roccia ne è completamente satura e la permeabilità relativa dell'acqua corrisponde a quella assoluta. Analogamente avviene per l'olio, che fluisce quando la sua saturazione è uguale o maggiore a quella critica, chiamata *saturazione di olio residuo* (S_{OI}).

L'andamento delle permeabilità relative rispetto alla saturazione del fluido si può modellare con l'equazione di Corey:

$$k_{rj} = k_{rj}^{0} \cdot S_{nj}^{nj}$$

Equazione I-3 – modello di Corey per le permeabilità relative

Dove $S_{nj} = \max\left(0, \frac{S_j - S_{jC}}{1 - S_{WC} - S_{Oi}}\right)$

Equazione I-4 - saturazioni normalizzate.

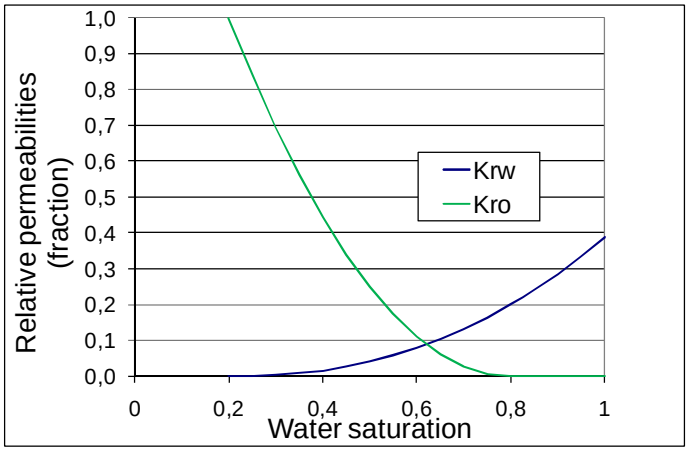

Figura I-1 – andamento delle permeabilità relative in funzione della saturazione d'acqua

I parametri k_{ro}, k_{rw}, S_{wr}, S_{or}, n_o, n_w devono essere determinati da prove sperimentali.

1.2.2.Equazione di diffusività

La principale equazione che governa il flusso all'interno del mezzo poroso è l'equazione di diffusività. E' ricavata a partire dalla legge di Darcy ed eseguendo un bilancio materiale su un elemento infinitesimale di roccia porosa attraversata dai fluidi.

$$\frac{\partial^2 P}{\partial x^2} = \left(\frac{\mu \cdot C \cdot \Phi}{k} \right) \cdot \frac{\partial P}{\partial t}$$

Equazione I-5 – equazione di diffusività

Il modello utilizzato dal simulatore fluidodinamico UtChem è basato su questa equazione, formulate includendo anche dei fenomeni diffusivi, di quelli legati alla gravità e alla pressione capillare:

$$\Phi \cdot C_t \cdot \frac{\partial P_1}{\partial t} + \nabla \vec{k} \cdot \lambda_{rTc} \cdot \nabla P_1 = -\nabla \sum_{l=1}^{np} \vec{k} \cdot \lambda_{rlc} \cdot \nabla h + \nabla \sum_{l=1}^{np} \vec{k} \cdot \lambda_{rlc} \cdot \nabla P_{cl1} + \sum_{k=1}^{nCV} Q_k$$

Equazione I-6 – equazione di pressione usata dal modello implementato in UtChem

1.3. Flussaggi e spiazzamento

La produzione secondaria di olio e gas è affidata principalmente all'iniezione di acqua da un pozzo iniettore. L'acqua iniettata fluisce dal pozzo iniettore al produttore, dislocando gli idrocarburi.

Il meccanismo dello spiazzamento di un fluido da parte di un altro è governato dalla differenza del rapporto tra permeabilità relativa e viscosità dei fluidi (k_r /μ). Tale rapporto è chiamato **mobilità del fluido** ed è indicato dal simbolo λ.

$$\lambda_W = k_W / \mu_W$$ **Equazione I-7 – mobilità dell'acqua.**

$$\lambda_O = k_O / \mu_O$$ **Equazione I-8 – mobilità dell'olio.**

Il rapporto tra la mobilità dell'acqua e quella dell'olio è chiamato *rapporto di mobilità* e quantifica il di scostamento dello spiazzamento dall'idealità.

Lo spiazzamento si definisce ideale, quando, dopo il passaggio della fase acquosa che sposta l'olio, c'è un passaggio netto dalla massima saturazione di olio (1-Swi) alla saturazione di olio irriducibile (Soi). Si tratta della condizione più favorevole, ma si verifica solo nei casi in cui il rapporto di mobilità all'interfaccia è minore o uguale a 1 (Equazione I-9).

$$M' = \lambda_W' / \lambda_O' \leq 1$$

Equazione I-9 – condizione per avere spiazzamento ideale

L'efficienza di recupero, chiamata anche "recovery factor" (RF), è di solito suddivisa come prodotto di tre fattori: un'efficienza areale, un'efficienza verticale e una microscopica.

L'efficienza areale è definita come il rapporto tra l'area del reservoir che viene in contatto dall'agente spiazzante e l'area totale. Quando l'acqua ha un'alta mobilità, tende a muoversi lungo canali preferenziali, creando un fenomeno noto come "fingering". In questo caso l'area di contatto con l'idrocarburo da muovere è bassa, risultando in una bassa efficienza di recupero.

L'efficienza verticale è la frazione di formazione lungo un piano verticale contatta dall'acqua. In caso di rapporto di mobilità minore o uguale a 1, l'olio è spinto da un fronte d'acqua, che si muove con moto a pistone.

Nella maggior parte dei casi l'acqua è più mobile dell'olio. Il risultato è che il flusso d'acqua aggira il banco di idrocarburi senza smuoverlo, in un fenomeno noto come "tonguing".

L'efficienza microscopica è la frazione di olio effettivamente mossa nella zona invasa dal flusso d'acqua.

1.4. Selezione della tecnica adeguata

I criteri per la selezione ("screening") della tecnica EOR adeguata sono stati ricavati dalla letteratura e da esperienze possitive passate.

Il reservoir oggetto del presente studio è caratterizzato da un olio ad alta viscosità, 23 cP, alta acidità, temperatura di 77 °C. L'acqua connata presente nel giacimento è caratterizzata da alta salinità e concentrazione di ioni bivalenti ("durezza" dell'acqua connata).

L'alta viscosità dell'olio ne limita fortemente la mobilità. Nel caso sia eseguito un semplice flussaggio con acqua, quindi, si avrebbe un alto rapporto di mobilità, che porterebbe ad avere una bassa efficienza di spiazzamento.

Il ricorso a tecniche di EOR è quindi necessario per aumentare l'efficienza di recupero, altrimenti troppo bassa.

Da una prima analisi la tecnica di iniettare una soluzione contenente polimero risulta la più compatibile con le proprietà del giacimento e la più promettente.

Aggiungere polimero all'acqua usata in un waterflooding consente, infatti, di aumentare la viscosità della soluzione da iniettare. Il rapporto di mobilità tra acqua e olio risulta quindi più basso, aumentando l'efficienza di spiazzamento, sia areale che verticale.

Il polimero iniettato, inoltre, tende ad otturare le zone del reservoir ad alta conduttività, bloccando i canali preferenziali del flusso acquoso e migliorando il contattamento acqua-olio.

1.5. Proprietà e scelta del polimero

I polimeri più usati commercialmente nell'ambito delle tecniche EOR rientrano nella classe delle poliacrilammidi.

La poliacrilammide usata nei casi di flussaggio con polimero è sottoposta a parziale idrolisi, che porta ad ottenere gruppi carbossilici anionici (COO^-) dispersi lungo la catena polimerica.

La carica negativa dei gruppi carbossilici è molto importante per le proprietà della soluzione polimerica. La repulsione tra i gruppi carbossilici aumenta il raggio idrodinamico della molecola e accentua la viscosità della soluzione. L'idrolisi, inoltre, permette la solubilità del polimero in acqua. Il grado di idrolisi ottimale non deve, però, essere troppo alto, per evitare la precipitazione di polimero in condizioni di alta salinità.

La salinità della soluzione è responsabile di un effetto di schermatura, attraverso il quale i cationi del sale tendono a formare legami deboli con i gruppi anionici sulla catena polimerica. Questo effetto annulla la repulsione elettrostatica tra i gruppi carbossilici, causando l'avvolgimento della molecola e il crollo della viscosità della soluzione.

Nel caso in esame l'ambiente in cui il polimero è iniettato è caratterizzato da un'alta salinità. Il polimero da utilizzare, quindi, deve essere modificato rispetto alla struttura originale della poliacrilammide, in modo da incrementarne la stabilità.

Il polimero scelto è stato l'AN-125, prodotto da SNF-Floerger. Si tratta di un co-polimero in cui alcuni gruppi acrilati sono stati sostituiti da monomeri anionici (acido sulfonico 2-acrilammide-2-metil propano, AMPS) più resistenti più resistenti alla schermatura cationica e alla precipitazione.

La viscosità di una soluzione acquosa contenente polimero è modellata usando l'equazione di Flory-Huggins:

$$\mu_p^0 = \mu_w \cdot \left(1 + \left(A_{p1} \cdot C_{pol} + A_{p2} \cdot C_{pol}^2 + A_{p3} \cdot C_{pol}^3\right) \cdot C_{SEP}^{Sp}\right)$$

Equazione I-10 – viscosità della soluzione con polimero

C_{pol} è la concentrazione di polimero in soluzione, espresso in frazione massica. A_{P1}, A_{P2}, e A_{P3} sono costanti tipiche del polimero. Insieme a C_{SEP} e a Sp sono determinati da prove sperimentali. In particolare A_{P1}, A_{P2}, e A_{P3} sono i coefficienti di una cubica che interpola i valori di viscosità della soluzione misurati per diverse concentrazioni di polimero. C_{SEP} e Sp sono determinati in modo analogo, misurando la viscosità della soluzione per diverse salinità.

L'abbassamento della mobilità di una soluzione contenente polimero all'interno di un mezzo poroso è misurato attraverso il "*fattore di resistenza*", R_F. Si tratta del rapporto tra la mobilità della brine e quella di una soluzione polimerica nelle stesse condizioni.

La mobilità risulta ridotta anche da una riduzione di permeabilità, misurata del "*fattore di riduzione di permeabilità*", R_K. La mobilità risulta ridotta anche dopo che l'iniezione di polimero è stata effettuata. Questo effetto è misurato dal "*fattore residuo di resistenza*", R_{RF}.

1.6. Riproduzione dati di laboratorio

Dopo la fase preliminare di screening, deve essere eseguita un'analisi più dettagliata, basata su misure sperimentali. L'obiettivo è trovare gli esatti parametri relativi a proprietà delle rocce costituenti il giacimento, come le permeabilità relative. Inoltre la compatibilità tra la soluzione iniettata e l'acqua connata presente nel giacimento deve essere verificata.

Per fare questo sono stati effettuati flussaggi su campioni sperimentali, in particolare su una carota di campo e un *sandpack*. Quest'ultimo è stato ottenuto macinando finemente sabbie e materiali prelevati dalla formazione e impaccandoli insieme.

In seguito sono state condotte simulazioni, riproducendo le condizioni degli esperimenti.

Le proprietà da determinare sono state inserite come input di primo tentativo nelle simulazioni. In questo modo è possibile capire se i valori implementati

sono quelli giusti verificando che i risultati delle simulazioni combacino correttamente con i risultati dai laboratori (fase di "*match*").

Le prove sperimentali sono state eseguite saturando il sandpack e la carota di campo prima con brine di salinità uguale a quella dell'acqua di formazione e poi flussando i campioni con olio prelevato dal campo spiazzando tutta l'acqua mobile. In questo modo si raggiunge la saturazione massima di olio, Soi, e si riproducono le condizioni presenti nel giacimento. In seguito, per simulare il recupero secondario con iniezione di acqua, una soluzione acquosa è fatta fluire attraverso il campione, fino a che tutto l'olio mobile non è stato spiazzato. E' eseguito, poi, un altro spiazzamento con una soluzione contenente l'agente chimico di cui si vogliono studiare gli effetti per simulare l'effetto di un recupero terziario.

I risultati dei flussaggi per sandpack e carota sono mostrati in

Figura **I-2** e

Figura I-3.

Sull'asse delle ascisse sono riportati i volumi porosi del campione che sono stati flussati. Quest'ultima è una scelta analoga a rappresentare il tempo di iniezione, ma consente di mantenere l'uniformità dei dati anche in presenza di variazioni di portata e di rendere confrontabili prove eseguite con diverse portate del fluido di iniezione.

Sull'asse delle ordinate è riportato il "recovery factor", la percentuale di olio presente all'interno del campione che è stato recuperato durante la prova.

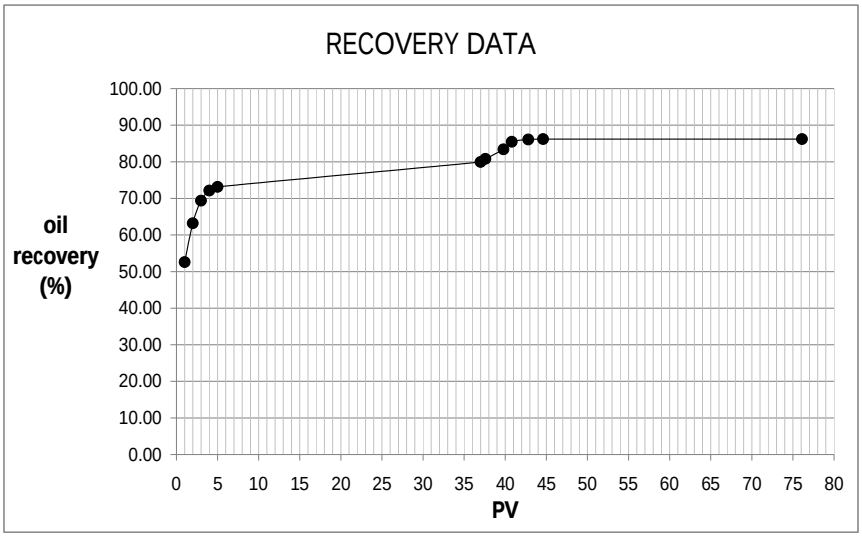

Figura I-2 – dati sperimentali dopo il flussaggio effettuato sul sandpack

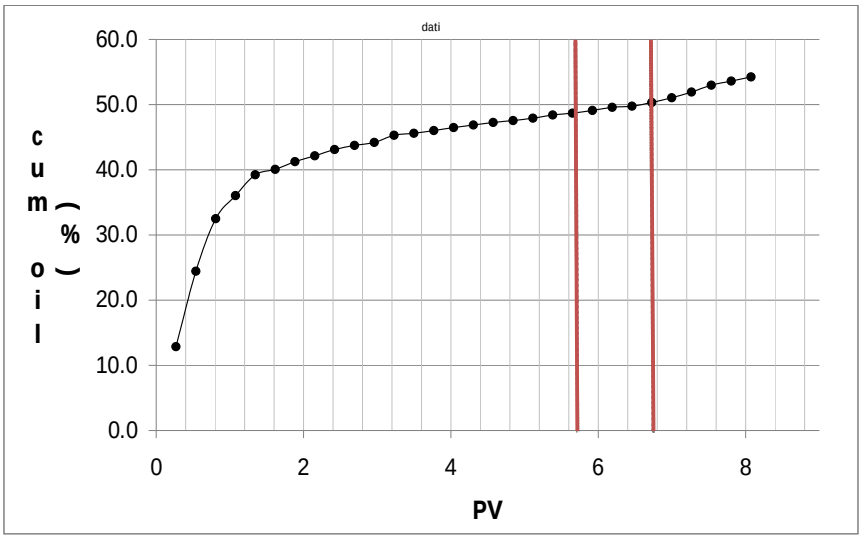

Figura I-3 – dati sperimentali dopo il flussaggio effettuato sulla carota di campo

In Figura I-4 e Figura I-5sono riportati i risultati del match tra simulazioni e dati sperimentali.

E' stato ottenuto un buon accordo implementando nelle simulazioni i parametri per sandpack e carota mostrati in Tabella 1 e Tabella 2.

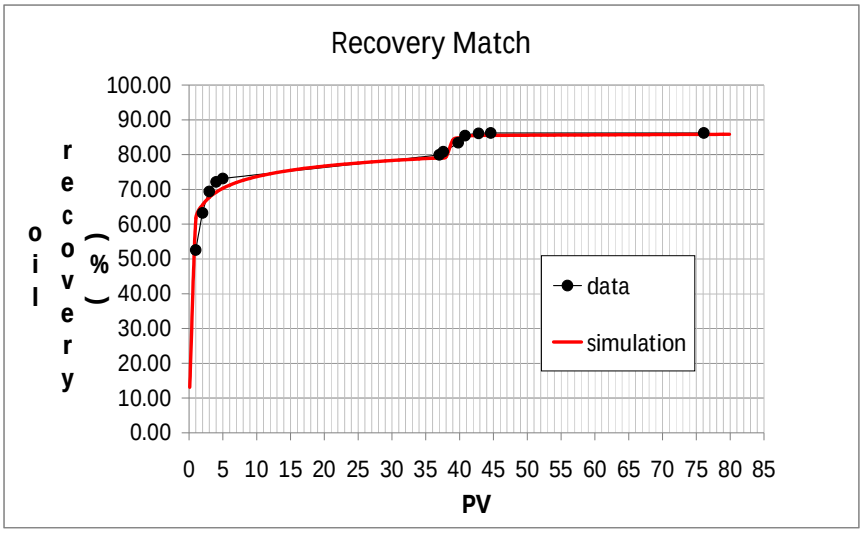

Figura I-4 –match tra simulazioni e dati sperimentali per il sandpack

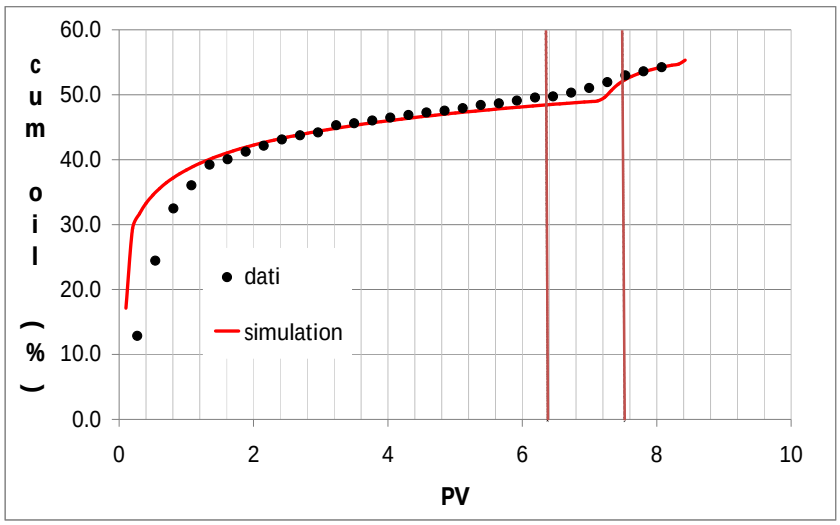

Figura I-5 – match per il flussaggio in carota

SANDPACK

nw	6
no	2.4
Sor	0.1
kwr	0.4
kor	0.9

Tabella 1 - parametri di Corey ottenuti da match sul sandpack

CORE

nw	3
no	4
Sor	0.15
kwr	0.25
kor	0.9

Tabella 2 – parametri di corey ottenuti da match sulla carota

Durante il flusso nel mezzo poroso, il polimero è soggetto ad uno sforzo di taglio, determinato da un gradiente di velocità esistente lungo il diametro dei canali percorsi dal fluido. Tale gradiente di velocità, chiamato "*shear rate*" ed indicato dal simbolo $\dot{\gamma}$, può essere definito come il rapporto tra la viscosità cinematica del polimero e l'altezza del condotto:

$$\dot{\gamma} = \frac{v}{h}$$ **Equazione I-11 – definizione di shear rate**

Per bassi valori di velocità, la viscosità della soluzione è indipendente dalla "*shear rate*" e il fluido mostra un comportamento newtoniano.

Per valori più alti la soluzione contenente polimero mostra un comportamento pseudoplastico e la viscosità diminuisce all'aumentare della velocità di deformazione.

La relazione tra la viscosità della soluzione e la shear rate è descritta dall'eqauzione di Meter:

$$\mu_{aq}^{I} = \mu_{aq}^{\infty} + \frac{\mu_{aq}^{0} - \mu_{aq}^{\infty}}{1 + \left(\frac{\dot{\gamma}}{\dot{\gamma}_{1/2}} \right)^{n_M - 1}}$$

Equazione I-12 – equazione di Meter: relazione tra viscosità e velocità di deformazione del fluido

Oltre all'effetto dello sforzo di taglio, per descrivere compiutamente gli effetti di flussaggio con polimero è necessario tenere conto anche del fenomeno dell'adsorbimento, cui il polimero va incontro su superfici permeabili. Dipende dal tipo del polimero, dalla soluzione in cui è inserito e dalle proprietà della roccia e spesso è unito all'intrappolamento delle molecole di polimero che avviene nei pori più piccoli. Causa la diminuzione della concentrazione di polimero all'interno della soluzione, portando ad una perdita sul controllo della mobilità.

Il valore di "*shear rate*" osservato nei due flussaggi è di circa 40 s^{-1}, mentre il valore di adsorbimento per il polimero varia tra 200 e 500 μg di polimero per grammo di volume poroso attraversato.

1.7. Simulazioni su scala di reservoir

I parametri identificati grazie ai test di laboratorio e alle simulazioni sono stati inseriti in un modello rappresentante un settore reale del giacimento da studiare.

La conformazione del giacimento, oltre alle proprietà petrofisiche, è stata ricavata attraverso LOG geofisici realizzati in campo ed è stata poi implementata nel simulatore UtChem descrivendo una griglia 3D.

Il settore è caratterizzato da una distribuzione di proprietà molto variabile, di conseguenza i parametri usati nel modello sono stati diversi secondo le zone. Sono stati usati i parametri ottenuti dal flussaggio in carota per le zone che presentano affinità alle proprietà della carota e analogamente è stato fatto per il caso del sandpack.

La prima simulazione ha riprodotto lo stesso procedimento già usato nella realtà per la coltivazione del giacimento, che sfrutta la pressione già presente nel reservoir. Il meccanismo di spinta è dato dall'espansione dei fluidi presenti. Tale fase è detta di "esaurimento naturale" o *natural depletion.* Dopo la simulazione si sono osservati gli andamenti risultanti di pressione media di giacimento, pressione al fondo dei due pozzi presenti nel modello, recupero percentuale di olio.

Il recupero di olio dipende fortemente dal "*water cut*", ovvero la frazione di acqua presente nella portata prodotta di liquido. Esso tende ad aumentare durante la produzione, abbassando costantemente la quantità di idrocarburi che si riesce a produrre.

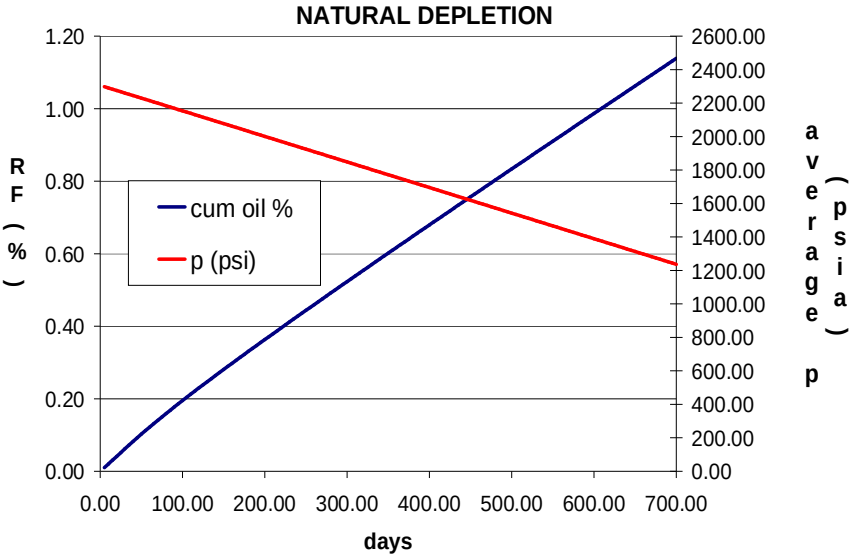

Figura I-6 – andamento della pressione media di giacimento e del recovery durante la fase di natural depletion

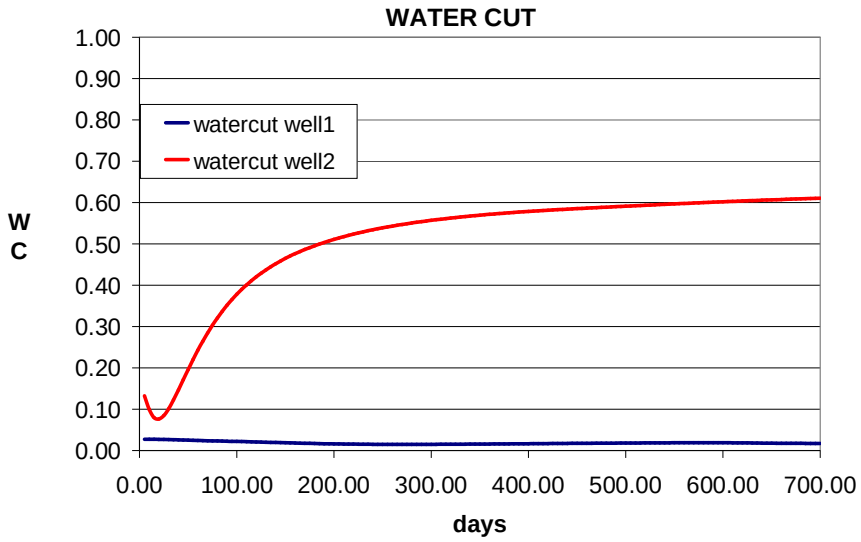

Figura I-7 – andamento del watercut per i due pozzi durante la fase di natural depletion

Quando il "*water cut*" diventa troppo elevato, si può procedere a simulare l'iniezione di polimero.

Due scenari sono stati messi a confronto: nel primo si inietta una normale soluzione acquosa, nel secondo una miscela di acqua e polimero.

Il confronto tra i due, in termini di "*water cut*" e di portata di olio prodotta, è mostrato in Figura I-8 e in Figura I-9.

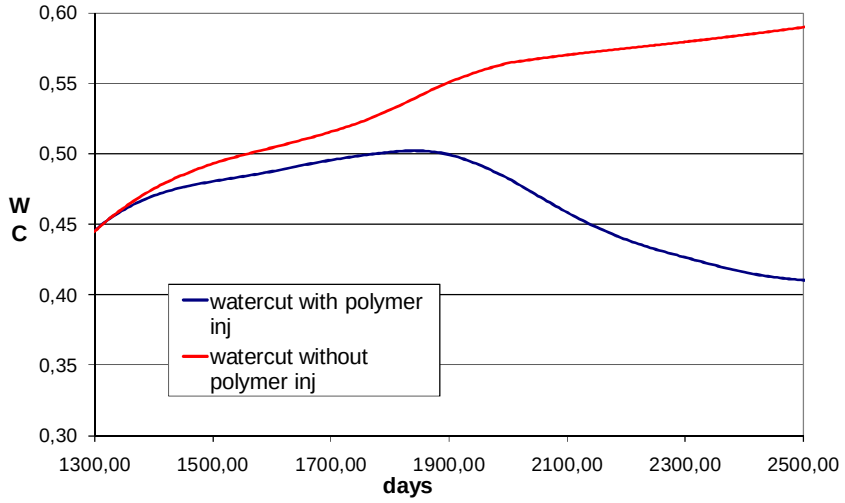

Figura I-8 – confronto dell'andamento del watercut per due simulazioni, una con iniezione di polimero e l'altra solo con iniezione di acqua

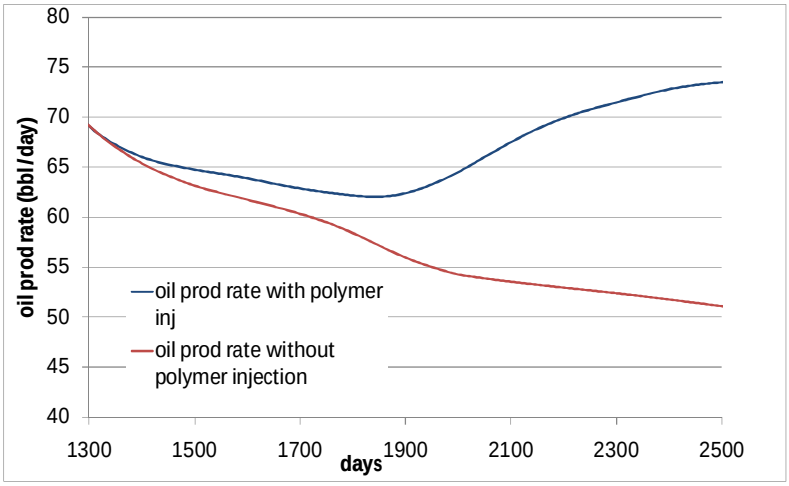

Figura I-9 - confronto dell'andamento della portata di olio prodotta per due simulazioni, con e senza iniezione di polimero.

Le simulazioni dei due scenari sono state condotte fino a 10000 giorni di iniezione. Alla fine, dopo circa 24 anni di coltivazione, il giacimento in cui è stato iniettato polimero presenta un recupero più alto del 38%.

Iniettare continuamente polimero potrebbe, però, non essere la strategia più conveniente. Il costo del polimero cui bisognerebbe far fronte potrebbe bilanciare il guadagno derivante dalla vendita dell'olio aggiuntivo prodotto.

Sono state eseguite, quindi, simulazioni con diverse configurazioni dei tempi di iniezione. Si è provato a fermare l'iniezione del polimero dopo 2000 giorni di produzione, poi dopo 3000, poi dopo 5000. In seguito si è voluto testare cosa accadrebbe iniettando il polimero fino a 2000 giorni e poi da 3000 a 4000. Successivamente si è provato a iniettare il polimero fino a 3000 giorni e poi da 6000 a 7000. Nell'ultima prova si è iniettato fino a 2000 giorni, poi da 3000 a 4000, poi da 6000 a 7000.

E' stato utilizzato, in seguito, un modello economico molto semplificato per determinare l'economicità delle diverse alternative

Il valore dell'investimento iniziale (capex) è costituito dal costo dell'impianto di miscelazione e iniezione della soluzione con polimero. L'esborso annuale (opex) è rappresentato dal costo del polimero da iniettare. Nota la quantità di petrolio aggiuntivo ottenuto grazie alla tecnica di EOR, è stato possibile calcolare il flusso di cassa netto per ciascuna simulazione.

Il flusso di cassa per ciascun anno è stato poi attualizzato, tenendo conto di un tasso di sconto del 10%.

La configurazione risultata più conveniente prevede l'iniezione di polimero fino a 5000 giorni dall'inizio della produzione del pozzo.

Noto questo risultato, si è provato a far girare una nuova simulazione in cui la soluzione polimerica è iniettata fino a 5000 giorni, ma con una concentrazione di polimero minore. Questo ha determinato una minore viscosità della soluzione

e un rapporto di mobilità più sfavorevole, ma il minore costo del polimero da iniettare rende comunque più competitiva tale scelta.

Effettuando un'analisi di sensitività al prezzo di petrolio. La soluzione in esame rimane economica per prezzi di greggio superiori a 48 $/bbl.

In Figura I-10 sono mostrate le portate di olio ottenute nel tempo confrontando la soluzione più competitiva, ovvero iniettare una soluzione con 1500 ppm di polimero fino a 5000 giorni, con le soluzioni limite (iniezione di sola acqua e di sola soluzione con polimero per tutta la durata della simulazione).

La quantità olio ottenuta in più con la soluzione più competitiva è evidenziata in rosso nel grafico. In giallo è evidenziato il periodo durante il quale il polimero è iniettato.

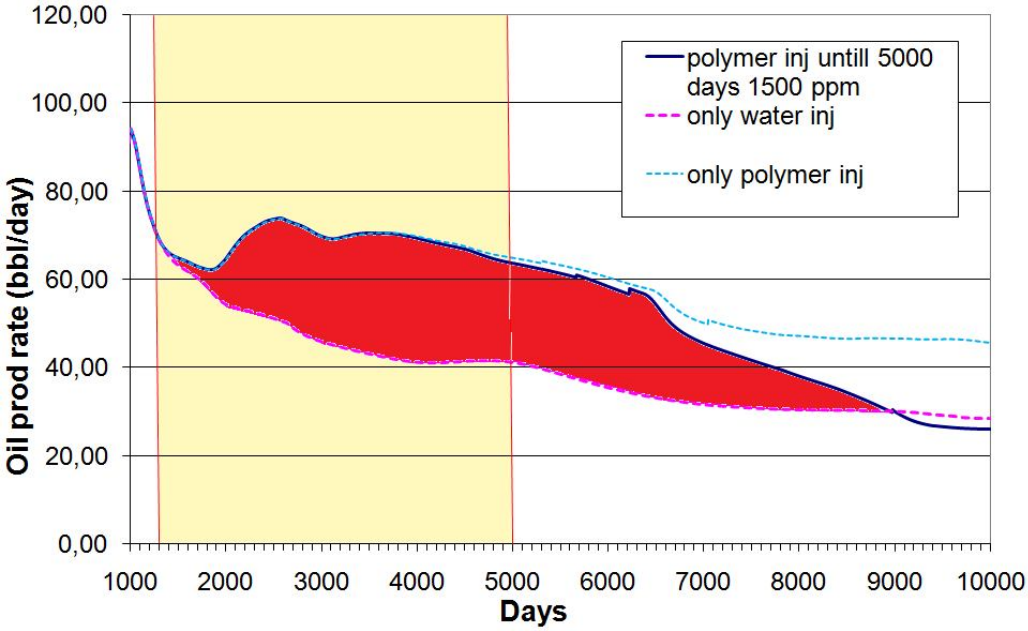

Figura I-10 - olio ottenuto in più, evidenziato in rosso, iniettando una soluzione con 1500 ppm di polimero rispetto ad iniettare solo acqua per tutto il tempo della simulazione.

1.8. Conclusioni

Le tecniche di EOR rappresentano una soluzione sempre più oggetto di studi e attenzioni, con il fine di mantenere una portata di produzione dai campi petroliferi in grado di soddisfare la crescente domanda di greggio.

In questo studio le possibilità di implementare una di queste innovative tecniche in un settore di un giacimento reale è stata efficacemente analizzata.

Dopo una fase di selezione preliminare, in cui si è tenuto conto delle principali caratteristiche del giacimento su cui intervenire, è emerso che la tecnica maggiormente applicabile e promettente consiste nell'iniezione in giacimento di una soluzione contenente polimero.

Sono state studiate le caratteristiche di diversi polimeri e il loro comportamento nelle condizioni dell'ambiente in cui sarebbero chiamati a operare. Considerando il pH, la temperatura e l'alta salinità dell'acqua di giacimento, è stato scelto un co-polimero di gruppi acril-ammide, acrilati e AMPS (2-metilpropano-2-acrilammide sulfonato).

Sono state poi effettuate prove di laboratorio su campioni di roccia prelevati direttamente dal giacimento, fatte poi combaciare con simulazioni numeriche, per determinare le proprietà specifiche della roccia serbatoio.

Il modello si è rivelato essere accurato nel riprodurre i dati sperimentali, derivanti dai flussaggi eseguiti in laboratorio.

Sono state così determinate le permeabilità relative della roccia nei confronti del moto dei fluidi al suo interno.

Le proprietà relative allo spiazzamento acqua-olio sono state poi implementate in un modello che riproduce un settore del giacimento.

Dopo aver riprodotto il suo comportamento reale, dall'inizio dello sfruttamento sino alla fase attuale, sono stati simulati diversi scenari di iniezione possibili.

I risultati hanno confermato quanto ci si aspettava dalla letteratura [16], in quanto, come si evince dalle simulazioni, nello scenario in cui si inietta polimero si arriva ad un recupero di olio maggiore rispetto allo scenario in cui si inietta solo acqua.

Per ottimizzare il guadagno derivante dal maggiore flusso di greggio, occorre determinare le migliori tempistiche di iniezione e la quantità di polimero più conveniente da iniettare.

Dopo aver stimato il capex e l'opex del progetto, è stato calcolato il flusso di cassa per ogni anno di simulazione, poi attualizzato per determinare la soluzione più competitiva.

Il flussaggio di polimero si conferma essere un metodo promettente per aumentare l'efficienza del recupero di greggio dal campo oggetto di questo studio e aumentare il guadagno netto, soprattutto se il prezzo del petrolio si mantiene ai livelli attuali.

Ulteriori aspetti legati all'iniezione di polimero devono essere studiati, ma richiedono la messa in opera di test pilota di iniettività effettuati direttamente sul campo.

1. INTRODUCTION

Fossil fuels are going to be the dominant sources of primary energy worldwide, according to the most probable scenario of world energy consumption (IEA, 2009, [1]), accounting for more than three quarters of the overall increase in energy use between 2007 and 2030. Oil is going to remain the single largest fuel in the primary fuel mix in 2030. Its demand is projected to grow by 1% per year on average on the projection period, from 85 barrels per day in 2008 to 105 barrels per day in 2030.

Oil extraction is a very important activity to support the global energy demand but, on average, about 70% of most proven oil reserves in the world remain untapped after primary oil recovery mechanism (Magbagbeola, [2]).

Secondary recovery techniques, like water injection into the field to improve the overall recovery, have been implemented, but a significant amount of unrecovered oil remains even after their extensive application.

The dropping of reserves and oil prices higher than 40 $ per barrel has stimulated interest in new methodologies, called EOR, Enhanced Oil Recovery techniques. They are getting renewed attention, as they would greatly increase the supply of oil and subsequently help meet the growing demand.

There are several different EOR methodologies, divided into thermal, chemical, or solvent methods.

In this work, after a preliminary introduction about the fundamentals of oil reservoir engineering and the principles governing the recovery, a state of art of the existing EOR tecniques is presented.

Then the possibility of implementation of an EOR technique in an oil reservoir in North Africa is studied.

First a screening phase, considering the overall characteristics of the oil field, is needed to choose the best technique to apply.

Then a study is conducted upon experimental samples, to find the correct properties of the reservoir rock, through laboratory experiments and subsequent matches with numerical simulations.

The simulator used was UtChem, a finite difference, three-dimensional, multiphase, multicomponent simulator of chemical flooding processes developed at the University of Texas at Austin. It implements an innovative model and was used to solve the pressure and flow equations governing the fluid dynamics inside the reservoir rock. It contains physicochemical advanced models able to simulate the flow of chemicals and their interactions. One of the targets of the work was to check the consistency of the model and its ability to reproduce the experimental data.

After that, simulations upon a real sector of the field are conducted. Their first aim is to check the properties found in the laboratory experiments by matching the real past history of the field sector. After that the EOR technique is

simulated to find the response of the field and check if the implementation leads to an effective improve in the amount of oil recovered.

2. BASICS OF RESERVOIR ENGINEERING REVIEW

Under a general point of view, a petroleum reservoir is composed by one or more layers of porous and permeable rock, delimited by impermeable formations of clays or by layers plenty of water, called aquifers.

Hydrocarbons saturate the pores of the rock-reservoir. They are the result of the transformations to which organic materials were undergone in past geologic ages. After the formation, they have accumulated in geologically favorable zones, filling the reservoirs.

They can be, depending by the thermodynamic conditions of the reservoir, in liquid or gaseous form [3].

Inside the reservoirs, the relative disposition of the different fluids present is gravity-regulated, as shown in the sketch in Figure 2-1.

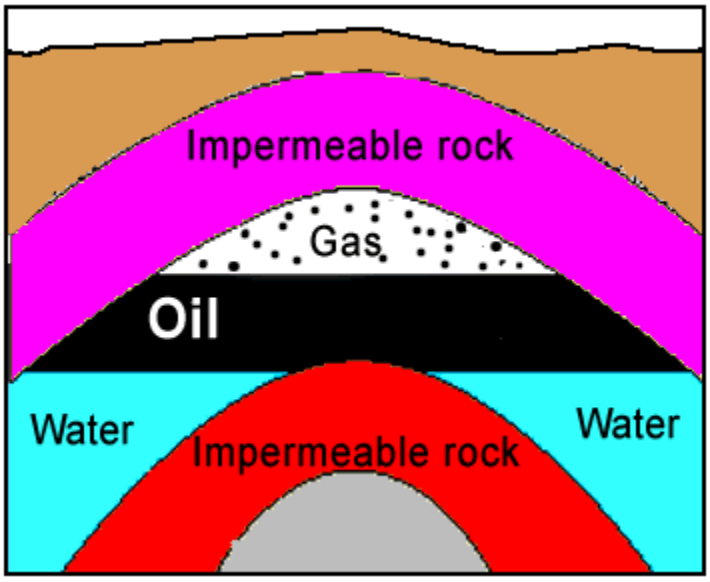

Figure 2-1 - Gas, oil, and water in a reservoir rock

In the zones with high concentration of oil and gas, a certain concentration of water is always present, under the form of a film, wrapping the grains of the reservoir rock. It is the remaining part of the water which saturated the pores before the hydrocarbon accumulation process. For this reason it is called “connate water”.

In the most of the cases, because of the wettability of the rock and interfacial tensions between non-miscible fluids, this water cannot be fluxed by the pressure gradients created during the depletion of the reservoir. For this reason it is also called “irreducible water”.

2.1. Properties of reservoir rock

In the most of the cases the reservoir rocks are sedimentary rocks: clastic or chemically generated.

The main properties of such rocks are porosity, permeability and compressibility.

2.1.1. Porosity

The porosity of a rock is the ratio between the total volume of pores and the total volume of the sample ($\Phi = \frac{V_P}{V_t}$ Equation 2-1).

In the computation of the pore volume, only the communicating pores are taken into consideration, since the others can't give any contribution to the production.

Porosity is a measure of the capacity of the rock to stock hydrocarbons.

$$\Phi = \frac{V_P}{V_t}$$ **Equation 2-1, definition of porosity**

Where:

Φ is the porosity

V_P is the volume of communicating pores, which can be occupied by fluids

V_t is the total volume of the sample rock considered

2.1.2. Absolute permeability

Absolute permeability is an intrinsic property of the rocks and it expresses the ability of the pore medium in allowing the flow through itself, without altering its structure.

Permeability is deductible from the Darcy law, obtained experimentally in the 1856:

$$\frac{q}{A} = v = -\frac{k}{\mu} \cdot \frac{dp}{dx}$$

Equation 2-2 - Darcy's law through a porous medium

Where:

q is the volumetric flow rate

A is the section of the porous sample

υ is the average speed of the flow

μ is the dynamic viscosity of the fluid

p is the pressure

x is the coordinate along the direction of the flow

k is the absolute permeability of the rock considered.

The Darcy equation describes the flow in porous granular media, under these hypotheses:

The saturation of the flowing fluid is equal to one.

The fluid does not chemically react with the porous rock.

The fluid is sufficiently dense.

Laminar flow.

Permeability is expressed in Darcy units. One Darcy measure the permeability of a rock sample with a section of 1 cm2 and a length of 1 cm, which, under a pressure difference of 1 atm, is crossed by a 1 cm3/s flow of a fluid with 1 cP viscosity.

2.1.3.- Compressibility of the rocks

The compressibility of a shape is defined as the fractionary variation of volume corresponding to a unitary variation of pressure.

Knowing this definition, it is possible to describe the coefficient of compressibility of the pore volume:

$$Cf = -\frac{1}{V_P}\left(\frac{\partial V_P}{\partial p}\right)$$ ***Equation 2-3, Definition of compressibility***

Where

Cf: Compressibility of the rock

V_P: reservoir pore volume

P: pressure

The negative sign convention is required, because compressibility is defined as a positive number, whereas the differential $\left(\partial V_P \big/ \partial p\right)$ is negative, since rocks expand while their confining pressure is decreased.

2.1.4.– Wettability

Wettability is defined as the tendency of one fluid to spread on or adhere to a solid surface in the presence of other immiscible fluids. When the fluids are water and oil, it measures the tendency for the rock to preferentially imbibe oil, water or both. The wettability of a rock is important, because it controls the location, flow, and distribution of fluids within reservoir rocks.

When a rock is water-wet, the aqueous phase is retained by capillary forces in the smaller pores and on the walls of the larger pores. The oleic phase, instead, occupies the center of the larger pores. The opposite happens for oil-wet reservoirs, where the oleic phase occupies the small pores and coats the walls of the large pores. The wettability can vary within the single reservoir and there can be no clear preference for one fluid or another. Many minerals, in fact, form the reservoir rock and they can have different surface chemistry and adsorption properties.

Several methods have been presented in literature for determining the wettability of a rock. The most common is the contact angle measurement.

When two immiscible fluids, such as oil and water, are together in contact with a rock, the surface of separation between them forms an angle with the solid wall.

This angle,θ, is called contact angle and can vary between 0° and 180° [4].

If $\theta < 90°$, the reservoir rock is described as being water wet, whereas if $\theta > 90°$ it is oil wet, as shown in Figure 2-2.

θ is the quantitative definition of the wettability.

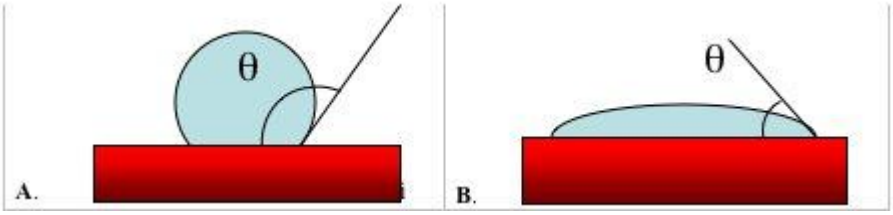

Figure 2-2 , wettability

– Capillary pressure

The fact that oil and water are immiscible is very important. When such fluids are in contact a clearly defined interface exists between them.

The molecules near the interface are unevenly attracted by their neighbors and this gives rise to a free surface energy per unit area, or interfacial tension. If the interface is curved the pressure on the concave side exceeds that on the convex.

The pressure difference between the two fluids along the separation surface is called Capillary Pressure.

It is an important reservoir property, because it directly or indirectly affects other properties such as residual saturations and relative permeabilities.

The general expression for calculating the capillary pressure is given by the Laplace equation:

$$P_C = p_O - p_W = \sigma \cdot \left(\frac{1}{r_1} + \frac{1}{r_2} \right)$$ **Equation 2-4, Laplace law for capillary pressure**

where Pw and P_O refer to the wetting and non-wetting phases.

σ is the interfacial tension between phases.

r_1 and r_2 are the principal radii of curvature at any point of the interface where the pressures in the oil and water are p_O and p_W.

2.2. Calculation of hydrocarbon volumes

Considering a reservoir initially filled with liquid oil, the oil volume in the reservoir is:

$$OIP = V \cdot \phi \cdot (1 - S_{WC})$$ **Equation 2-5, calculation of oil in place**

Where

V: net bulk volume of reservoir rock

ϕ: Porosity of the rock

S_{WC}: Connate or irreducible water saturation, expressed as fraction of pore volume.

The product $V \cdot \phi$ is the pore volume (V_P or PV).

The product $V \cdot \phi \cdot (1 - S_{WC})$, similarly, is called hydrocarbon pore volume (HCPV) and is the total reservoir volume which can be filled with hydrocarbons.

The oil volume calculated using Equation 2-5 is expressed as a reservoir volume.

Since all oils, at the high pressures and temperatures in reservoirs, contain different amount of dissolved gas, it is more meaningful to express oil volumes at surface conditions, at which oil and gas will be separated.

Thus the stock tank oil initially in place is:

$$STOIIP = N = V \cdot \phi \cdot (1 - S_{WC}) / B_{Oi}$$

Equation 2-6, Stock Tank Volume of oil in place

Where BO_i is the oil formation volume factor, under initial conditions. Its units are reservoir volume/stock tank volume. Thus a volume of BOi reservoir barrel (rb) of oil will produce one standard barrel (stb) of oil at the surface.

Equation **2-6** can be converted into an equation for calculating the ultimate recovery multiplying by the recovery factor (RF). It is a number between zero and unity representing the fraction of recoverable oil. Thus:

$$Ultimate\ \text{Recovery} = \left(V \cdot \phi \cdot \left(1 - S_{WC}\right) / B_{Oi}\right) \cdot RF$$

Equation 2-7, Ultimate recovery

There are two main categories of hydrocarbon recovery, called primary and supplementary.

Primary recovery is the volume of oil which can be produced utilizing only the natural energy available in the reservoir and its adjacent aquifer.

Supplementary recovery is the oil obtained by adding energy to the reservoir-fluid system.

The most common type of supplementary recovery is water flooding, which consists in injecting water in the reservoir. Water displaces oil towards the producing wells, increasing the natural energy of the system.

The primary recovery relies on the expansion of fluids in the reservoir and can be described using the definition of isothermal compressibility:

$$C = -\frac{1}{V}\left(\frac{\partial V}{\partial p}\right)\Bigg|_T$$

Equation 2-8, Isothermal compressibility

This definition applies to all fluids.

According to a reasonable approximation, as the fluids are produced, and so remove heat from the reservoir by convection, the base rock, considered as infinite sources of heat, immediately replaces the heat by conduction.

To describe reservoir depletion, it is more illustrative to express the compressibility in the form:

$$\Delta V = C \cdot V \cdot \Delta p$$

Equation 2-9

Where ΔV is an expansion and Δp a pressure drop, both of which are positive.

If Δp is taken as the pressure drop from initial to some lower pressure, then ΔV will be the corresponding fluid expansion.

2.3. - PVT Analysis for oil

If the pressure is above the bubble point of the oil mixture, only one phase exists in the reservoir, the liquid oil.

If a quantity of this undersaturated oil is produced to the surface, gas will separate from the oil.

Control in relating surface volumes of production to underground withdrawal is gained by defining the following three PVT parameters, which can be measured by laboratory experiments [5].

- Rs $\left[\frac{scf\ \ gas}{stb\ \ oil}\right]$: The solution gas oil ratio, which is the number of standard cubic feet of gas which will dissolve in one stock tank barrel of oil when both are taken down to the reservoir at the prevailing reservoir pressure and temperature.
- Bo $\left[\frac{rb\ \ oil}{stb\ \ oil}\right]$: The oil formation volume factor, which is the volume in barrels occupied in the reservoir, at the prevailing pressure and temperature, by one stock tank barrel of oil plus its dissolved gas.
- Bg $\left[\frac{rb\ \ gas}{stb\ \ oil}\right]$: The gas formation volume factor, which is the volume in barrels that one standard cubic foot of gas will occupy as free gas in the reservoir at the prevailing reservoir pressure and temperature.

2.4. – Two Phase flow in reservoir

2.4.1.– Relative permeabilities

In hydrocarbons reservoir the porous medium is usually saturated with two or three fluids: water, oil and gas. So there is the need to generalize the Darcy law to compute the contemporaneous flow of several fluids.

If the saturation of a fluid is less than one, the porous rock has, respect to it, a value of permeability less than absolute permeability. In this case each fluid has its own, so called, effective permeability.

These permeabilities are dependent on the saturations of each fluid and the sum of the effective permeabilities is always less than the absolute permeability.

The relative permeability of a fluid, instead, is defined as the ratio between the effective permeability of the fluid and the absolute permeability of the medium in which it flows [6]:

$$kr_{FL} = \frac{permeability\ \ referred\ \ to\ \ the\ \ phase\ \ considered}{rock\ \ absolute\ \ pereability}$$

Equation 2-10, definition of relative permeability

Relative permeabilities are dependent, in addition to the saturation of the fluids, also from the pore dimensions and their distribution.

Considering the relative permeability curve for water, two points on this curve are known. When $S_W=S_{WC}$, the connate or irreducible water saturation, the

water will not flow and k_W=0. Also, when SW=1 the rock is entirely saturated with water and k_W=k (Figure 2-3).

Similarly for the oil, when S_W=0 (and S_O=1) then k_O=k. When the oil saturation decreases to S_{OR}, called oil residual saturation, there will be no oil flow and k_O=0.

The main influence on the shape of the curves appears to be the wettability.

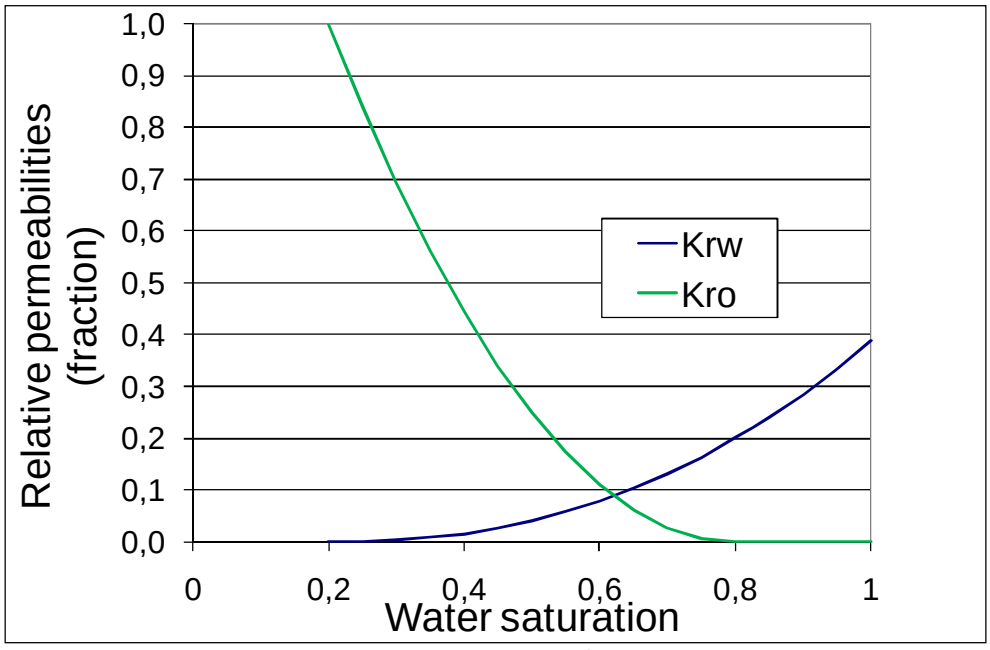

Figure 2-3, relative permeability curves for a water – oil system

2.4.2. Imbibition and drainage

Imbibition is a dynamic situation in which the wetting phase saturation is increasing.

Drainage, instead, is characterized by the decrease of the wetting phase saturation. It has been determined experimentally that the contact angle is larger when the wetting phase is advancing over the rock face than when retreating. This difference is described as the hysteresis of the contact angle, as it is possible to see in Figure 2-4 .

Both drainage and imbibitions curves may be required in studies of oil-water systems. Although most processes of interest involve displacement of oil by water, or imbibitions, the reverse may take place in parts of the reservoir, due to geometrical effects, or to changes in injection and production rates resulting in reversal of flow directions [7].

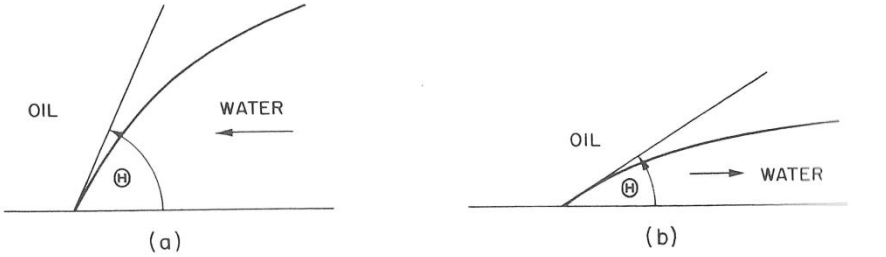

Figure 2-4, Contact angle in a water wet reservoir, (a) wetting phase increasing (imbibition); (b) wetting phase decreasing (drainage)

Starting with the porous rock completely filled with water, and displacing by oil, the drainage relative permeability and capillary pressure curves will be defined:

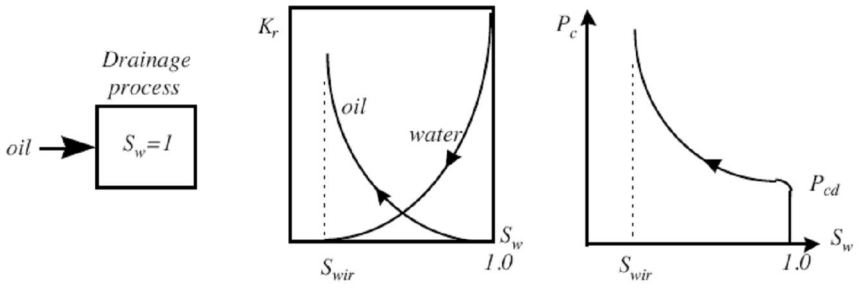

Figure 2-5, permeability and capillary pressure curves for a drainage process

Reversing the process when all mobile water has been displaced, by injecting water to displace the oil, imbibitions curves are defined:

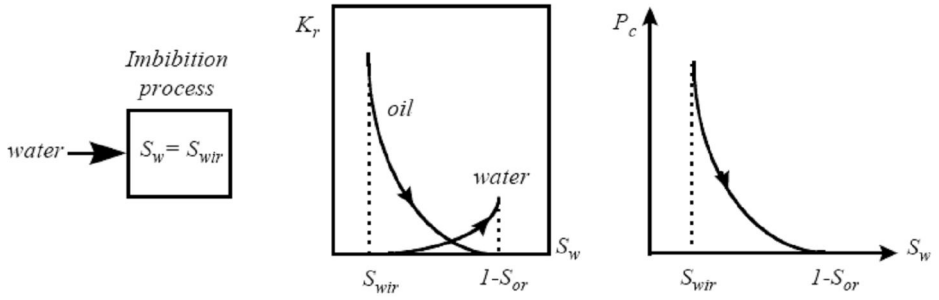

Figure 2-6, permeability and capillary pressure curves for an imbibitions process

The above curves (Figure 2-5 and Figure 2-6) are typical ones for a completely water-wet system.

2.5. – Material balance applied to oil reservoirs

The general form of material balance is derived as a volume balance which equates the cumulative observed production, expressed as an underground withdrawal, to the expansion of the fluids in the reservoir resulting from a finite pressure drop.

Principle of material conservation

$$\left\{\begin{matrix}Amount of\ \ fluids\ present\\ initially in\ the\ reservoir\\ (st.\ vol.)\end{matrix}\right\}-\left\{\begin{matrix}Amount of\\ fluids\ produced\\ st.\ vol.\end{matrix}\right\}=\left\{\begin{matrix}Amount of\ \ fluids\ remaining\\ in\ the\ reservoir\ finally\\ (st.\ vol.)\end{matrix}\right\}$$

Equation 2-11, principle of material conservation

To derive the material balance, it is necessary to describe the fluid behavior, as follows:

Oil density:

$$\rho_O = \frac{\rho_{OS} + \rho_{gS} \cdot R_{SO}}{B_O}$$

Equation 2-12

Water compressibility:

$$C_W = -\left(\frac{1}{V_W}\right) \cdot \left(\frac{\partial V_W}{\partial p}\right)_T$$

Equation 2-13

Water volume change:

$$B_{W2} = B_{W1} \cdot \exp\left(-C_W \cdot \Delta p\right) \approx B_{w1} \cdot \left(1 - C_W \cdot \Delta p\right)$$

Equation 2-14

Finally, we need to quantify the behavior of the pores during pressure change in the reservoir.

It is assumed that, while the pore volume decrease, the bulk volume of the rock itself does not change.

Rock compressibility: $$Cf = -\frac{1}{V_P}\left(\frac{\partial V_P}{\partial p}\right)$$ **Equation 2-15**

Porosity change: $$\Phi_{W2} = \Phi_{W1} \cdot \exp\left(C_R \cdot \Delta p\right) \approx \Phi_{W1} \cdot \left(1 + C_R \cdot \Delta p\right)$$

Equation 2-16

2.5.1.– Oil material balance

$$\left\{\begin{matrix} oil\ \ present \\ initially\ \ in\ \ the\ \ reservoir \\ \left(st.\ \ vol.\right) \end{matrix}\right\} - \left\{\begin{matrix} oil\ \ produced \\ st.\ \ vol. \end{matrix}\right\} = \left\{\begin{matrix} oil\ \ remaining \\ in\ \ the\ \ reservoir\ \ \ finally \\ \left(st.\ \ vol.\right) \end{matrix}\right\}$$

Equation 2-17

$$N - N_P = V_{P2} \cdot S_{O2} / B_{O2}$$ **Equation 2-18**

Where N in the initial oil in place, in stock tank barrels,
N_P is the cumulative oil production in stock tank barrels,
V_{P2} is the final pore volume
S_{O2} is the final oil saturation
B_{O2} is the oil formation volume factor

Rearranging the equation:

$$S_{O2} = \frac{\left(N - N_P\right) \cdot B_{O2}}{V_{P2}}$$ **Equation 2-19**

2.5.2. Water material balance

$$\begin{Bmatrix} water\ present \\ initially\ in\ the\ reservoir \\ (st.\ vol.) \end{Bmatrix} - \begin{Bmatrix} water \\ produced \\ st.\ vol. \end{Bmatrix} + \begin{Bmatrix} water \\ injected \\ st.\ vol. \end{Bmatrix} + \begin{Bmatrix} aquifer \\ \inf lux \\ st.\ vol. \end{Bmatrix} = \begin{Bmatrix} water\ remaining \\ in\ the\ reservoir\ finally \\ (st.\ vol.) \end{Bmatrix}$$

Equation 2-20

Or

$$V_{P1} \cdot S_{W1} / B_{W1} - W_P + W_i + W_e = V_{P2} \cdot S_{W2} / B_{W2} \qquad \textbf{Equation 2-21}$$

B_W: water formation volume factor
W_P: cumulative water produced (stock tank barrels)
W_i: cumulative water injected (stock tank barrels)
W_e: aquifer influx

2.5.3.– Complete material balance

$$S_W + S_O = 1 \qquad \textbf{Equation 2-22}$$

Knowing that the sum of saturations must be one, as shown in Equation 2-22, it is possible to write the final form of material balance [8]:

$$\underbrace{N_P \cdot B_{O2} + W_P \cdot B_{W2}}_{\text{Production term}} = N \cdot \left[\underbrace{\left(B_{O2} - B_{O1}\right)}_{\text{Oil expansion term}} - \underbrace{B_{O1} \cdot \frac{C_r + C_W \cdot S_{W1}}{1 - S_{W1}} \cdot \Delta p}_{\text{Rock and water expansion term}} \right] + \underbrace{\left(W_i + W_e\right) \cdot B_{W2}}_{\text{External water influence}}$$

Equation 2-23

2.6. – Fluid flow differential equations

Flow equations for flow in porous media are based on a set of mass, momentum and energy conservation equations, and constitutive equations for the fluids and porous material involved.

Assuming isothermal conditions, it is possible to derive the constitutive equations describing a single-phase flow in linear, one dimensional, horizontal system.

2.6.1.– Conservation of mass

Mass conservation may be formulated across a control element of the slab, with one fluid of density ρ flowing through it at a velocity u, as shown in Figure 2-7.

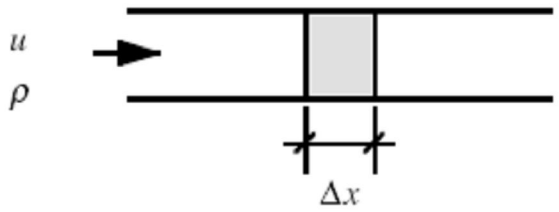

Figure 2-7, mass balance across a control element

The mass balance for the control element may the written as:

$$\begin{Bmatrix} Mass \ \text{int}\, o \ the \\ element \ at \ x \end{Bmatrix} - \begin{Bmatrix} Mass \ out \ of \ the \\ element \ at \ x+dx \end{Bmatrix} = \begin{Bmatrix} Rate \ of \ change \ of \ mass \\ inside \ the \ element \end{Bmatrix}$$

Equation 2-24

The balance above can be written as:

$$\{u \cdot \rho \cdot A\}_X - \{u \cdot \rho \cdot A\}_{X+\Delta X} = \frac{\partial}{\partial t}(\rho \cdot \Phi) \qquad \textbf{Equation 2-25}$$

Dividing by ΔX and making it approaches to zero, and considering constant the cross-sectional area, we get the continuity equation:

$$-\frac{\partial}{\partial x}(\rho \cdot u) = \frac{\partial}{\partial t}(\Phi \cdot \rho)$$

Equation 2-26 Continuity equation, for a constant cross-sectional area

2.6.2.– Conservation of momentum

Conservation of momentum is governed by Navier-Stokes equations, but it is normally simplified for low velocity flow in porous materials to be described by the Darcy's equation [9]:

$$\frac{q}{A} = v = -\frac{k}{\mu} \cdot \frac{dp}{dx}$$

Equation 2-27, Darcy's law through a porous medium

2.6.3.– Constitutive equation for porous materials

To include pressure dependency in the porosity, it is possible to use the definition of rock compressibility:

$$Cf = -\frac{1}{V_P}\left(\frac{\partial V_P}{\partial p}\right) \qquad \textbf{Equation 2-28, Definition of compressibility}$$

2.6.4. Constitutive equation for fluids

For the fluids it is possible to recall the fluid compressibility definition:

$$C = -\frac{1}{V}\left(\frac{\partial V}{\partial p}\right)\Bigg|_T$$

Equation 2-29, Isothermal compressibility

For more general purposes, such as in reservoir simulation models, it is also possible to use the so-called Black Oil fluid description, or compositional fluid description.

The standard Balck Oil model includes the formation volume factor, B, and the solution Gas-Oil ratio, Rs.

The density of oil at reservoir conditions is then:

$$\rho_O = \frac{\rho_{OS} + \rho_{GS} \cdot R_{SO}}{B_O}$$

Equation 2-30, density of oil in reservoir condition according to the Black Oil model

2.6.5.– Diffusivity equation

Substituting the Darcy equation into the continuity equation, after few passages it is possible to derive the diffusivity equation [10]:

$$\frac{\partial^2 P}{\partial x^2} = \left(\frac{\mu \cdot C \cdot \Phi}{k}\right) \cdot \frac{\partial P}{\partial t}$$

Equation 2-31, diffusivity equation

Where C is the sum of the rock and fluid compressibilities.

Assumptions made in the derivation of the equation above:

1. One dimensional flow
2. Linear flow
3. Horizontal flow
4. One phase flow
5. Darcy's equation applies
6. Small fluid compressibility
7. Constant permeability and viscosity

– Generalizations

MULTIPHASE FLOW

A continuity equation may be written for each fluid phase flowing:

$$-\frac{\partial}{\partial x}\left(\rho_l \cdot u_l\right) = \frac{\partial}{\partial t}\left(\Phi \cdot \rho_l \cdot S_l\right) \qquad \text{l = water, oil, gas} \qquad \textbf{Equation 2-32}$$

And the corresponding Darcy equations are:

$$u_l = -\frac{k \cdot k_{rl}}{\mu_l} \cdot \frac{dp_l}{dx}, \quad l = o, w, g \qquad \textbf{Equation 2-33}$$

NON – HORIZONTAL FLOW

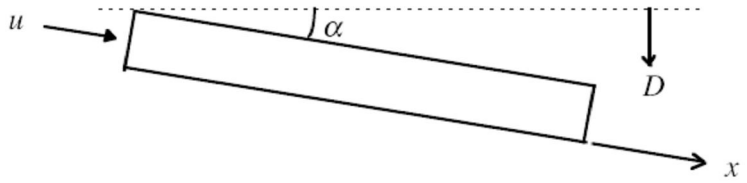

Figure 2-8

For one-dimensional, inclined flow, as shown in Figure 2-8, the Darcy equation becomes:

$$v = -\frac{k}{\mu} \cdot \left(\frac{dp}{dx} - \rho \cdot g \cdot \frac{dD}{dx}\right) \qquad \textbf{Equation 2-34}$$

MULTIDIMENSIONAL FLOW

The continuity equation becomes:

$$-\nabla\left(\rho \cdot v\right) = \frac{\partial}{\partial t}\left(\Phi \cdot \rho\right) \qquad \textbf{Equation 2-35}$$

And the Darcy law:

$$v = -\frac{k}{\mu} \cdot \left(\nabla p - \rho \cdot g \cdot \nabla D\right) \qquad \textbf{Equation 2-36}$$

Where the operator ∇ is defined as:

$$\nabla(\ ) = \frac{\partial}{\partial x}(\ ) + \frac{\partial}{\partial y}(\ ) + \frac{\partial}{\partial z}(\ ) \qquad \textbf{Equation 2-37}$$

3. WATERFLOODING AND DISPLACEMENT

Most oil and gas production (primary and secondary recovery) relies on the process of immiscible displacement of fluids in the reservoir, which is exactly what happens in a waterflood. Water is injected in a well or pattern of wells to displace oil from an injector towards a producer.

3.1. Mobility

The mechanics of displacement of one fluid with another are controlled by differences in the ratio of effective permeability and viscosity (k /μ).

Recalling the Darcy law:

$$q_W = -\left(\frac{k \cdot k_{rw}}{\mu_w}\right) \cdot \nabla\left(p_w + \gamma_w \cdot D\right) \qquad \textbf{Equation 3-1}$$

$$q_O = -\left(\frac{k \cdot k_{ro}}{\mu_o}\right) \cdot \nabla\left(p_O + \gamma_O \cdot D\right) \qquad \textbf{Equation 3-2}$$

The specific discharge for each phase depends on k /μ. This is called the fluid **mobility** (λ):

$$\lambda_w = k_w / \mu_w \qquad \textbf{Equation 3-3, mobility of water}$$

$$\lambda_O = k_O / \mu_O \qquad \textbf{Equation 3-4, mobility of oil}$$

Mobility controls the relative ease with which fluids can flow through a porous medium.

The mobility ratio is expressed as:

$$M = \lambda_w / \lambda_O \qquad \textbf{Equation 3-5, mobility ratio}$$

In ideal displacement, there is a sharp transition from residual oil saturation (S_{oi}) to maximum oil saturation ($1 - S_{wi}$) at the oil-water interface.

Ahead of the interface, oil alone is flowing at the end-point mobility $\lambda o' = ko'/\mu o$. Behind the interface, water alone is flowing at the end-point mobility $\lambda w' = kw'/\mu w$.

Ideal displacement is the most favorable condition for production but only occurs if the end-point mobility ratio is less than or equal to unity.

$$M' = \lambda_w' / \lambda_O' \leq 1$$ **Equation 3-6 – condition for ideal displacement**

3.2. Ideal and non- ideal displacement

If the mobility ratio is less than or equal to one, oil can flow at a rate greater than or equal to that of water and is pushed ahead by the water bank in a piston-like fashion (Figure 3-1).

The moveable oil volume (MOV) is given by:

$$MOV = (1 - S_{Oi} - S_{Wi}) \cdot PV$$ **Equation 3-7, movable oil in ideal displacement**

Where PV is the pore volume. For a waterflood under ideal displacement conditions, the volume of oil recovered is exactly equal to the volume of water injected.

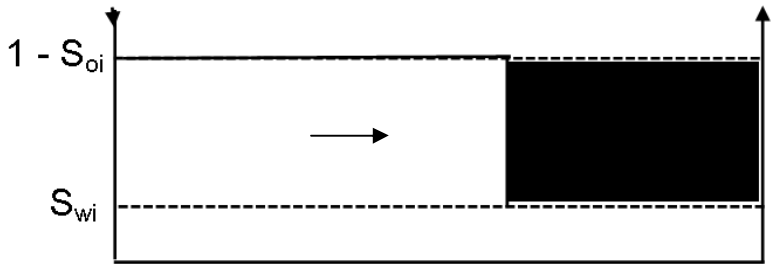

Figure 3-1, piston-like displacement

Under most circumstances, water is found to be more mobile than oil [11]. As a result, tongues of water bypass the oil leading to much less favorable saturation profiles.

Some distance ahead of the water front, oil alone flows at the end-point mobility $\lambda_o' = k_o'/\mu_o$.

At some point nearer the water front there is a sharp change in water saturation called the ***shock front***. Behind the shock front there is a transition zone where both water and oil flow (Figure 3-2).

At the end of the transition zone, water alone is flowing at the end-point mobility $\lambda_w' = k_w'/\mu_w$.

When the shock front reaches the production well there is a sharp increase in water produced. This event is called ***breakthrough***.

In contrast to the ideal displacement case, at breakthrough, only a fraction of the MOV has been recovered.

Addition water injection is required to recover the moveable oil. Several MOV's of water may be needed to displace a single MOV of oil.

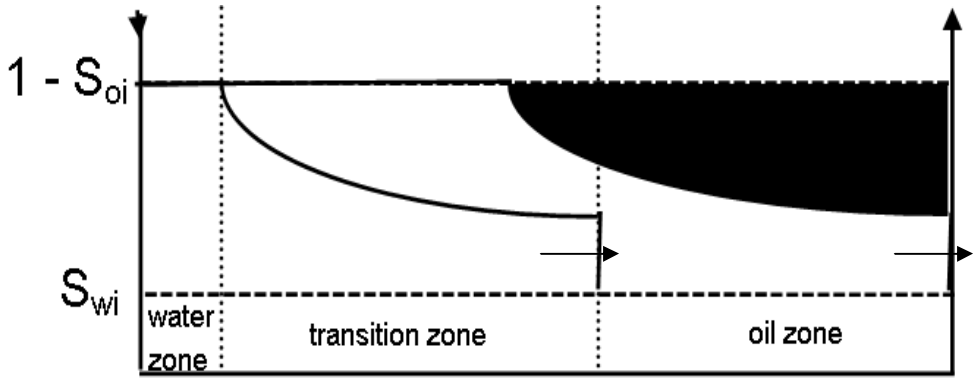

Figure 3-2, non-ideal displacement

The diagram in Figure 3-2 shows two saturation profiles with the shock front to the right. Before breakthrough, there is a water zone, a transition zone and an oil zone. At breakthrough, the shaded area represents moveable oil that remains between the injector and producer.

In the reservoir an oil-water transition zone forms, as shown in Figure 3-4.

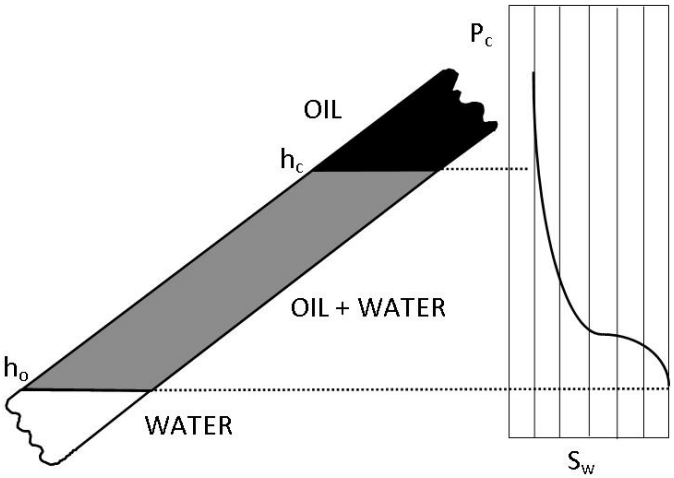

Figure 3-3, oil- water transition zone

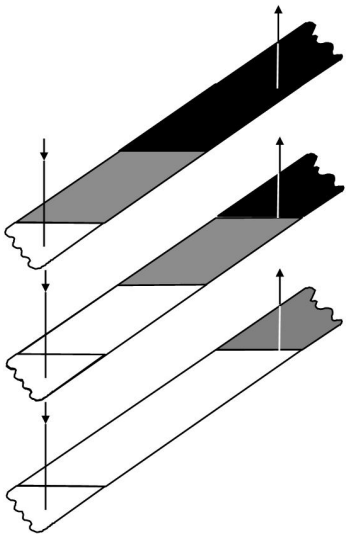

Figure 3-4, displacement process

At elevations greater than the capillary head, h_c, the oil saturation is $(1 - S_{wi})$. At the OWC (Oil-Water Contact), h_o, the water saturation is 1. Between h_o and h_c the saturations vary continuously through the capillary transition zone.

When the leading edge of the capillary transition zone reaches the producer ***breakthrough*** occurs.

After breakthrough, both oil and water are produced and the ***watercut*** increases progressively.

Eventually the trailing edge of the capillary zone reaches the producer and only water is produced.

3.3. Recovery efficiencies

The recovery efficiency, also known as recovery factor (RF), is usually broken as the product of three factors: an areal sweep efficiency (E_A), a vertical sweep efficiency (E_V), and a microscopic displacement efficiency (E_D) [11].

$$RF = \frac{N_P}{N} = E_A \cdot E_V \cdot E_D \qquad \textbf{Equation 3-8}$$

3.3.1.Areal sweep efficiency

Areal sweep efficiency can be defined as:

$$E_A = \frac{Area\ \ contacted\ \ by\ \ displacing\ \ agent}{Total\ \ Area} \qquad \textbf{Equation 3-9}$$

When oil is produced from patterns of injectors and producers, the flow is such that only part of the area is swept at breakthrough.

The expansion of the waterbank is initially radial from the injector but eventually is focused at the producer.

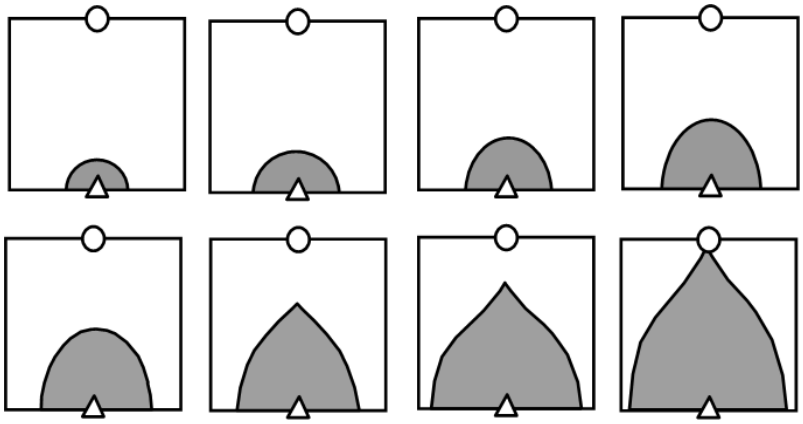

Figure 3-5, areal sweep efficiency

The pattern in Figure 3-5 is illustrated for a direct line drive at a mobility ratio of unity. At breakthough, a considerable area of the reservoir is unswept.

Mobility ratio (M) has a strong influence on areal sweep efficiency (ASE) at breakthrough. For five-spot patterns, areal sweep efficiency at breakthrough depends on the mobility ratio.

$M < 0.2$, $E_A > 95\%$
$M = 1.0$, $E_A = 67\%$
$M = 10$, $E_A = 50\%$.

Viscous fingering

The mechanics of displacing one fluid with another are relatively simple if the ***displaced fluid*** (oil) has a tendency to flow faster than the ***displacing fluid*** (water).

Under these circumstances there is no tendency for the displaced fluid to be overtaken by the displacing fluid and the fluid-fluid (oil-water) interface is ***stable***.

If the displacing fluid has a tendency to move faster than the displaced fluid, the fluid-fluid interface is ***unstable.*** Tongues of displacing fluid propagate at the interface. This process is called ***viscous fingering*** (Figure 3-6).

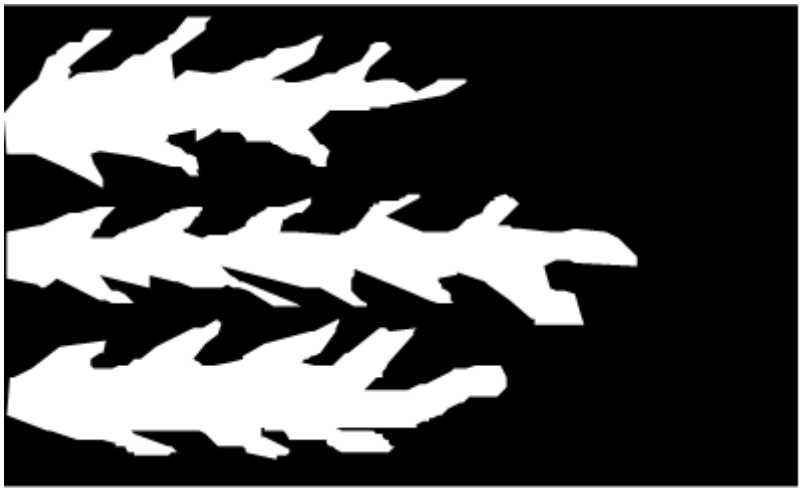

Figure 3-6, viscous fingering

3.3.2.Vertical Sweep Efficiency

Vertical sweep efficiency for a waterflood is the fraction of a formation in a vertical plane that the water will contact.

Vertical sweep efficiency depends primarily on the degree of reservoir stratification.

High k lenses and layers that extend from injector to producer can adversely affect vertical sweep efficiency by providing “short-circuits” for the displacing fluid leading to premature breakthrough (Figure 3-7).

Other factors on which the vertical sweep efficiency depends upon are:

- Heterogeneity
- Gravity
- Mobility ratio
- Capillary forces

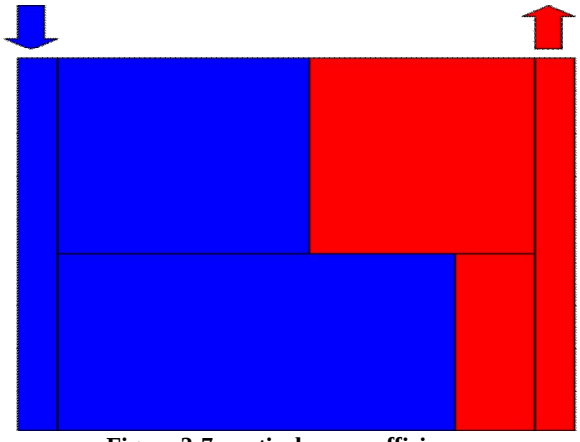

Figure 3-7, vertical sweep efficiency

Gravity effect

Gravity affects the vertical efficiency not only in heterogeneous reservoirs but in homogenous as well.

Gravity effects are important when vertical communication is good and when gravity forces are larger than viscous forces.

Vertical communication is good when R_L factor is large:

Errore. Non si possono creare oggetti dalla modifica di codici di campo.
Equation 3-10

L is the length of the sector considered, H is the depth. K_V is the permeability along the vertical direction.

Gravity forces, instead, are strong compared to viscous forces when capillary number N_g is large

$$N_g = \frac{k \cdot \lambda \cdot \Delta\rho \cdot g}{v}$$ **Equation 3-11, capillary number**

Where:

λ: relative mobility of displacing fluid

Δρ: density difference (displaced - displacing)

v: superficial velocity

Both R_L and N_g are dimensionless.

Gravity effect is responsible of the "tonguing" phenomenon (Figure 3-8).

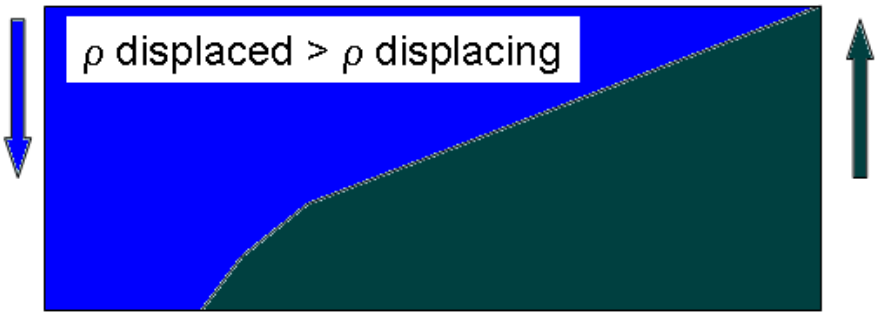

Figure 3-8, Tongue over

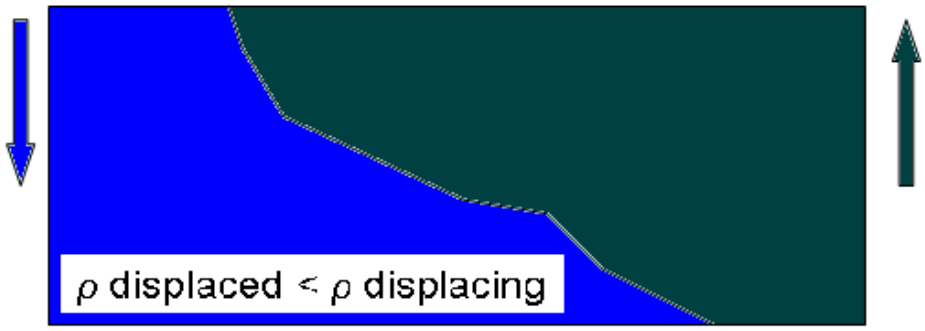

Figure 3-9, Tongue under

In the “tongue over” the density of displacing fluid is lower than the density of displaced fluid.

In the “tongue under” the Density of displacing fluid is higher.

Tonguing will occur when M < 1 as long as R_L and N_g are large. The effect of heterogeneity and gravity can be mitigated by a favorable mobility ratio. Gravity tonguing is important in steam flooding applications.

Areal and vertical sweep efficiencies can be combined together, to give the “Volumetric Sweep Efficiency”.

$$E_V = E_v \cdot E_A$$

Equation 3-12, volumetric sweep efficiency

It can be defined as:

$$E_V = \frac{\text{Reservoir volumes of oil contacted by displacing agent}}{\text{Reservoir volumes of oil originally in place}}$$

Equation 3-13 - volumetric sweep efficiency

3.3.3.Microscopic Displacement efficiency

The microscopic displacement efficiency is the fraction of oil which water will displace in the invaded zone.

It can be defined as:

$$E_D = \frac{\text{Reservoir volumes of oil mobilized by water}}{\text{Reservoir volumes contacted by water}}$$

Equation 3-14 - microscopic displacement efficiency

This efficiency is measured directly from a laboratory core flood (where EV=1).

For an immiscible displacement ED is bounded by a residual phase saturation of the displaced phase Sor. Miscible displacements can eliminate - in principle - Sor.

ED is a function of:

- Mobility ratios
- Wettability
- Dip angle
- Capillary number

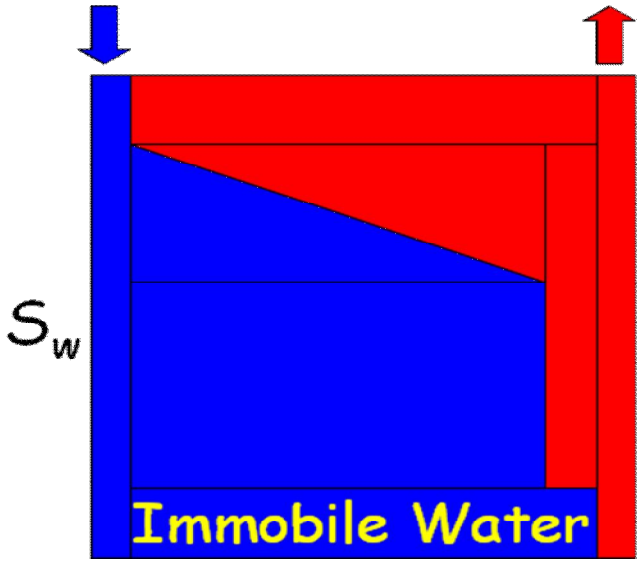

Figure 3-10 - microscopic displacement efficiency

4. INTRODUCTION TO ENHANCED OIL RECOVERY TECHNIQUES

METHODS TO IMPROVE RECOVERY EFFICIENCY

The producing life of a reservoir is divided into three phases: primary, secondary and tertiary. Primary recovery is recovery by natural drive mechanisms. They include solutions gas drive, water influx, gas cap drive and gravity drainage. If there is not enough natural reservoir energy for wells to flow, some form of artificial lift may be used to provide energy to lift the produced fluids to surface.

In addition to conventional recovery processes, there are a variety of methods that are available to improve recovery efficiency. The techniques whose aim is to raise or maintain reservoir pressure, like water or gas injection, are referred to as “secondary recovery”.

Any technique applied after secondary recovery is referred to as tertiary recovery, as shown in Figure 4-1.

Secondary and tertiary methods are grouped into three main categories: Enhanced Oil Recovery (EOR), strategic wellbore placement, production/injection control [12].

High oil prices and dropping reserves replacement has stimulated interest in these technologies, particularly for applications in mature waterfloods. Depending upon the perspective of investors, the decision to proceed with an oil field EOR process may depend upon projected: rate of return, return of investment, $/bbl of injected reserves and cumulative cash flow [13].

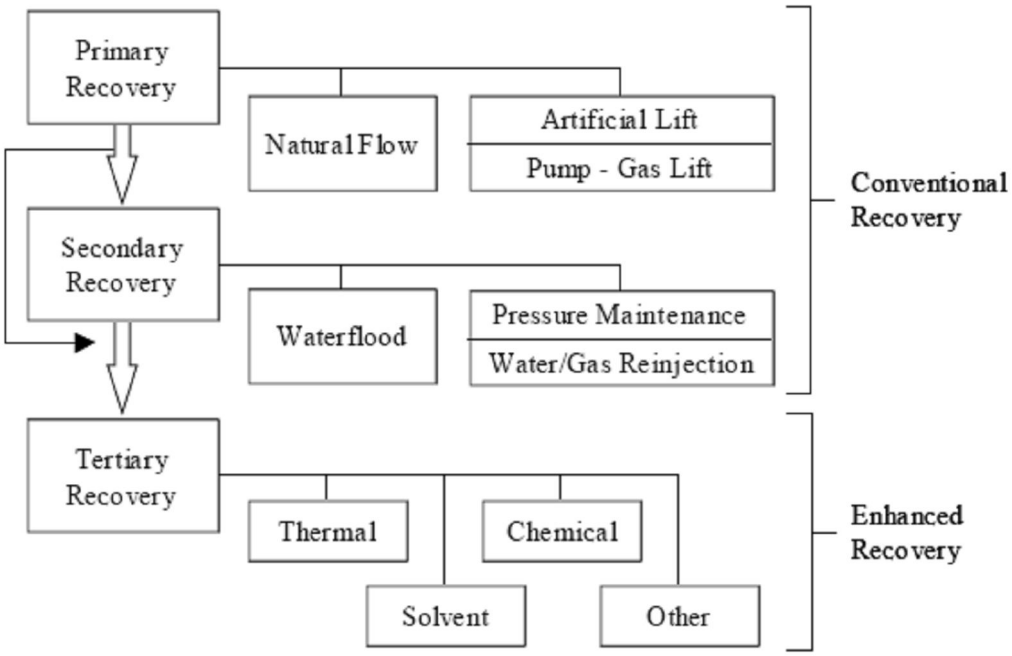

Figure 4-1 - Oil recovery classifications (from Oil&Gas Journal biennial surveys)

4.1. IMPROVED RECOVERY TECNIQUES

In the last decade, the term "Improved Oil Recovery" (IOR) has been used interchangeably with EOR or even in place of it. Although there is not exact definition, IOR typically refers to any process or practice that improves oil recovery.

IOR includes EOR, but also regards other practices, like waterflooding and pressure maintenance.

4.1.1.WATERFLOODING

Waterflooding consists of injecting water into the reservoir.

It is the most widely used post-primary recovery method. Water can be injected along the periphery of the reservoir or along specific patterns.

It is conceived to use the water drive to displace part of the oil remaining in the reservoir after the natural depletion.

Furth more, injecting water helps in maintaining high the reservoir pressure, supporting the pressure difference-based recovery.

The use of waterfloding has little results in presence of high-viscosity oil. In this case the water has a high mobility and it bypasses the oil in the reservoir, without mobilizing it.

When the reservoir has a fractured structure, with rock matrixes surrounded by channels, the water has the tendency to flow only in the fractures, bypassing the rock and the most of the reservoir, giving a very little oil recovery.

For these reasons waterflooding is not recommended with an oil viscosity higher than 30 cP and with fractured reservoirs.

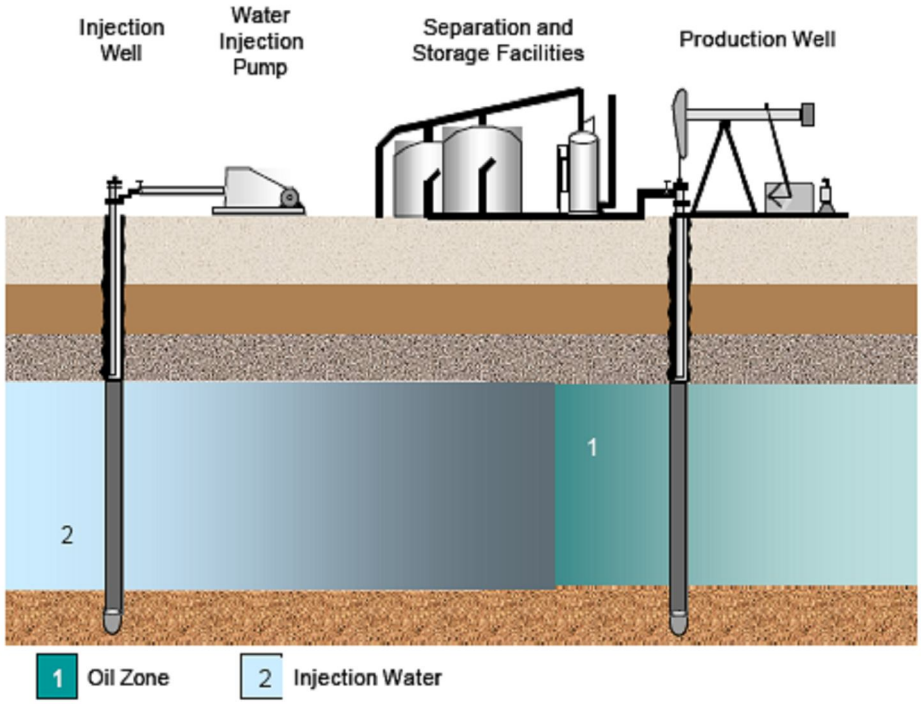

Figure 4-2 - sketch of a waterflooding process (Class Notes for PETE 609 – Module 1- Dr. Maria Antonieta Barrufet – Fall, 2001)

4.2. Enhanced Oil Recovery

EOR processes include all methods that use, to recover oil, injection of materials not normally present in the reservoir [11].

This definition covers all modes of oil recovery processes and most of oil recovery agents.

The definition given above excludes waterflooding, but is intended to exclude all pressure maintenance processes. Moreover, agents such as methane, in high pressure gas drive, or carbon dioxide, in a reservoir with initial presence of CO_2, do not satisfy the definition, yet both are clearly EOR processes.

EOR techniques include:

- Thermal methods, like steam stimulation

- Miscible methods, like hydrocarbon gas, CO_2, N_2 injection
- Chemical methods. These are polymer, surfactant, caustic and micellar/polymer flooding.

The target of any EOR process is to mobilize the remaining oil that is the amount unrecoverable by conventional means [12].

This is achieved by enhancing oil displacement and volumetric sweep efficiency.

Oil displacement efficiency is improved by reducing oil viscosity (thermal floods), or reducing capillary forces or interfacial tension between phases (miscible floods).

Volumetric sweep efficiency is improved by developing a more favourable mobility ratio between the injected fluid and the oil to mobilize (polymer floods).

4.2.1.Improved Waterflooding Processes

Improved waterflooding processes consist in changing the properties of the brine used by adding some chemicals.

The target of these chemicals is to increase the water viscosity to improve mobility ratios, or to lower the IFT between oil and water by using surfactants, or a combination of both.

Polymer Flooding

Polymer flooding consists of adding polymer to the water of a waterflood to decrease its mobility.

The resulting increase in viscosity, as well as a decrease in aqueous phase permeability that occurs with some polymers, causes a lower mobility ratio.

This lowering increases the efficiency of the waterflood through greater volumetric sweep efficiency and lower swept-zone oil saturation. Irreducible oil saturation does not decrease although the remain saturation does. The greater recovery efficiency constitutes the economic incentive for polymer flooding when applicable.

Generally, a polymer flood will be economic only when the waterflood mobility ratio is high, the reservoir heterogeneity is high, or a combination of these two occurs [14].

Micellar-polymer flooding

Any immiscible displacement leaves oil behind, trapped. This trapping can be expressed as a competition between viscous forces, which mobilize the oil, and capillary forces, which trap the oil.

The dimensionless ratio of viscous to capillary forces is expressed by the capillary number:

$$N_c = \frac{k \cdot |\nabla P_w|}{\sigma}$$

Equation 4-1

Where:

K: absolute permeability of rock $[L^2]$

∇P_w: gradient of pressure $[F/L^3]$

σ: interfacial tension $[F/L]$

This is the most general definition of capillary number [14].

To lower the residual oil saturation, a very low IFT, around 1 mN/m, is required, and it is reached using surface-active chemicals, or surfactants.

Micellar flooding consists of injecting a slug that contains water, surfactant,

electrolyte (salt), usually a co-solvent (alcohol), and possibly a hydrocarbon (oil), followed by polymer-thickened water.

The surfactant injected lowers the interfacial tension (IFT) between oil and water, and thereby recovers the residual oil that normally remains after water flood.

Lowering interfacial tension the capillary forces are reduced, aiding the recovery of oil.

SURFACTANTS USED:

A typical surfactant monomer is composed of a polar (hydrophilic) portion, and a nonpolar (lypophilic) portion. The entire monomer is sometimes called amphiphile because of this dual nature.

Surfactants are classified in 4 groups based on their polar groups. These are:

- Anionics: The monomer is associated with an inorganic metal (a cation, which is usually sodium). In an aqueous solution the molecule dissociates into free cations (positively charged), and the anionic monomer (negatively charged). The solution is electroneutral, which means positive and negative charges balance. Anionic surfactants are the most common in MP flooding because they are good surfactants, relatively resistant to retention, stable, and can be made relatively cheap.
- Cationic: In this case the surfactant molecule contains a an inorganic anion to balance the charge. In solution it ionizes into a positively charged monomer, and the anion. Cationic surfactants are highly adsorbed by clays and therefore have not much use in MP flooding.

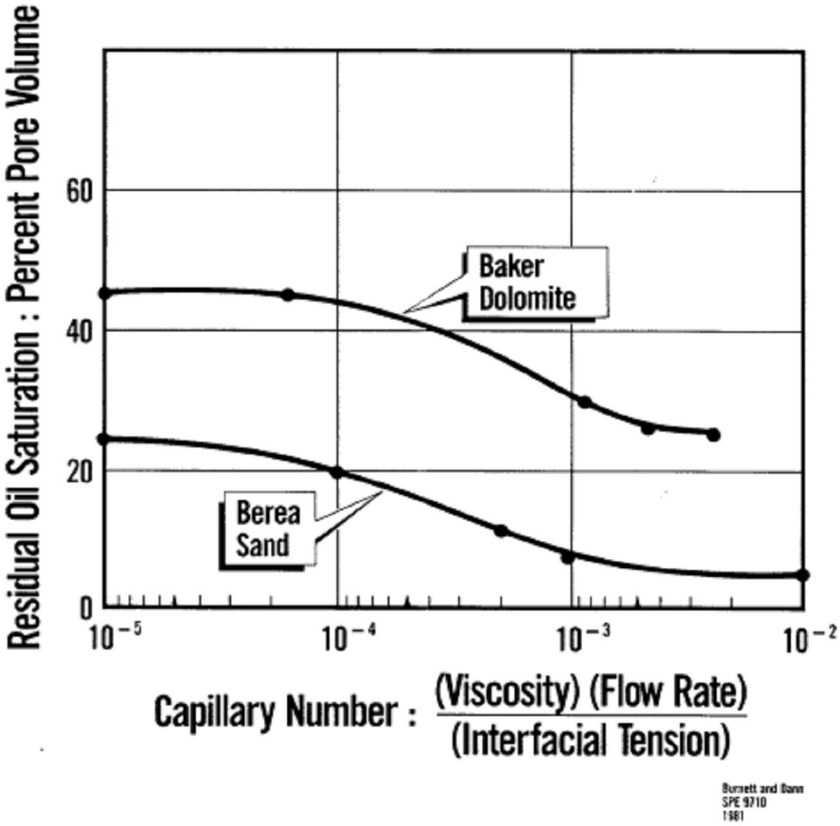

Figure 4-3 – Residual oil saturation as a function of Capillary number and rock type

- Non-ionic: This class of surfactant does not have ionic bonds, but when dissolved in aqueous solutions, exhibits surfactant properties mainly by electronegativity contrasts among its constituents. Non-anionic surfactants are much more tolerant to high salinities than anionic, but they are poorer surfactants. The non-ionic surfactants are used extensively in MP floods mainly as co-surfactants.
- Amphoteric: This class of surfactant has not been used in oil recovery. They contain aspects of two or more of the previous classifications.

The success of a MP flooding process depends upon meeting certain criteria.

First, the surfactant slug must be propagated in its interfacial active mode. This is accomplished through the chemical formulation steps.

Second, the amount of surfactant injected must be enough to overcome the retention by the porous media [14]. This is accomplished by using some sacrificial agents, scale-up studies, laboratory experiments, and numerical simulation.

Third, the MP displacement must be designed such that dissipation due to dispersion and channeling are minimized.

CRITICAL MICELLE CONCENTRATION

If an anionic surfactant is dissolved in an aqueous solution the surfactant dissociates into a cation and a monomer. If the surfactant concentration is increased, the lypophilic portions (moieties) of the surfactant begin to cluster among themselves to form aggregates, or micelles, containing several monomers each. A plot of the surfactant monomer concentration versus the total surfactant concentration, as indicated in Figure 4-, shows a curve that begins at the origin, increases monotonically with init slope, then levels off at the so called critical micelle concentration CMC. Above the CMC, all further increases in surfactant concentration cause increases in the micelle concentration only.

CMC's are typically small, and the surfactant in oil applications is in the micellar state.

That is the reason of the name Micellar flooding. Typical CMC values are 10-5 – 10-4 kg-mol/m3. And the size of the micelles is 10-4 to 10-6 mm.

When the surfactant solution contacts an oleic phase, the surfactant tends to accumulate at the interface. The lypophilic tail "dissolves" in the oil phase, and the hydrophilic end "dissolves" in the aqueous phase. The surfactant prefers the interface over the micelle. Now it becomes clear the purpose of the dual nature of the surfactant since its accumulation at the interface will lower the IFT between the oleic and the aqueous phase. This interface blurs in the same manner as do interfaces in vapour-liquid-equilibrium (VLE) near a critical point. We need to design the surfactant to maximize the solubility in this interface, however brines affect greatly the surfactant behaviour. Therefore we need to analyze the interactions surfactant-oil-brine. Depending on the salinity, micelles may form either with water or oil as the external phase.

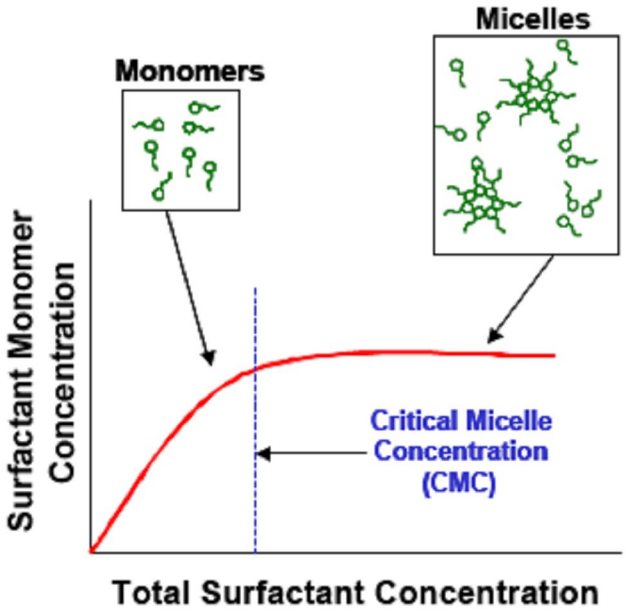

Figure 4-4 - Surfactant monomer concentration versus total surfactant concentration

Alkaline Flooding

Alkaline flooding is a high pH chemical EOR method which has many similarities with micellar flooding. The difference is that in micellar flooding the surfactant is injected; while in alkaline (or caustic) flooding the surfactant is generated in situ.

High pH's indicates large concentrations of the hydroxide anions OH^- .

OH- by itself is not a surfactant since the absence of a lypophilic tail makes it exclusively water soluble. However, if the oil contains acidic hydrocarbon components (HAo), some of it may partition into the aqueous phase.

We assume that the acid species in the oil is represented by a generic single component named HAo. This acid component will not be soluble in an aqueous phase with neutral pH (i.e., 7). However if the pH is increased with a caustic solution the acid will be extracted from the oil to the aqueous phase.

The exact nature of the acidic component is unknown, but it is probably highly dependent on the crude oil type. The deficiency of protons (high PH) in the aqueous phase will promote the chemical reactions of acid dissociation to the right:

$$HA_O = H^+ + A^-$$

The anionic species A^- is a surfactant with many of the properties described in MP flooding [14].

If no acidic species are present in the crude, no surfactant can be generated.

4.2.2.Miscible Gas Flooding (CO2 Injection)

CO_2 flooding consists of injecting large quantities of CO_2 (15% or more hydrocarbon pore volumes) in the reservoir to form a miscible flood.

CO_2 extracts the light-to-intermediate components from the oil, and, if the pressure is high enough, develops miscibility to displace oil from the reservoir (vaporizing gas drive).

If the viscosity of CO_2 is low, it results in poor mobility control.

There can be also problems if a early breakthrough of CO_2 happens, and there can be corrosion phenomena in the producing wells.

Furthmore, CO_2 produced needs to be separated from sellable hydrocarbons.

4.2.3.Miscible Gas Flooding (Hydrocarbon Injection)

Hydrocarbon gas flooding consists of injecting light hydrocarbons through the reservoir to form a miscible flood.

It uses as mechanism of recovery the viscosity reduction, the oil swelling and the condensing or vaporizing gas drive.

Minimum depth is set by the pressure needed to maintain the generated miscibility. The required pressure ranges from about 1,200 psi for the LPG process to 3,000-5,000 psi for the High Pressure Gas Drive, depending on the oil [14].

If the horizontal sweep efficiency is poor, viscous fingering results.

In addition to this problem, large quantities of expensive products are required.

4.2.4.Nitrogen / Flue Gas Flooding

Nitrogen or flue gas injection consists of injecting large quantities of gas that may be miscible or immiscible depending on the pressure and oil composition. Large volumes may be injected, because of the low cost.

Nitrogen or flue gas are also considered for use as chase gases in hydrocarbon- miscible and CO2 floods.

Nitrogen flooding vaporizes the lighter components of the crude oil and generates miscibility if the pressure is high enough. In addition it provides a gas drive where a significant portion of the reservoir volume is filled with low-cost gases.

Miscibility can only be achieved with light oils at high pressures; therefore, deep reservoirs are needed.

A steeply dipping reservoir is desired to permit gravity stabilization of the displacement, which has a very unfavorable mobility ratio.

4.2.5.Thermal (Steamflooding)

Steamflooding consists of injecting ±80% quality steam to displace oil. Normal practice is to precede and accompany the steam drive by a cyclic steam stimulation of the producing wells (called huff and puff).

Injecting steam adds energy and increase the temperature of the oil in the reservoir. As a result, the viscosity decreases. The injection supplies also pressure to drive oil to the producing wells.

It is applicable to viscous oils in massive, high permeability sandstones or unconsolidated sands.

Oil saturations must be high, and pay zones should be > 20 feet thick to minimize heat losses to adjacent formations. Less viscous crude oils can be steamflooded if they don't respond to water.

Steamflooded reservoirs should be as shallow as possible, because of excessive wellbore heat losses.

Since about one third of the additional oil recovered is consumed to generate the required steam, the cost per incremental barrel of oil is high.

5. SCREENING STUDIES

With the increasing importance of new improved hydrocarbon recovery techniques, it is vital to develop the necessary tools and methodologies required to effectively screen and prioritize assets for IOR opportunities.

In addition to merely identifying the most appropriate IOR process, it is of equal importance to be able to predict reservoir performance of an IOR project.

The IOR evaluation workflow is usually divided in steps (Dickson, Dios, Wylie, [15]). The first step is to identify the most promising injection type and processes for a given reservoir and to complete preliminary screening economics to ensure feasibility. The initial screening step is followed by a more in-depth investigation, including laboratory studies on reservoir's cores and mechanistic simulations.

The simulations are first performed to fit the laboratory results from the core studies, in order to determine several reservoir properties, like the relative permeabilities.

Afterwards, simulations are conducted to study the behaviour of the reservoir segment on which the IOR process is intended to be run.

When a proposed project demonstrates potential for field implementations, pilot tests may be conducted to resolve any key uncertainties [16] (Figure 5-1 and Figure 5-2).

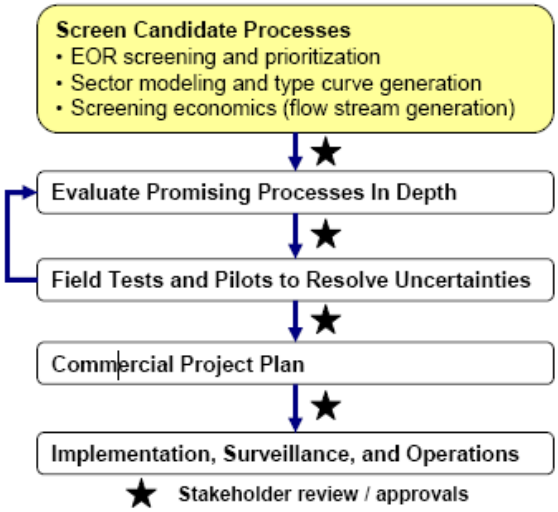

Figure 5-1 – ExxonMobil's IOR evaluation workflow (adapted from Selamat et al. 2008 [16])

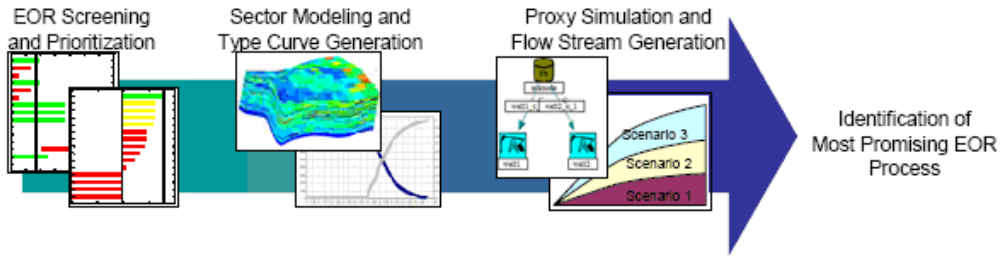

Fig 2–IHR screening workflow.

Figure 5-2 – IOR screening workflow

5.1. Screening criteria

Screening criteria for various recovery techniques can be compiled, and are presented below.

These criteria are a combination of literature values and values gained after successful recovery experiences.

5.1.1.Waterflooding

- Oil saturation > 50%
- Oil viscosity < 2000 cP
- Oil mobility > 0.1 mD/cP
- Current water oil ratio < 10%

Poor compatibility between the injected water and the reservoir may cause formation damage.

5.1.2.Polymer flooding

- Oil saturation > 10% of pore volume
- Oil viscosity < 200 cP
- Permeability > 50 mD to prevent plugging
- Water salinity < 100000 ppm
- Temperature < 350 K to avoid degradation

Lower injectivity than with water can adversely affect oil production rates in the early stages of the polymer flood.

5.1.3.Surfactant flooding

- Oil saturation > 20%
- Reservoir temperature < 70 °C
- Oil viscosity < 150 cP
- Water salinity < 50000 ppm

Furthmore, there must not be any gas cap in the reservoir, neither bottom water or an active water drive. The clay content must be low.

5.1.4.Alkali – surfactant flooding

- Oil saturation > 35%
- Oil viscosity < 150 cP
- Water salinity < 50000 ppm
- Acid number > 0.1 mg KOH/g

The best performance is obtained with sandfstone reservoirs, with no anhydride or gypsum present, and with minimal amounts of clay and shale.

5.1.5.Carbon dioxide miscible gas injection

- Oil saturation > 25%
- Oil viscosity < 10 cP
- Oil gravity > 22° API (oil density < 920 Kg/m^3)

The low oil viscosity is required to avoid problems of early breakthrough of CO_2, which can cause problems and corrosion in the producing wells.

5.1.6.Steam flooding

- Net thickness > 20 feet
- Oil saturation > 40-50% of PV
- Reservoir pressure < 1500 psi
- Permeability > 200 mD

Oil saturations must be high, and pay zones should be greater than 20 feet thick to minimize heat losses to adjacent formations.

Steamflooded reservoirs should be as shallow as possible, because of excessive wellbore heat losses.

5.2. CASE STUDY: RESERVOIR IN NORTH AFRICA

The objective of this work is to study the possibilities of implementing an EOR technique in an oil reservoir, situated in North Africa.

The characteristics of the reservoir are:

- Permeability: variable, depending upon the rock layer and the position in the reservoir. Most of values are between 200 and 100 mD
- Oil viscosity: 23 cP. It's an high-viscosity oil
- Reservoir temperature: 77 °C
- Salinity of reservoir water: 72 g/l, comprehensive of 2000 ppm Ca^{2+} ions and 600 ppm Mg^{2+} ions.
- Porosity: around 20%
- Acid number of oil : 1.9 mg/g of KOH

The use of the screening criteria and the experimental activity enabled to reach some conclusions about the best techniques available to enhance the oil production.

- The high acid number of the oil highlights its high ability of forming natural surfactants in situ, through an alkaline treatment. So an alkaline flooding could be performed. The high presence of divalent ions (Ca^{2+} and Mg^{2+}) in the formation water, however, makes an alkaline flooding unfeasible, since it would cause the precipitation of calcium and magnesium salts.
- The high hardness present in injection and formation water severely limited the performance of classical surfactants.
- The high temperature of the reservoir could cause the problem to the surfactants. They could be made unstable.
- A waterflood can be implemented, but there are concerns, including: viscous fingering through viscous oil zone, injection water may channel into the water leg, bypassing oil.

The use of a polymer, from a first analysis, results to be the most compatible with the reservoir properties and the most promising. The polymer solution viscosity corrects the poor water/oil mobility ratio responsible for conformance control issues leading to poor waterflood performance on intermediate heavy oils.

6. POLYMER FLOODING

Polymer flooding consists of adding polymer to the water of a waterflood to decrease its mobility. Adding a polymer leads to an increase in viscosity, as well as to a decrease in aqueous phase permeability and a lower mobility ratio.

The remaining oil saturation decreases, due to the increased efficiency of the waterflood, even if the irreducible oil saturation is not affected by this technique [17].

The polymer is used not only to affect the mobility of the injected solution, but also to plug high conductivity zones, that can be near the wells as well as deep in the reservoir.

Polymer injection sequence consists of: a preflush with low-salinity brine; the polymer solution itself; a freshwater buffer to protect the polymer solution from backside dilution; and, finally, drive water.

Since the water used in the injection is usually a dilution of an oil-field brine, interactions with salinity are important, particularly for certain classes of polymers.

Salinity is the total dissolved solids (TDS) content of the aqueous phase. All chemical flooding properties depend on the concentration of specific ions rather than salinity only. In particular the total divalent cation content, also called *hardness*, is critical to the chemical flood properties.

6.1. Chemistry of the polymers

The most used commercially polymers for EOR techniques fall into the class of polyacrylamides.

The monomeric unit is the acrylamide molecule is shown in Figure 6-1. As used in the polymer flooding, polyacrylamides have undergone partial hydrolysis, which causes anionic (negatively charged) carboxyl groups (COO^-) to be scattered along the backbone chain (Figure 6-2). For this reason the polymers are called “Partially Hydrolized PolyacrylAMide” (HPAM). Typical degrees of hydrolysis are between 15% and 40% (Levitt, Pope [18]).

The hydrolysis makes the molecule negatively charged, which accounts for many of its physical properties. Water solubility, viscosity and retention of polymer are optimized through the selection of the degree of hydrolysis. If it is too small, the polymer will not be water soluble. If it is too large, its properties will be too sensitive to salinity and hardness.

The anionic repulsion between carboxyl groups increases the hydrodynamic radius[1] of the polymer molecules and hence accentuates the solution viscosity. The repulsion is both between polymer molecules and segments on the same molecule. It accentuates the mobility reduction, since the molecules in solution elongate and snag on others similarly elongated.

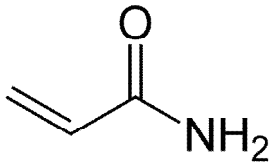

Figure 6-1 – Acrylamide molecule

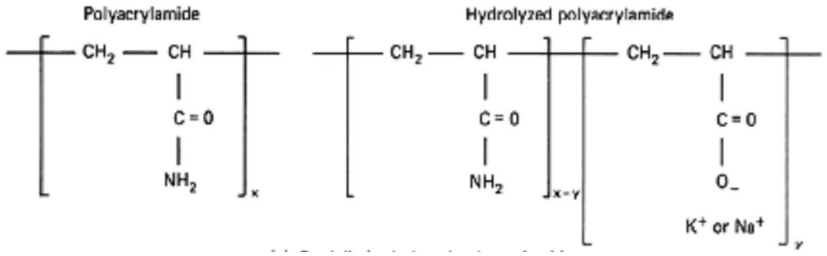

Figure 6-2 – Partially Hydrolized polyacrylamide

If the brine salinity is high, the repulsion is greatly decreased through ionic shielding and the freely rotating carbon-carbon bonds allow the molecule to coil up (

Figure 6-3). As a result, the effectiveness of the polymer solution is greatly decreased [17].

[1] The hydrodynamic radius of a polymer molecule is also known as radius of gyration. It is difficult to experimentally determine this parameter. However, a theoretical expression has been proposed: the Flory- Fox equation:

$$\Omega_P = \left[\frac{[\mu]\cdot M}{\Phi}\right]^{1/3}$$

Where Ω_P is the hydrodynamic radius of polymer molecule and Φ is a universal constant.

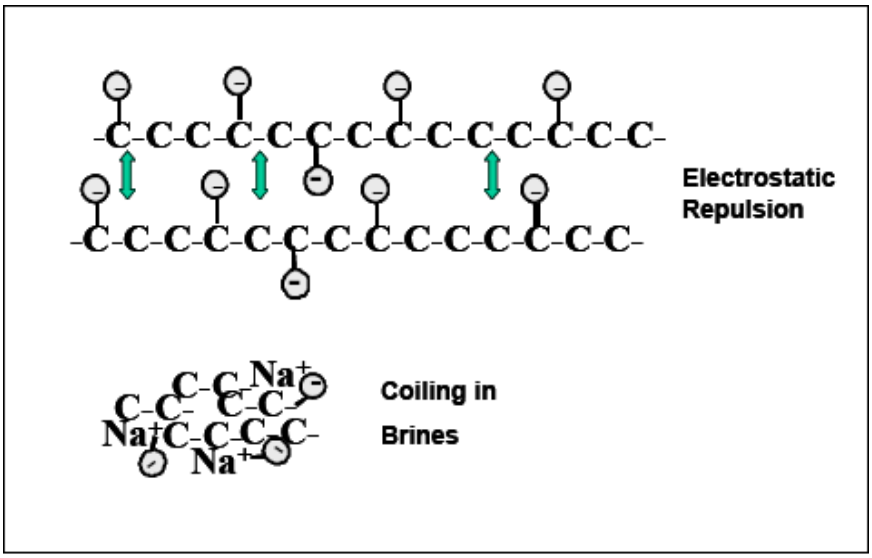

Figure 6-3 – Shielding effect, causing the coiling up of the polymer molecules

6.2. Properties of the polymers

6.2.1.Viscosity relations

The molecular weight is a very important characteristic of polymers, since it determines the viscosifying potential.

The viscosity of a solution of brine containing the polymer can be modeled using the Flory-Huggins equation:

$$\mu_{aq}^{I} = \mu_{aq} \cdot \left[1 + a_1 \cdot C_{pol} + a_2 \cdot C_{pol}{}^{2} + a_3 \cdot C_{pol}{}^{3} + \ldots\right]$$

Equation 6-1 – Flory-Huggins equation

Where C_{pol} is the polymer concentration in the aqueous phase, usually expressed in g/m^3 of solution, which is approximately the same as ppm; μ_{aq} is the brine viscosity; a_1, a_2 and so on are constants.

The linear term in the equation accounts for the dilute range, where polymer molecules act independently. The equation can be truncated at the cubic term for most purposes.

To measure the thickening power of the polymer is possible to rely on the intrinsic viscosity, defined as:

$$[\mu] = \lim_{Cpol \to 0} \left[\frac{\mu_{aq}^{I} - \mu_{aq}}{\mu_{aq} \cdot C_{pol}} \right]$$

Equation 6-2 – Intrinsic viscosity

Intrinsic viscosity is the same as a_1 term in Equation 6-2.

6.2.2. Non-Newtonian effects

Shear rate, $\dot{\gamma}$, is the velocity gradient measured across the diameter of a fluid-flow channel, be it a pipe, annulus or other shape. It is the rate of change of velocity at which one layer of fluid passes over an adjacent layer.

It is defined as:

$$\dot{\gamma} = \frac{v}{h}$$ **Equation 6-3 – definition of shear rate**

At low shear rates, the viscosity of the solution is independent from $\dot{\gamma}$, showing a Newtonian behavior. At higher $\dot{\gamma}$, μ_{aq}^{I} decreases, approaching a limiting value, μ_{aq}^{∞}, value not much greater than the water viscosity.

This type of behavior, with the viscosity decreasing while the shear rate is increasing, is called *shear thinning*. It is physically caused by the uncoiling and unsnagging of the polymer chains when they are elongated in shear flow.

This behavior is favorable: for the bulk of a reservoir's volume, $\dot{\gamma}$ is usually low, making it possible to obtain a favorable mobility ratio with a minimum amount of polymer. But near the injection wells, $\dot{\gamma}$ can be quite high, lowering the viscosity and decreasing the pressure needed for the injection.

The relationship between polymer-solution viscosity and shear rate may be described by the Meter model:

$$\mu_{aq}^{I} = \mu_{aq}^{\infty} + \frac{\mu_{aq}^{0} - \mu_{aq}^{\infty}}{1 + \left(\frac{\dot{\gamma}}{\dot{\gamma}_{1/2}} \right)^{n_M - 1}}$$

Equation 6-4 – Meter and Bird equation

Where n_M is an empirical coefficient, $\dot{\gamma}_{1/2}$ is the shear rate at which the viscosity is an average between μ_{aq}^{0} and μ_{aq}^{∞} [2].

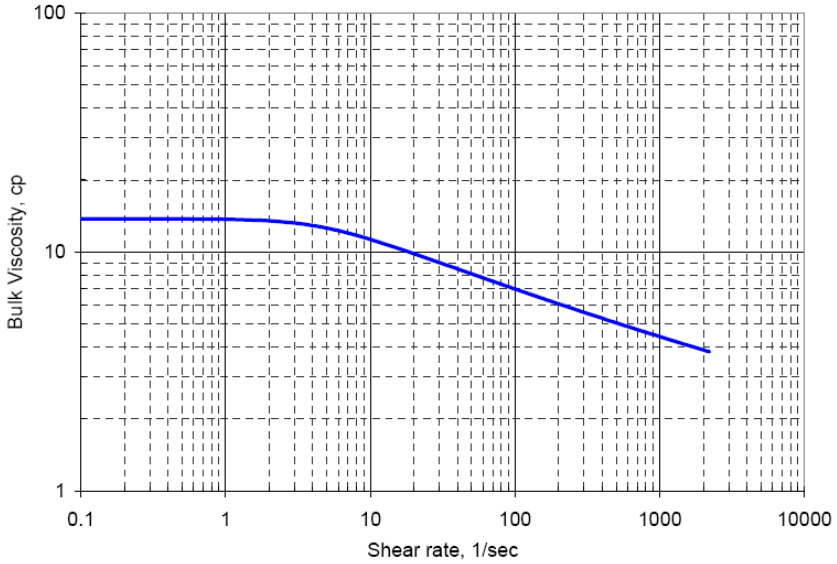

Figure 6-4 – Schematic of shear rate dependence of polymer bulk or shear viscosity

6.2.3.Retention

All polymers experience retention in permeable media because of adsorption onto solid surfaces or trapping within small pores. This phenomenon depends upon polymer type, molecular weight, rock composition, brine salinity, brine hardness, flow rate and temperature.

It causes the loss of polymer from solution, which can lead to lose the mobility control effect.

It is usually expressed as mass of polymer per mass of rock.

It can be represented with a Langmuir-type isotherm:

$$C_{pol-ads} = \frac{a_4 \cdot C_{pol}}{1 + b_4 \cdot C_{pol}}$$

Equation 6-5 – Concentration of adsorbed polymer

a_4 and b_4 are adsorption parameters typical of the polymer.

Considering the anionic character of water-soluble polymers, the mechanism governing the adsorption is chemical. In fact, polymer adsorption increases with increasing salinity and hardness [17].

6.2.4.Inaccessible Pore Volume

Inaccessible pore volume is an effect consisting in the acceleration of the polymer solution through the permeable medium. It can happen because the smaller portions of the pore space will not allow polymer molecules to enter because of their size. Thus a portion of the total pore space is inaccessible, and this accelerates the flux. Furth more, in water-wet reservoirs, the smallest pores does not contain oil to displace, but only connate water.

A wall exclusion effect can also play a role: the polymer fluid layer near the pore wall has a lower viscosity than the fluid in the center, which causes an apparent fluid slip.

IPV depends on polymer molecular weight, permeability, porosity and pore size distribution [17].

6.2.5.Permeability reduction

The total mobility lowering contribution of a polymer is measured by the *resistance factor,* R_F. It is the ratio of the mobility of brine to that of a single-phase polymer solution flowing under the same conditions.

$$R_F = \frac{\lambda_{aq}}{\lambda_{aq}^I} = \left(\frac{k_{aq}}{\mu_{aq}}\right) \cdot \left(\frac{\mu_{aq}^I}{k_{aq}^I}\right)$$

Equation 6-6 – Resistance factor

For the polymers based on HPAM structure, mobility is reduced also by a permeability reduction, in addition to the viscosity increase.

The *permeability reduction factor*, R_K, is defined as:

$$R_k = \frac{k_{aq}}{k_{aq}^I}$$

Equation 6-7 – Permeability reduction factor

Finally, it is possible to define the *residual resistance factor,* R_{RF}, which is the ratio of the mobilities of a brine solution before and after (λ_{aq}^1) polymer injection;

$$R_{RF} = \frac{\lambda_{aq}}{\lambda_{aq}^1}$$

Equation 6-8 – Residual resistance factor

R_{RF} indicates the permanence of the permeability reduction effect caused by the polymer solution. R_k and R_{RF} are nearly equal for the most of cases, while R_F is much larger, since it contains both the viscosity enhancing and the permeability-reducing effect [19].

Polymers that have undergone even a small amount of mechanical degradation seem to lose most of their permeability reduction effect. For this reason R_k is difficult to control, being sensitive to even small deteriorations in the polymer quality.

Thank to the permeability reduction, it is possible to achieve the mobility control with less polymer.

6.2.6.Mechanical Degradation

All polymers mechanically degrade when they are exposed to high-velocity flows, which can be present both in surface equipment as in downhole conditions.

HPAM polymers are most susceptible to mechanical degradation, particularly if the salinity or hardness of the brine is high. Elongational and shear stresses are both destructive to polymer solutions. Mechanical degradation usually begins for shear rates near the value of minimum-viscosity shear rate.

6.2.7.Chemical Degradation

The residence time in a reservoir is typical very long, so degradation reactions, even the slow ones, are potentially dangerous. At very low or high pH, especially at high temperatures, degradation will be significant.

In the case of HPAM, hydrolysis reactions can occur, increasing the degree of hydrolysis (τ) selected initially for the product. This will increase the sensitivity to hardness (Figure 6-5). Furth more, molecules with a high degree of hydrolization can give precipitation in presence of divalent ions of calcium [20].

During hydrolysis the acrylamide (AM) moieties are converted to acrylic acid sites or its salt, the acrylate (AA).

At high salinity, the acrylate moieties on HPAM are strongly associated with cations, and the viscosity approaches that of non-hydrolyzed polyacrylamide. If τ exceeds approximately 0.33 (Zaitoun and Potie, 1983, [20]) the precipitation is possible.

The kinetics of hydrolysis is a strong function of pH. It is a combination of acid and basic mechanisms and neighbor effects. The rate is lowest at neutral pH and increases linearly as pH rises or falls.

Also oxidation reactions can happen. Therefore, oxygen scavengers and antioxidants are often added to prevent or retard them.

High temperatures in the reservoir can lead to a radical induced breakdown of the acrylic backbone, resulting in molecular weight reduction. This phenomenon is usually referred to as "*Thermal degradation*".

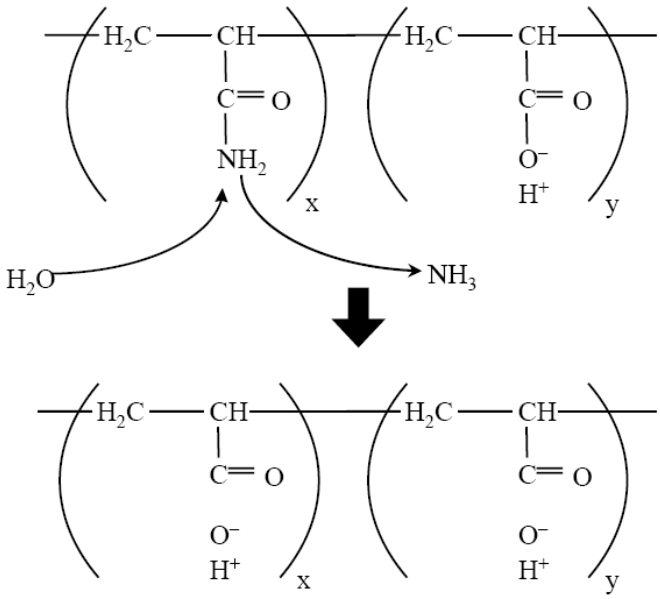

Figure 6-5 – Advancement of hydrolysis reaction

6.2.8.Requirements for EOR polymers

1. Good thickening: high mobility reduction per unit cost
2. High water solubility.
3. Low retention: less than 20 μg/g rock
4. Shear stability: the molecule must not break apart when is subjected to stress
5. Chemical stability.
6. Biological stability.
7. Good transport in permeable media. Ability to propagate the polymer through the rock intact and without excessive plugging or pressure drop [18].

6.3. Choice of the polymer for the case study in North Africa

Several researches have examined the possibilities of modifying the structure of HPAM to improve chemical stability or viscosity in presence of salt, by adding, for example, co monomers.

This may be achieved either by reducing the extent of hydrolysis or by finding other ways to increase the viscosity, to negate the reduction of hydrodynamic radius due to shielding by cations.

A solution consists in substituting some of the acrylate moieties with another anionic monomer more resistant to cation shielding and precipitation, and which may also stabilize neighboring acrylamide moieties [21].

The monomer chosen is the 2-acrylamid-2-methylpropane sulfonate (AMPS). The result is a terpolymer of AMPS, AA and AM (Figure 6-6). The molar fraction of AMPS moieties on a polymer is represented by the symbol σ.

Using this solution, it is possible to obtain the same anionicity of HPAM, with a lower proportion of amide groups hydrolyzed.

The calcium tolerance, as a strong function of the degree of hydrolysis, is greatly increased by the presence of AMPS moieties (Levitt and Pope, 2008, [18]) (Figure 6-7).

Poly(AM-co-AMPS) is desirable in situations where 200 ppm or more of divalent ions will be present and moderate or extensive hydrolysis is expected. This is the case of the reservoir considered, which is characterized by a 2000 ppm concentration of Ca^{2+} ions and 600 ppm of Mg^{2+} ions.

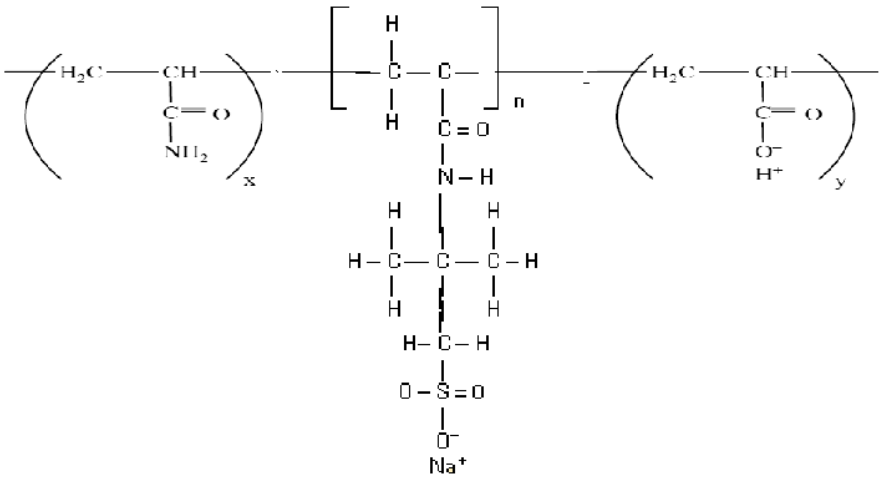

Figure 6-6 – Poly(Am-co-AMPS), AN-125

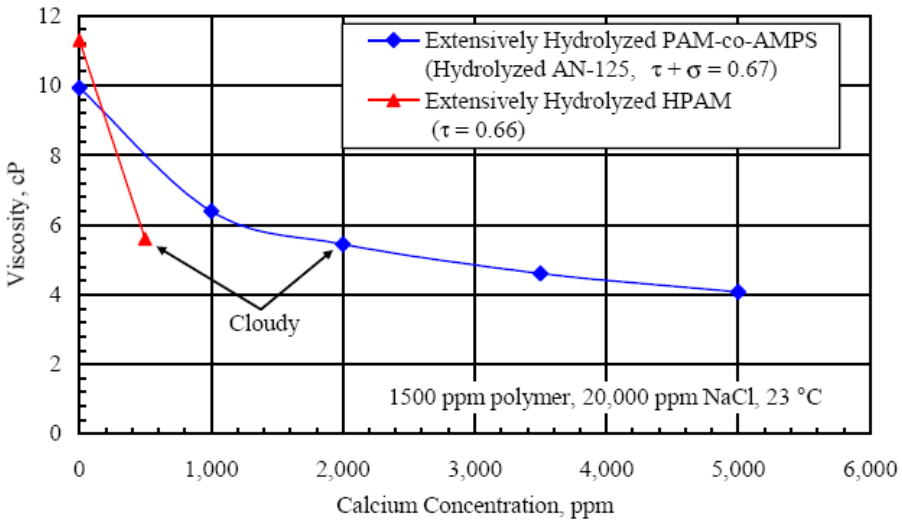

Figure 6-7 – Effect of the presence of 20-30% AMPS moieties on the calcium tolerance of extensively hydrolyzed polymers, 23°C (Levitt and Pope, 2008)

After a preliminary screening, the polymer chosen for enhanced waterflooding was AN-125, a co-polymer of acrylamide, acrylate and AMPS moieties. AN 125 is also the lowest molecular weight compound so it is expected to have the most favourable behaviour as far as retention on porous rock is concerned.

7. INVESTIGATION THROUGH LABORATORY MATCHES

After a preliminary study, in which the overall properties of the reservoir are taken into consideration, a more in-depth analysis is performed.

The aim is to find out parameters regarding the rock properties, like oil-water relative permeabilies. Another relevant issue to analyze within the water injection studies is the compatibility between the water that will be injected and the reservoir water.

To do this, reservoir samples are needed to perform experimental analysis.

The reservoir samples used belong to two typologies: cores and sandpacks.

A core is a cylindrical sample of geologic formation, usually reservoir rock, taken during or after drilling a well. Cores can be full-diameter cores (that is, they are nearly as large in diameter as the drill bit) taken at the time of drilling the zone, or sidewall cores (generally less than 1 in. [2.5 cm] in diameter) taken after a hole has been drilled.

Sandpacks are made with sands and materials taken from the formation. The rock from the formation is finely crushed and crumbled, to obtain thin sand. The sand is poured in a core-holder, which is fully filled at a time and vibrated for about one hour. The aim is to obtain a packed core which should have the same characteristics of the reservoir rock.

Usually the main analysis consists in waterflooding conducted upon the samples. It allows to perform on a smaller scale the same action that can be run upon the reservoir, and observe the possible results.

Coreflooding tests are performed to determinate the recovery factor and permit to analyze the viscous forces equilibrium during the displacement, to calculate the sweep efficiency and the microscopic displacement efficiency.

Water injection coreflooding tests are furthermore performed to compare the recovery factor of waterflooding with different techniques of enhanced oil recovery for secondary or tertiary recovery.

After the experimental step, simulations are conducted, which reproduce the conditions of the experiments. The aim is to find the correct properties of the formation. The properties to find are included in the simulations, and if the result matches correctly the results from the laboratory, it means that the properties used are the right ones [22].

For the simulation step specific finite-difference programs are used.

7.1. Conduction of the experiments

7.1.1.Brine preparation

As first step, the synthetic brine, with the same properties of the formation brine of the reservoir studied, has to be prepared.

Below are listed the chemical properties of the formation water present in the field studied:

		Formation water	Injection water
salinity (as NaCl)	mg/L	63400	71600
sodium	"	23200	24500
potassium	"	614	754
lithium	"	3.5	3.6
calcium	"	1930	3890
magnesium	"	586	739
barium	"	0.9	0.6
strontium	"	8.20	10
iron	"	57	58
manganese	"	0.6	1.5
silicon dioxide	"	25	16
chloride	"	38400	43400
sulphate	"	533	690
bromide	"	161	177
formate	"	<15	< 15
acetate	"	< 15	< 15
propionate	"	<15	< 15
butyrate	"	<15	< 15
alkalinity (as HCO_3)	"	241	167
pH		7.00	6.57

Table 7-1 – Analysis formation water and injection water

The synthetic brine has been prepared scaling 64.5 g of NaCl and 14.1 g of $CaCl_2.2H_2O$, and adding demineralized water until 1 liter volume was reached.

The brine obtained has a 72 g/l total salinity and a 3840 ppm concentration of Ca^{2+}. Its pH is 6.91.

7.1.2.Polymer preparation

Proper polymer solubilization in brine is a task that must be carefully accomplished. Polymer hydration can be a lengthy process due to the very high polymer molecular weight (ranging from 2 to 20 million Dalton). Incomplete dissolution, caused by a wrong hydratation procedure, can lead to loss of product and to low performance solutions [23].

Hydrolyzed polyacrylamide (HPAM) and AMPS co-polymer solutions are prepared from powder form of the polymer. The powder must be kept out of contact from moisture. The dry form of polymer may absorb water if not stored in a dry environment and consequently can make accurate polymer concentrations difficult to prepare.

Polymer solutions were prepared as follows:

• Polymer powder was slowly added to the synthetic brine under magnetic stirring.

• The solution was let hydrate properly for 8 hours under weak stirring.

• Polymer was filtered through a 5 μm polycarbonate filter. During this operation the filtration ratio was measured by comparing the time to filter equal volumes at the beginning of the filtration toward the end of the filtration. Values of filtration ratio around 0.7-1.0 were considered acceptable for polymer proper preparation.

7.1.3.Core preparation

Core preparation is divided into three steps.

First saturation with brine is done, with the same weight concentration NaCl of the reservoir to study, and 20 days aging, to allow the achievement of the equilibrium between solid and aqueous phase, at ambient temperature.

Then a flooding with brine is performed, at 20°C. When stability is reached, the rate and pressure drop are measured and the absolute permeability is determined, by using the Darcy's equation ($\frac{q}{A} = v = -\frac{k}{\mu} \cdot \frac{dp}{dx}$

Equation 2-2 - Darcy's law through a porous medium).

Finally the sample is saturated with oil, through a flooding at the reservoir temperature (77°C). The flooding is carried out until the saturation of water remained in the sample coincides with the irreducible water saturation (S_{WC}).

7.1.4.Flooding modality

Oil displacement is usually carried out in three phases.

First with a waterflooding, to simulate the secondary recovery, using the synthetic brine previously produced. This step is conducted until a volume of water corresponding to several sample's volumes has been fluxed.

Then another displacement with brine is performed, with the addition of the chemical agent to study. It consists in flowing with of 1-2 pore volumes of chemical slug, followed by the synthetic brine (tertiary recovery).

Finally a displacement with the addition of a chemical solvent is carried out, to remove from the sample all the oil remained. This action allows measuring the fraction of oil recovered with the EOR technique and the amount of oil still retained by the rock [23].

A scheme of core flooding apparatus used is reported in

Figure 7-2.

Plug is prepared in the core holder placed inside an oven at reservoir temperature (Figure 7-3).

Water is pumped inside the plug and displaces the oil. Obtaining an outlet from the core can be a critical issue due to the flow resistance of the oil. A procedure was developed that uses a solvent injection to reduce the viscosity. This approximation can be used when quantitative analysis must be executed on outlet fractions.

Data acquisition system quality is important to allow accurate monitoring of the tests. Electronic transducers are used to measure the pressure drop between core or sandpack inlet and outlet.

The oil extracted by solvent (usually dichloromethane) is collected in volumetric flasks and quantified by UV quantitative analysis. Using the pressure drop values it is possible to study the displacement system and to calculate the end-point relative permeabilities.

7.1.5.Quantitative recovery calculations

Produced oil volumes after water flooding and chemical flooding cannot be determined by visual evaluation in graduated collection tubes when dealing with heavy oil. Heavy oils are sticky and may adhere to the walls of the glass tubes preventing accurate volume measurements. As a consequence all the collected fractions are extracted with tetrahydrofurane (THF) and subsequently oil is precisely quantified by UV-Vis spectroscopy with the external standard method.

Quantization is performed by reading absorbance of THF solutions in the visible region at 446 nm.

Tetrahydrofurane is known to be a very good oil solvent able to keep into solution almost all the components of oil, even the most polar asphaltene fraction. Furthermore tetrahydrofurane is lighter than brine (water plus electrolytes) and not miscible with it. As a consequence the recovery of the upper phase from the collection tubes after oil extraction is quite simple.

Tetrahydrofurane is also used to wash the core after chemical flooding to collect the residual oil not recovered by the chemicals. The sum of oil volumes from waterflooding, chemical flooding and tetrahydrofurane wash is used to calculate the initial oil saturation.

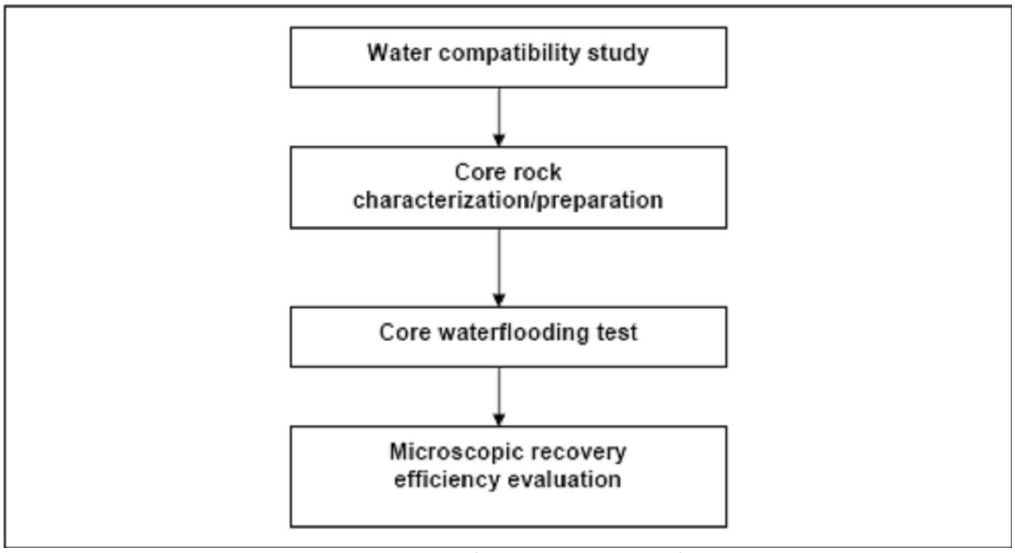

Figure 7-1 – Waterflooding study workflow

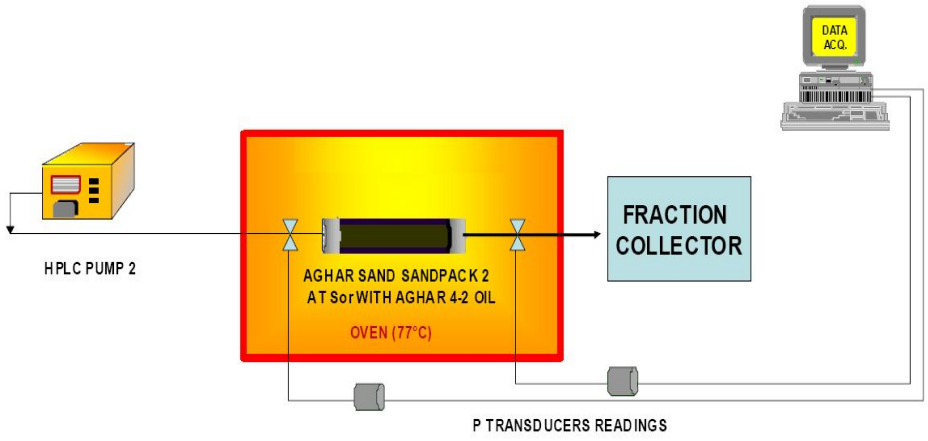

Figure 7-2 – Core flooding apparatus scheme

Figure 7-3 – Instrumentation used for core flooding

7.2. Numerical simulations

After the flooding experiments, simulations are run, to estimate the parameters of the reservoir rock. Solving the flow equations involved is needed. Analytical solutions to flow equation, however, are only obtainable after making simplifying assumptions in regard to geometry, properties and boundary conditions. For most real fluid flow problems, such simplifications are not valid. Hence, the equations have to be solved numerically.

To represent the core used in laboratory experiments, it is possible to consider a simple horizontal slab of porous material, where initially the pressure everywhere is P_0, and then at time zero, the left side pressure (at x=0) is raised to P_L while the right side pressure (at x=L) is kept at $P_R=P_0$ (Figure 7-4).

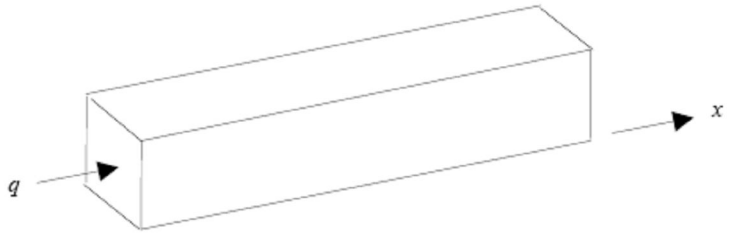

Figure 7-4 - representation of reservoir core flooding

The initial core-flooding may be represented by modeling a one-phase flow.

The equation governing the flow through this porous medium is the diffusivity equation ($\frac{\partial^2 P}{\partial x^2} = \left(\frac{\mu \cdot C \cdot \Phi}{k}\right) \cdot \frac{\partial P}{\partial t}$ Equation **2-31, diffusivity equation**).

It is possible to solve this equation by using standard finite difference approximation for the two derivative terms $\frac{\partial^2 P}{\partial x^2}$ and $\frac{\partial P}{\partial t}$.

First, the x-coordinate must be subdivided into a number of discrete grid blocks (Figure 7-5), each of length Δx, and the time coordinate must be divided into discrete time steps.

Then, the pressure in each block can be solved numerically for each time step.

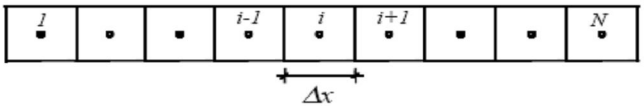

Figure 7-5 – Block-centered grid

The grid created is called a *block-centered grid.* The grid blocks are assigned indices, *i*, referring to the midpoint of each block, representing the average property of the block [24].

Using the Taylor series approximation, the pressure function may be expanded forward and backwards:

$$P(x+\Delta x,t)=P(x,t)+\frac{(\Delta x)}{1!}\cdot P'(x,t)+\frac{(\Delta x)^2}{2!}\cdot P''(x,t)+\frac{(\Delta x)^3}{3!}\cdot P'''(x,t)+\ldots$$

Equation 7-1 – forward expansion of pressure equation

$$P(x-\Delta x,t)=P(x,t)+\frac{(-\Delta x)}{1!}\cdot P'(x,t)+\frac{(-\Delta x)^2}{2!}\cdot P''(x,t)+\frac{(-\Delta x)^3}{3!}\cdot P'''(x,t)+\ldots$$

Equation 7-2 – backward expansion of pressure equation

By adding these two expressions, and solving for the second derivative, we get:

$$P''(x,t)=\frac{P(x+\Delta x,t)-2\cdot P(x,t)+P(x+\Delta x,t)}{(\Delta x)^2}+\frac{(\Delta x)^2}{12}\cdot P'''(x,t)+\ldots$$

Equation 7-3

Or, by employing the grid index system, and using superscript to indicate time level:

$$\left(\frac{\partial^2 P}{\partial x^2}\right)_i^t=\frac{P_{i+1}^t-2\cdot P_i^t+P_{i-1}^t}{(\Delta x)^2}+o(\Delta x^2)$$

Equation 7-4 – approximation of the second order pressure derivative

The term $o(\Delta x^2)$ is the error term, also called *discretization error*, and is neglected in the numerical solution. The smaller the grid blocks used, the smaller will be the error involved.

By using a similar proceeding, it's possible to get the time derivative approximation:

$$\left(\frac{\partial P}{\partial t}\right)_i^t=\frac{P_i^{t+\Delta t}-\cdot P_i^t}{\Delta t}+o(\Delta t)$$

Equation 7-5 – time derivative approximation

7.2.1. Explicit difference equations

It's possible to substitute the approximations into the linear flow equation, to obtain the following set of difference equations:

$$\frac{P_{i+1}^{t} - 2 \cdot P_i^t + P_{i-1}^t}{(\Delta x)^2} = \left(\frac{\Phi \cdot \mu \cdot C}{k}\right) \frac{P_i^{t+\Delta t} - \cdot P_i^t}{\Delta t} \qquad i = 1,\ldots, N$$

Equation 7-6 – Finite difference equation

These equations can be solved explicitly for average pressures in the grid blocks ($i=1\ldots N$) for each time step:

$$P_1^{t+\Delta t} = P_1^t + \frac{4}{3} \cdot \left(\frac{\Delta t}{\Delta x^2}\right) \cdot \left(\frac{k}{\Phi \cdot \mu \cdot c}\right) \cdot \left(P_2^t - 3P_1^t + 2 \cdot P_L\right)$$

Equation 7-7 – solution for the first block, derived from the boundary conditions

$$P_N^{t+\Delta t} = P_N^t + \frac{4}{3} \cdot \left(\frac{\Delta t}{\Delta x^2}\right) \cdot \left(\frac{k}{\Phi \cdot \mu \cdot c}\right) \cdot \left(2P_R^t - 3P_N^t + 2 \cdot P_{N-1}\right)$$

Equation 7-8 – solution for the last block

$$P_i^{t+\Delta t} = P_i^t + \frac{4}{3} \cdot \left(\frac{\Delta t}{\Delta x^2}\right) \cdot \left(\frac{k}{\Phi \cdot \mu \cdot c}\right) \cdot \left(P_{i+1}^t - 2P_i^t + 2 \cdot P_{i-1}\right)$$

Equation 7-9 – solution for the intermediate blocks

7.2.2.Implicit difference equations

In the case of implicit formulations, a set of N equations with N unknowns is obtained, which must be solved simultaneously.

In this case all time levels in the approximation are changed to $t+\Delta t$, except for in the time derivative approximation, which now will be of backward type[24] .

$$\frac{P_2^{t+\Delta t} - 3P_1^{t+\Delta t} + 2P_L}{\frac{3}{4}\Delta x^2} = \left(\frac{\Phi \cdot \mu \cdot C}{k}\right) \cdot \frac{P_i^{t+\Delta t} - P_i^t}{\Delta t} \qquad (i = 1)$$

Equation 7-10

$$\frac{P_{i+1}^{t+\Delta t} - 3P_i^{t+\Delta t} + 2P_{i-1}}{\Delta x^2} = \left(\frac{\Phi \cdot \mu \cdot C}{k}\right) \cdot \frac{P_i^{t+\Delta t} - P_i^t}{\Delta t} \qquad (i = 2,\ldots, N-1)$$

Equation 7-11

$$\frac{P_R^{t+\Delta t} - 3P_N^{t+\Delta t} + 2P_{N-1}}{\frac{3}{4}\Delta x^2} = \left(\frac{\Phi \cdot \mu \cdot C}{k}\right) \cdot \frac{P_i^{t+\Delta t} - P_i^t}{\Delta t} \qquad (i = N)$$

Equation 7-12

For simplicity, the set of equations may be written in the linear form:

$$a_i \cdot P_{i-1}^{t+\Delta t} + b_i \cdot P_i^{t+\Delta t} + c_i \cdot P_{i+1}^{t+\Delta t} = d_i \qquad i = 1,\ldots,N$$

Equation 7-13

Then the equations may be solved for average block pressures using for instance the Gaussian elimination method.

7.2.3.Discussion on the formulations

The explicit formulation requires less computational time, as explicit expressions for pressure are obtained directly. This formulation, however, becomes unstable for large time steps. It has, indeed, the following stability requirement [24]:

$$\Delta t \le \frac{1}{2} \cdot \left(\frac{\Phi \cdot \mu \cdot C}{k}\right) \cdot \Delta x^2 \qquad \textbf{Equation 7-14}$$

As a consequence, the time step size is limited by both grid block size and properties of the rock and fluid.

Implicit formulation, instead, is unconditionally stable for all time step sizes.

The additional computational work per time step is usually compensated by permitting much larger time steps.

7.2.4. Oil – water simulation - IMPES solution

Considering the fluid phases of oil and water only, and substituting Darcy's equations and standard Black Oil fluid descriptions into the continuity equations, the following flow equations for the two phases will result:

$$\frac{\partial}{\partial x}\left(\frac{k \cdot k_{ro}}{\mu_o B_o} \cdot \frac{\partial P_o}{\partial x}\right) - q_o^I = \frac{\partial}{\partial t}\left(\frac{\Phi \cdot S_o}{B_o}\right)$$

Equation 7-15 – flow equation for oil

$$\frac{\partial}{\partial x}\left(\frac{k\cdot k_{rw}}{\mu_w B_w}\cdot\frac{\partial P_w}{\partial x}\right)-q_w^I=\frac{\partial}{\partial t}\left(\frac{\Phi\cdot S_w}{B_w}\right)$$

Equation 7-16 – Flow equation for water

Similar approximations as the ones used for one-phase flow can be utilized. In this case the left side flow terms become:

$$\frac{\partial}{\partial x}\left(\frac{k\cdot k_{ro}}{\mu_o B_o}\cdot\frac{\partial P_o}{\partial x}\right)\approx T_{xoi+1/2}\cdot\left(P_{oi+1}-P_{oi}\right)+T_{xoi-1/2}\cdot\left(P_{oi-1}-P_{oi}\right)$$

Equation 7-17

And

$$\frac{\partial}{\partial x}\left(\frac{k\cdot k_{rw}}{\mu_w B_w}\cdot\frac{\partial P_w}{\partial x}\right)_i\approx T_{xwi+1/2}\cdot\left(P_{wi+1}-P_{wi}\right)+T_{xwi-1/2}\cdot\left(P_{wi-1}-P_{wi}\right)$$

Equation 7-18

In these expressions, the term $T_{Xli+1/2}$ is the phase transmissibility, defined as:

$$T_{xoi+1/2}=\frac{2\cdot\lambda_{oi+1/2}}{\Delta x_i\cdot\left(\frac{\Delta x_{i+1}}{k_{i+1}}+\frac{\Delta x_i}{k_i}\right)}$$

Equation 7-19 – Phase transmissibility

And λ_i is the mobility term, defined as:

$$\lambda_o=\frac{k_{ro}}{\mu_o\cdot B_o};\qquad \lambda_w=\frac{k_{rw}}{\mu_w\cdot B_w}$$

Equation 7-20 – Mobility term

The right hand sides of Equation 7-15 and Equation 7-16 become:

$$\frac{\partial}{\partial t}\left(\frac{\Phi\cdot S_o}{B_o}\right)\approx C_{pooi}\cdot\left(P_{oi}-P_{oi}^{\ t}\right)+C_{swoi}\cdot\left(S_{wi}-S_{wi}^{\ t}\right)$$

Equation 7-21

$$\frac{\partial}{\partial t}\left(\frac{\Phi\cdot S_w}{B_w}\right)\approx C_{powi}\cdot\left(P_{oi}-P_{oi}^{\ t}\right)+C_{swwi}\cdot\left(S_{wi}-S_{wi}^{\ t}\right)$$

Equation 7-22

So the discrete forms of the oil and water equations may be written:

$$T_{xoi+1/2} \cdot \left(P_{oi+1} - P_{oi}\right) + T_{xoi-1/2} \cdot \left(P_{oi-1} - P_{oi}\right) - q_{oi}^{I} = C_{pooi} \cdot \left(P_{oi} - P_{oi}^{\ t}\right) + C_{swoi} \cdot \left(S_{wi} - S_{wi}^{\ t}\right), \qquad i = 1, N$$

Equation 7-23

$$T_{xwi+1/2} \cdot \left[\left(P_{oi+1} - P_{oi}\right) - \left(P_{cowui+1} - P_{cowi}\right)\right] + T_{xwi-1/2} \cdot \left[\left(P_{oi-1} - P_{oi}\right) - \left(P_{cowui+1} - P_{cowi}\right)\right] - q_{wi}^{I} = C_{powi} \cdot \left(P_{oi} - P_{oi}^{\ t}\right) + C_{swwi} \cdot \left(S_{wi} - S_{wi}^{\ t}\right), \qquad i = 1, N$$

Equation 7-24

In the equations above, oil pressure, P_{oi}, and water saturation, S_{wi}, are the primary variables, and unknowns to be solved for.

It is not possible to solve the equations before the coefficients and the capillary pressures are calculated, and both the coefficient and capillary pressure are functions of the unknowns. Therefore, a solution method is needed that either iterates on the solution and updates coefficients and capillary pressures until convergence is reached.

IMPES is one of the most used methods. The acronym IMPES stands for IMplicit Pressure, Explicit Saturation method.

In the IMPES method, the key lies in the approximation of coefficients and capillary pressures. It simply evaluates these at time level t, and thus allows solving for pressures and saturations without having to iterate on the solution.

7.2.5.Grid Effects

The most important numerical errors associated with finite difference type simulation models are numerical dispersion and grid orientation effects.

Numerical dispersion has the effect of smearing displacement fronts and arises because of the upstream evaluation of the coefficients in the interblock flow terms. The effect is illustrated in Figure 7-6.

There are three important considerations:

1) For a given grid and the same timestep sizes, the numerical dispersion is always larger with a fully implicit method than with IMPES.

2) For a fully implicit method, the numerical dispersion effect is increasing with timestep size.

3) For IMPES, the numerical dispersion is decreasing with timestep size. (Kleppe and Skjaeveland, 1992, [25])

The grid-orientation effect is another important characteristic of conventional finite-difference methods. The effect is illustrated in Figure 7-7,

where the results of simulations with similar gridblock sizes but different grid orientation are compared.

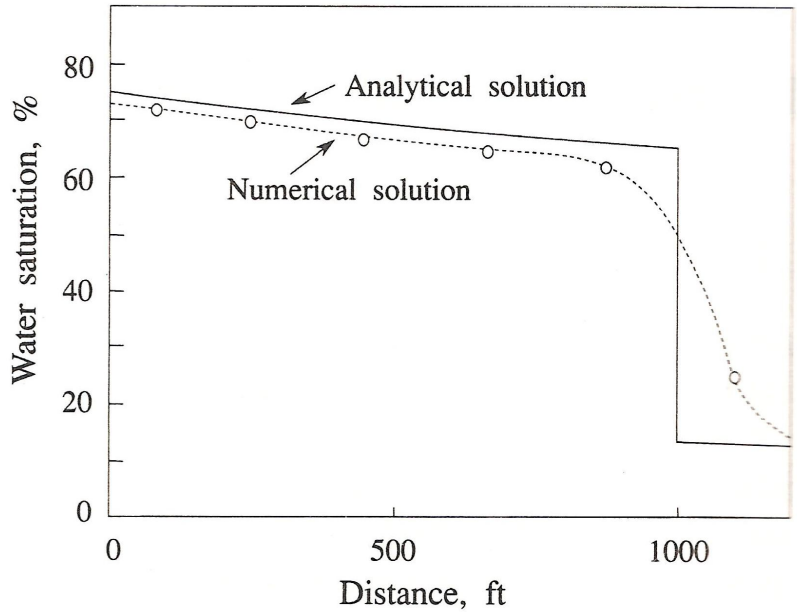

Figure 7-6 - Numerical dispersion effect illustarted for a one-dimensional displacement of oil by water

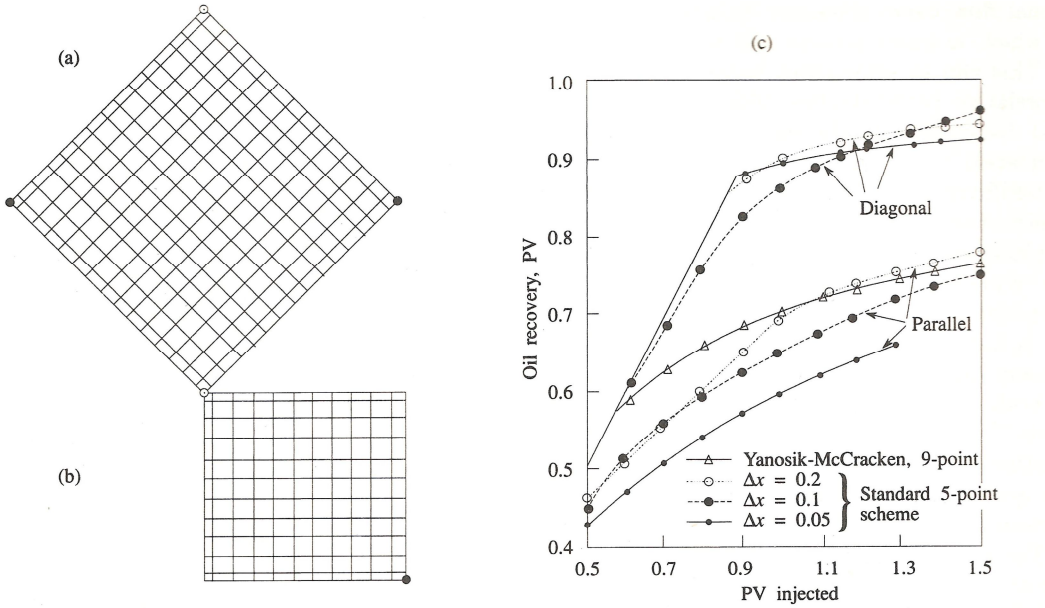

Figure 7-7 - Grid orientation effect illustrated for an unfavorable mobility ratio. (a): diagonal grid. (b): parallel grid. (c): confrontation of results

7.3. Review of UTCHEM

The reservoir simulator used in this work was UTCHEM, a three-dimensional, multiphase, multicomponent chemical flooding simulator developed in the Center for Petroleum and Geosystem Engineering at the University of Texas at Austin. UTCHEM can be described as an implicit pressure explicit saturation formulation that has the option to simulate several species such as water, oil, surfactant, co-solvent, polymer, cations, anions, and tracers [26].

Numerous phenomena are modeled such as: microemulsion phase behavior, three phase relative permeability, capillary desaturation of oil, water and microemulsion phases, shear thinning polymer viscosity, adsorption, cation exchange, tracer partitioning and reaction. It is used for many applications including polymer and surfactant flooding.

7.3.1.UTCHEM model formulation

The basic governing differential equations consist of: a mass conservation equation for each component, an overall mass conservation equation that determines the pressure (the pressure equation), an energy balance, and Darcy's Law generalized for multiphase flow. The resulting flow equations are solved using a block-centered finite difference scheme.

The flow equations allow for compressibility of soil and fluids, dispersion and molecular diffusion, chemical reactions, and phase behavior.

Mass Conservation Equations

The assumptions imposed when developing the flow equations are the local thermodynamic equilibrium, immobile solid phases, slightly compressible soil and fluids, Fickian dispersion, ideal mixing, and Darcy's law. The boundary conditions used are no flow and no dispersive flux across the impermeable boundaries [27].

The continuity of mass for component in association with Darcy's law is expressed in terms of overall volume of component per unit pore volume ($\tilde{C}_k$) as

$$\frac{\partial}{\partial t}\left(\Phi \cdot \tilde{C}_k \cdot \rho_k\right) + \nabla\left[\sum_{l=1}^{np} \rho_k \cdot \left(C_{kl} \cdot \vec{u}_l - \tilde{D}_{kl}\right)\right] = R_k$$

Equation 7-25

Where n_p is the phase number; l is the phase index; R_K is the total source/sink for species k. R_K is a combination of all rate terms for a particular component and may be expressed as:

$$R_k = \Phi \cdot \sum_{l=1}^{np} S_l \cdot r_{kl} + (1-\Phi) \cdot r_{ks} + Q_k$$

Equation 7-26

r_{Kl} is the reaction rate for species k in phase l.

The phase flux from Darcy's law is

$$\vec{u}_l = -\frac{k_{rl} \cdot \vec{k}}{\mu_l} \cdot (\nabla P_l - \gamma_l \cdot \nabla h)$$

Equation 7-27

where $\vec{\vec{k}}$ is the intrinsic permeability tensor and h is the vertical depth.

Pressure equation

The pressure equation is developed by summing the mass balance equations overall volume-occupying components, substituting Darcy's law for the phase flux terms, using the definition of capillary pressure, and noting that $\sum_{K=1}^{n_{CV}} C_{Kl} = 1$, where n_{CV} is the number of components.

$$\Phi \cdot C_t \cdot \frac{\partial P_1}{\partial t} + \nabla \vec{k} \cdot \lambda_{rTc} \cdot \nabla P_1 = -\nabla \sum_{l=1}^{np} \vec{k} \cdot \lambda_{rlc} \cdot \nabla h + \nabla \sum_{l=1}^{np} \vec{k} \cdot \lambda_{rlc} \cdot \nabla P_{cl1} + \sum_{k=1}^{nCV} Q_k$$

Equation 7-28 – pressure equation

Where

$$\lambda_{rlc} = \frac{k_{rl}}{\mu_l} \cdot \sum_{k=1}^{nCV} \rho_k \cdot C_{kl}$$

Equation 7-29

and total relative mobility with the correction for fluid compressibility is

$$\lambda_{rTC} = \sum_{l=1}^{nP} \lambda_{rlc}$$

Equation 7-30

The total compressibility, Ct, is the volume-weighted sum of the rock or soil matrix (Cr) and component compressibilities (C_O^k):

$$C_t = C_r + \sum_{k=1}^{nCV} C_k^o \cdot \tilde{C}_k$$

Equation 7-31

Where

$$\Phi = \Phi_R \cdot \left[1 + C_r \cdot \left(P_R - P_{R0}\right)\right]$$

Equation 7-32

Adsorption

UTCHEM uses a Langmuir-type isotherm to describe the adsorption level of surfactant or polymer which takes into account the salinity, surfactant/polymer concentration, and soil permeability. The adsorption is irreversible with concentration and reversible with salinity. The adsorbed concentration is given by:

$$\hat{C}_k = \min\left(\tilde{C}_k, \frac{a_k \cdot \left(\tilde{C}_k - \hat{C}_k\right)}{1 + b_k \cdot \left(\tilde{C}_k - \hat{C}_k\right)}\right)$$

Equation 7-33

K indicates the polymer or the surfactant.

The minimum is taken to guarantee that the adsorption is no greater than the total surfactant concentration.

Adsorption increases linearly with effective salinity and decreases as the permeability increases:

$$a_K = \left(a_{K1} + a_{K2} \cdot C_{SE}\right) \cdot \left(\frac{k_{ref}}{k}\right)^{0.5}$$

Equation 7-34

The value of a_K/b_K represents the maximum level of component adsorbed and b3 controls the curvature of the isotherm. The adsorption model parameters a_{K1}, a_{K2}, and b_K are found by matching laboratory surfactant adsorption data. The reference permeability kref is the permeability at which the input adsorption parameters are specified.

CSE is the effective salinity:

$$C_{SEP} = \frac{C_{51} + (\beta_P - 1) \cdot C_{61}}{C_{11}}$$

Equation 7-35

Where C51, C61, and C11 are the anion, calcium, and water concentrations in the aqueous phase and βP is measured in the laboratory and is an input parameter to the model.

Capillary pressures and relative permeabilities

The Corey model for capillary pressure is used:

$$P_{cOW} = CPC \cdot \sqrt{\frac{\Phi}{k}} \cdot (1 - S_{nj})^{EPC}$$

Equation -7-36

CPC and EPC are experimental parameters. S_{nj} is the normalized saturation of the species j, defined as:

$$S_{nj} = \max\left(0, \frac{S_j - S_{jr}}{1 - S_{wr} - S_{or}}\right)$$

Equation 7-37

The Corey model is used also for relative permeabilities:

$$k_{rj} = k_{rj}^0 \cdot S_{nj}^{nj}$$

Equation 7-38 – Corey's model for relative permeabilities

K_{rj}^0 is the end-point relative permeability for species j.

To determine the relative-permeability curves, the main input parameters are: k_{ro}, k_{rw}, S_{wr}, S_{or}, n_o, n_w.

Viscosity

The viscosity of a polymer solution depends on the concentration of polymer and on salinity. The Flory-Huggins equation (Equation 6-1) was modified to account for variation in salinity:

$$\mu_p^0 = \mu_w \cdot \left(1 + \left(A_{p1} \cdot C_{pol} + A_{p2} \cdot C_{pol}^2 + A_{p3} \cdot C_{pol}^3\right) \cdot C_{SEP}^{Sp}\right)$$

Equation 7-39 – Viscosity of solution as a function of polymer concentration

C_{pol} is the concentration of polymer in the aqueous phase, expressed in weight fraction; μ_W is the water viscosity; A_{P1}, A_{P2}, and A_{P3} are constants. The factors C_{SEP} and Sp allows for dependence of polymer viscosity on salinity and hardness.

The reduction in polymer solution viscosity as a function of shear rate (μ_P) is modelled by Meter's equation (Equation 6-4):

$$\mu_p = \mu_w + \frac{\mu_p^0 - \mu_2}{1 + \left(\frac{\dot{\gamma}}{\dot{\gamma}_{1/2}}\right)^{P\alpha - 1}}$$

Equation 7-40 – Viscosity as a function of shear rate

$\gamma_{1/2}$ is the shear rate at which viscosity is the average of $\mu_P{}^o$ and μ_w and S_P is an empirical coefficient. When the above equation is applied to flow in permeable media, μ_P is usually called "apparent viscosity" and the shear rate is an equivalent shear rate $\dot{\gamma}_{eq}$.

Polymer permeability reduction

Polymer solutions reduce both the mobility of the displacing fluid and the effective permeability of the porous medium, as discussed in section 6.2.5.

The permeability reduction factor in UTCHEM is modelled as:

$$R_k = 1 + \frac{\left(R_{k\max} - 1\right) \cdot b_{rk} \cdot C_{pol}}{1 + b_{rk} \cdot C_{pol}}$$

Equation 7-41

Where

$$R_{k\max} = \min\left\{\left[1 - \frac{c_{rk} \cdot \left(A_{p1} \cdot C_{SEP}^{Sp}\right)^{1/3}}{\left(\frac{\sqrt{k_x \cdot k_y}}{\Phi}\right)^{1/2}}\right]^{-4}, 10\right\}$$

Equation 7-42

b_{rk} and C_{rk} are input parameters, experimentally determined.

The effect of permeability reduction is assumed to be irreversible i.e., it does not decrease as polymer concentration decreases and thus $R_{RF}=R_k$.

The viscosity of the phase that contains the polymer is multiplied by the value of the R_k to account for the mobility reduction in the simulator [27].

Polymer inaccessible pore volume

The reduction in porosity due to inaccessible or excluded pores to the large size polymer molecules is called inaccessible pore volume. The resulting effect is a faster polymer velocity than the velocity of water. This effect is modeled by multiplying the porosity in the conservation equation for polymer by the input parameter of effective pore volume.

8. MATCH OF EXPERIMENTAL DATA

For the screening phase based on the investigation upon the laboratory experiments, two reservoir samples were available. They were a sandpack and a reservoir core.

8.1. Sandpack experiment

The sandpack was prepared with crushed core material. The flooding procedure was followed as described in chapter 7.1.

Below are listed the sandpack and fluid characteristics:

SANDPACK PROPERTIES		
DIMENSIONS	Length L(cm) Diameter D(cm) Pore Volume PV(ml) Porosity Φ(fraction)	10 1 6.38 0.414
PERMEABILITY	K mD	1624
INITAL SATURATIONS	Water Initial S_{Wi} Residual water saturation $S_{W}r$ Residual oil Saturation $S_{O}r$	0.2 0.4 0.1

Table 8-1 – Properties of sandpack used during the experiments

FLUID PROPERTIES (AT 77°C)	
BRINE DENSITY (Kg/m^3)	1.07
BRINE VISCOSITY (cP)	0.395
BRINE COMPRESSIBILITY (Psi^{-1})	2.66*10^{-6}
OIL DENSITY (Kg/m^3)	0.925
OIL VISCOSITY (cP)	24
OIL COMPRESSIBILITY (Psi^{-1})	4.2*10^{-6}

Table 8-2 – Fluid properties

Oil displacement has been performed at reservoir temperature, 77°C, in three steps:

1) Displacement with brine, with 1.7% NaCl concentration, for about 38 pore volumes;
2) Displacement with brine, with 1.7% NaCl concentration and 2500 ppm of AN125 polymer. This step has been run for 4 PV's;
3) Displacement with reservoir brine for other 42 PV's.

The flooding has been performed with a fixed injection rate of 0.2 ml/min.

Data regarding the recovery and the pressure difference between the ends of the sample have been recovered from the flooding, and are shown in Figure 8-1 and Figure 8-2.

In Figure 8-1 the recovery data graph is shown. On the x-axis the pore volumes fluxed are reported. Putting the pore volumes on the x-axis is similar to represent the injection time, but it allows keeping the uniformity of the data even if flow rate variations are present. Furth more, in this way trials performed with different flow rates are comparable.

On the y-axis is shown the percentage of total oil recovered.

In Figure 8-2 the pressure data graph is reported. On the y axis is shown the pressure difference between the extremes of the sample.

It is possible to note that, as soon as the flooding with polymer begins, there is a sudden increase in the recovery of oil and in the ΔP between the sample's ends.

The ΔP decreases after the polymer injection is stopped, but remains fixed to a value higher than the initial one. This can be explained by the residual resistance factor, which causes permeability reduction effects.

According to the Darcy law ($\frac{q}{A} = v = -\frac{k}{\mu} \cdot \frac{dp}{dx}$

Equation 2-2 - Darcy's law through a porous medium) a decrease in permeability, with constant rate, causes an increase in the ΔP.

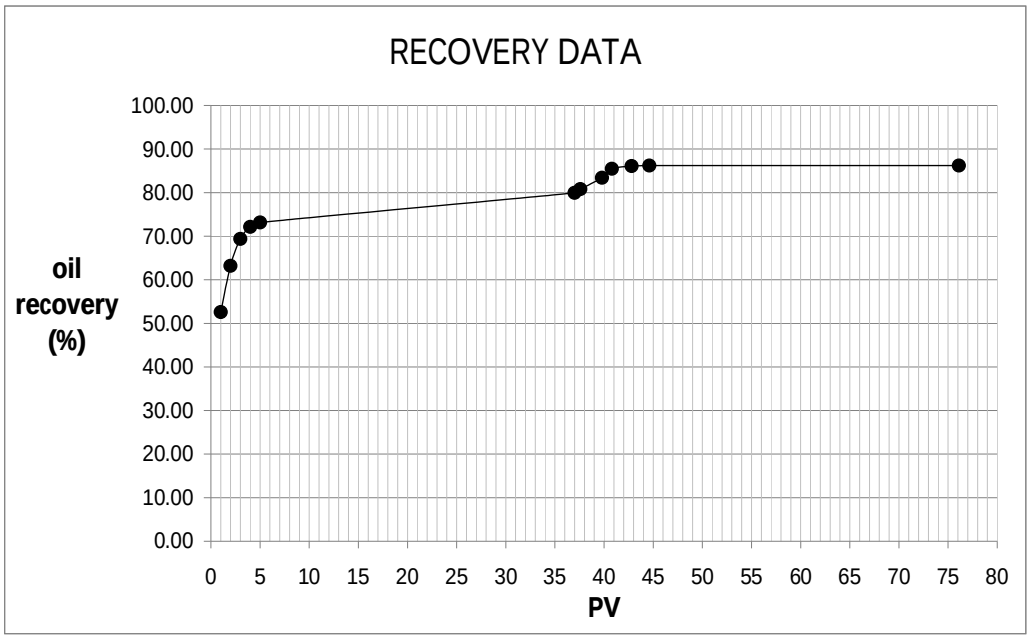

Figure 8-1 – Recovery data from sandpack flooding

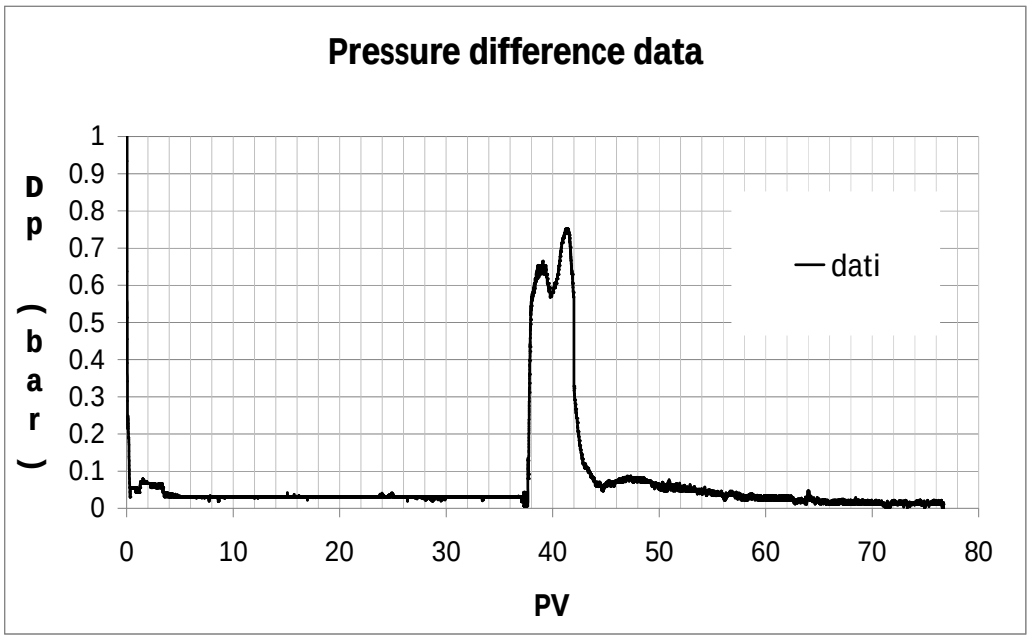

Figure 8-2 – Pressure data from sandpack flooding

8.2. Waterflooding matches

The first simulations to be run concern the waterflooding step, before the treatment with the chemical agent.

8.2.1. Permeability effect upon ΔP

The earliest simulation was performed to observe the variation of pressure trend changing the rock permeability.

The results are in according with the Darcy law: the pressure difference increases with the decreasing of the rock permeability, if the rate is kept constant.

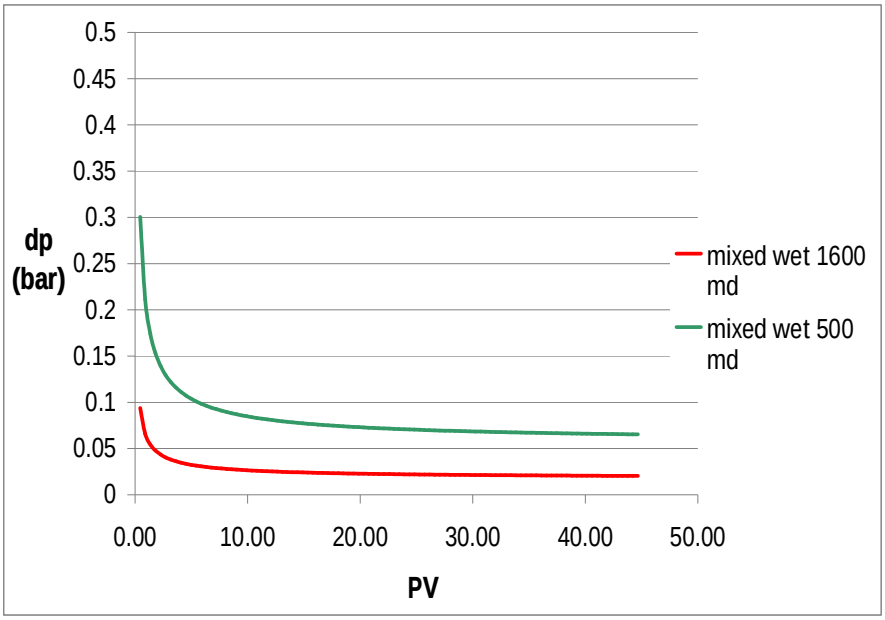

Figure 8-3 – permeability effect upon the ΔP

8.2.2. Effect of wettability upon recovery

Changing the wettability of the rock sample modeled the recovery changes significantly. As expected, if an oil-wet rock is modeled, the recovery is less respect to the case of water-wet rock (Figure 8-4 – Effect of wettability upon recovery). This is because the oil adheres preferentially to the rock in the oil-wet sample and the displacement with water results more difficult.

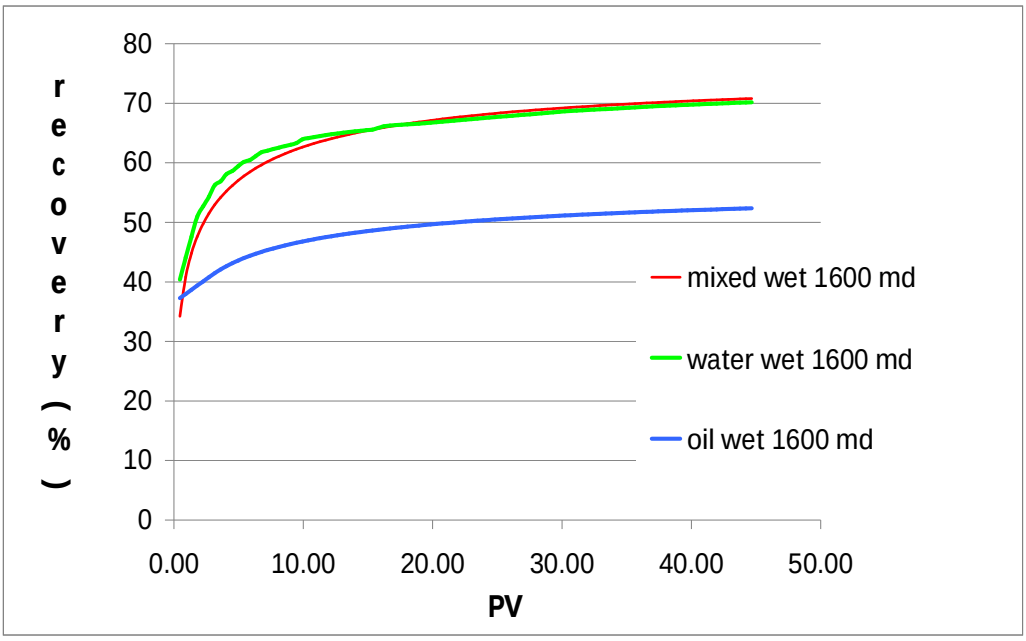

Figure 8-4 – Effect of wettability upon recovery

8.2.3.Corey's parameters estimation

Several simulations have been run to reproduce the experimental recovery data. The main parameters that influence the shape of the recovery curve are the Corey exponents, n_w and n_o, present in Equation 7-38 – Corey's model for relative permeabilities ($k_{ro} = k_{ro}^0 \cdot S_{n_o}^{no}$; $k_{rw} = k_{rw}^0 \cdot S_{n_w}^{nw}$).

The results of the simulations and their match with experimental data are shown in Figure 8-5. The reason why the behavior of the sample is so influenced by the Corey exponents is explained observing the changing of the relative permeability curves (Figure 8-6). If the exponent of the water relative permeability curve switches from the value of 6 to the value of 2, the relative permeability of water is higher even for small water saturation. As a consequence, water has a higher mobility and the mobility ratio is more unfavorable for the oil recovery. This explains the less recovery percentage in the recovery graph.

If, on the other hand, the oil exponent is less, the oil mobility will be increased even at small oil concentration and the final recovery of oil will be higher.

The Corey parameters which best fit the experimental data are shown in Table 8-3 and the relative permeability curves resulting are shown in Figure 8-7.

The effects of capillary pressure are negligible for a flooding experiment.

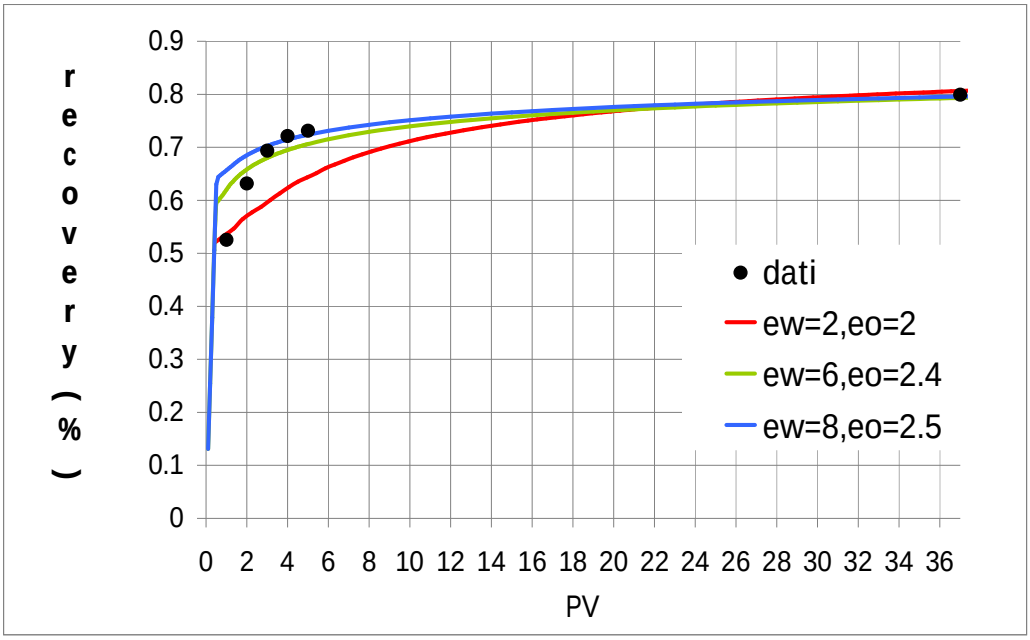

Figure 8-5 – effect of Corey exponents on the recovery curve

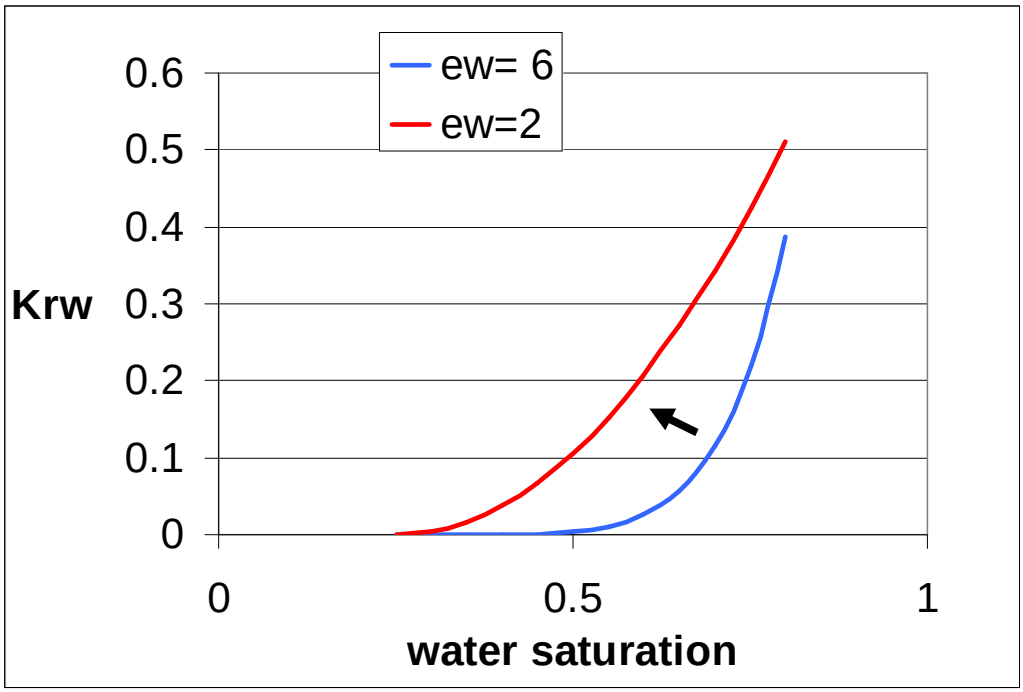

Figure 8-6 – effect of Corey exponent change on the water relative permeability curve

nw	6
no	2.4
Sor	0.1
kwr	0.4
kor	0.9
CPC	0
EPC	0

Table 8-3 – Corey parameters from matches with experimental sandpack flooding

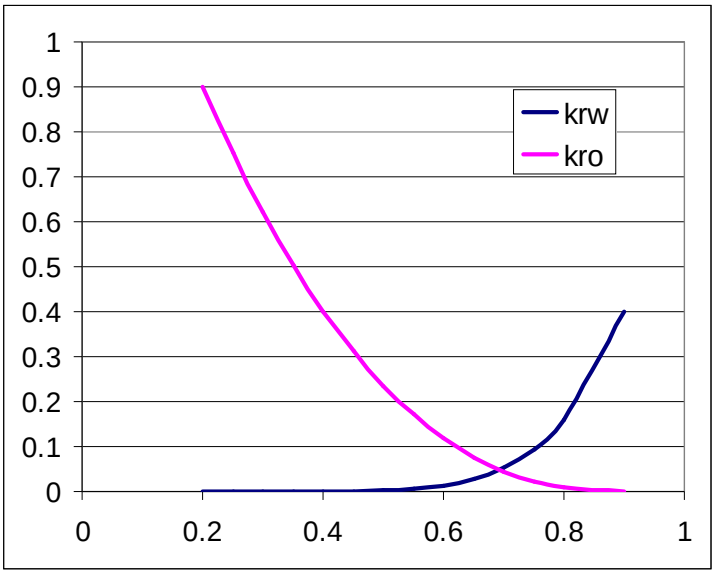

Figure 8-7 – relative permeability curves resulting from sandpack matches

8.3. Polymer flooding matches

Experimental tests with the polymer are needed to determine the input parameters required to model the polymer behavior in porous media.

The first parameter needed is the one which control the salinity dependence of the viscosity of the polymer solution. The experimental data are shown in Figure 8-8.

The data are then reported in a log-log graph, on which on the x-axis is reported the salinity, in meq/ml, and on the y-axis the normalized difference between the densities of polymer solution and the brine.

The slope of the curve obtained through the interpolation of the data is the input parameter needed (Figure 8-9).

The next information needed is the trend of the viscosity changing the polymer concentration. The experimental data and their match are shown on

Figure 8-10. The coefficients of the cubic curve that match the experimental data are the input parameters required by the UtChem model (Equation 7-39).

To complete the modeling of the polymer solution, the behavior in presence of shear rate is needed.

In

Figure **8-11** is shown the variation of the polymer solution with the shear rate. The parameters of the Meter's equation (Equation 7-40 – Viscosity as a function of shear rate), which is represented by the red curve, need to be adjusted to fit the experimental data, represented by the black points in the figure.

Retention of the polymer in porous media is a function of polymer concentration. It is possible to refer to a value given by the polymer suppliers, according to which 500 μg of polymer are adsorbed for every g of porous material.

Once the parameters are known, it is possible to extend the simulation to the part where the polymer solution was used in the flooding. The results are shown in Figure 8-12 and Figure 8-13.

It is possible to observe a good representation of the experimental data. It was obtained simulating a Residual Resistance Factor (R_{RF}) of 3.5 and a shear rate of 40 s^{-1}.

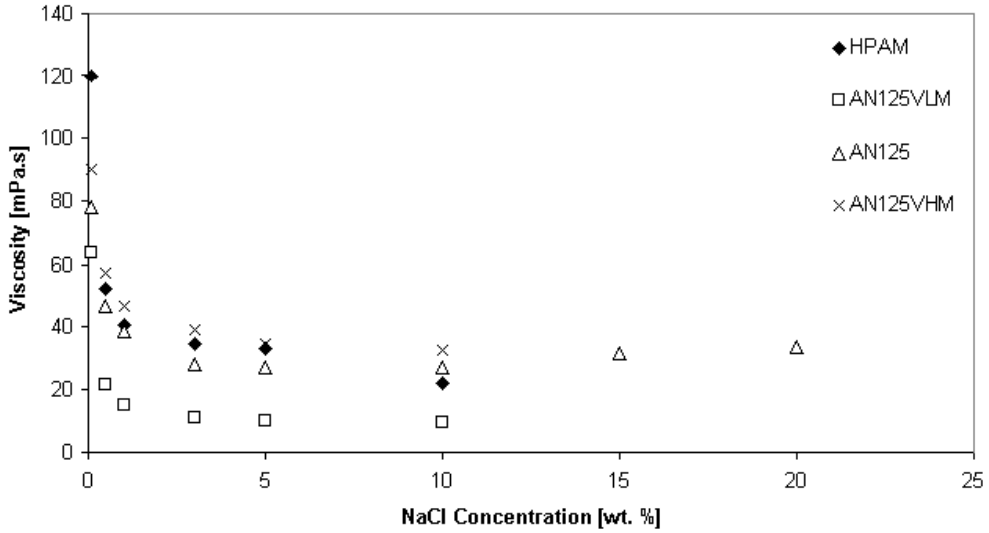

Figure 8-8 – salinity dependence of the polymer, from Norwegian Centre for Integrated Petroleum Research

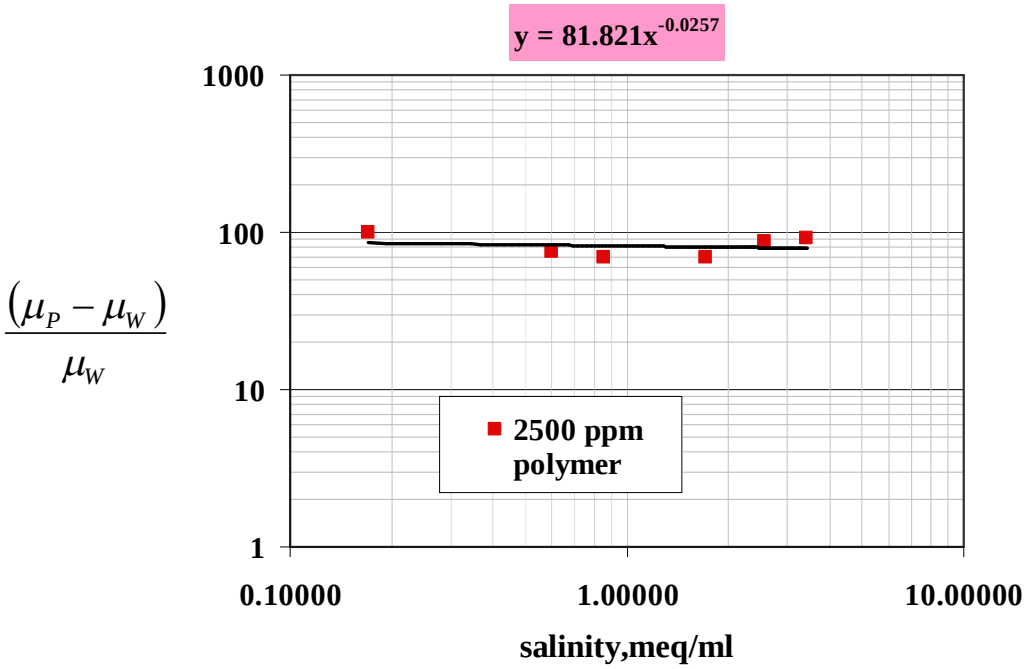

Figure 8-9 – Interpolation of experimental data of viscosity

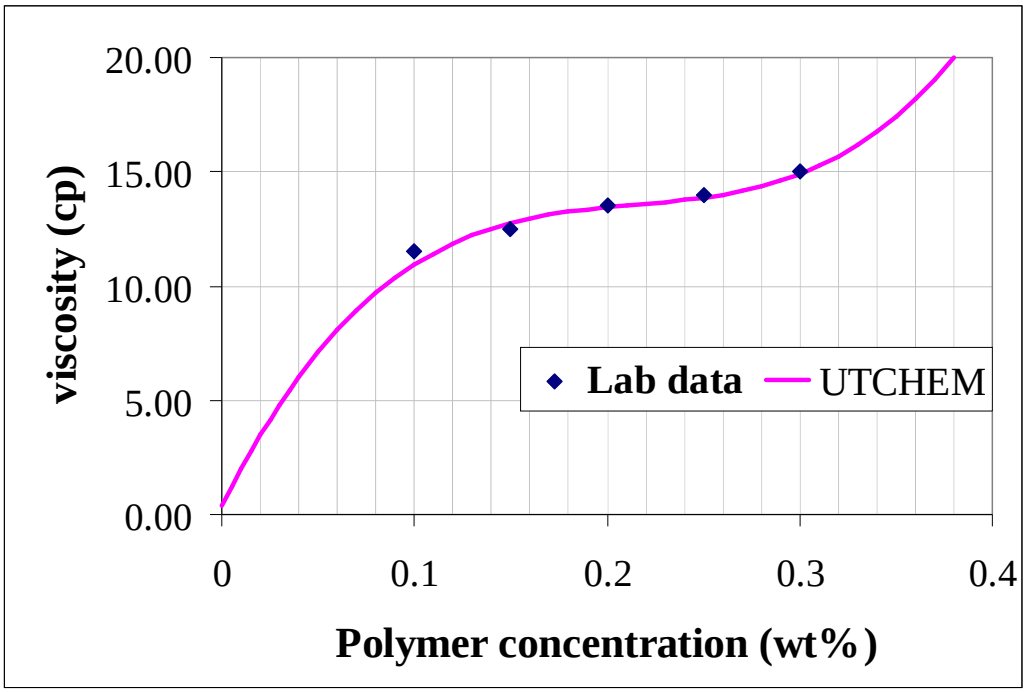

Figure 8-10 – Viscosity vs. polymer concentration

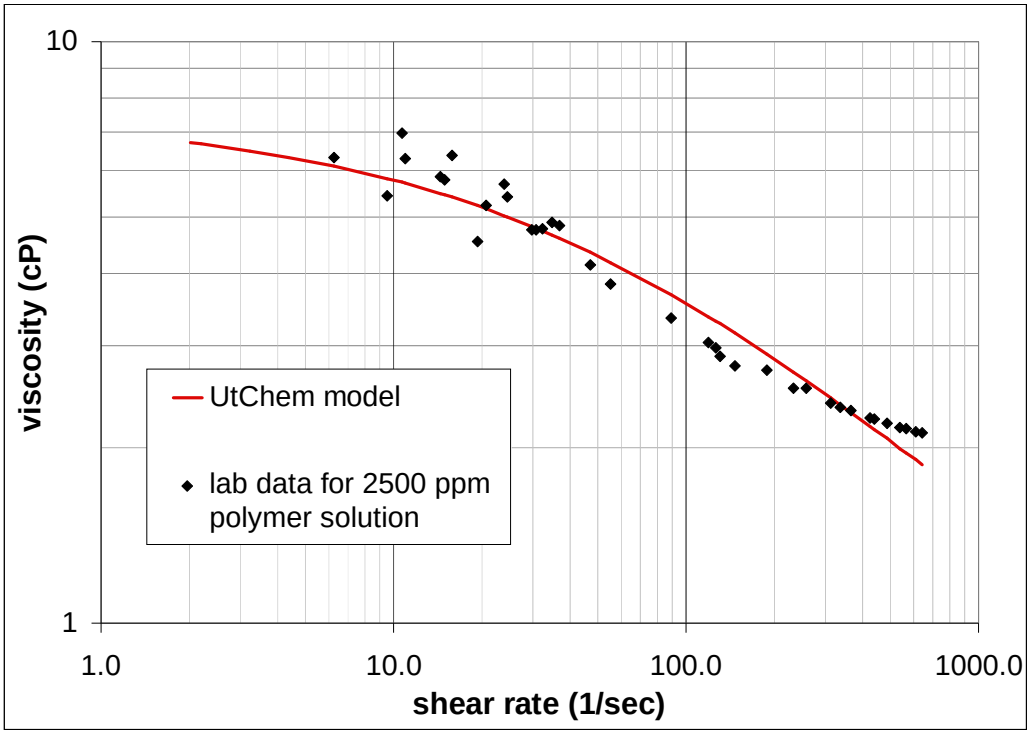

Figure 8-11 – Viscosity vs. shear rate

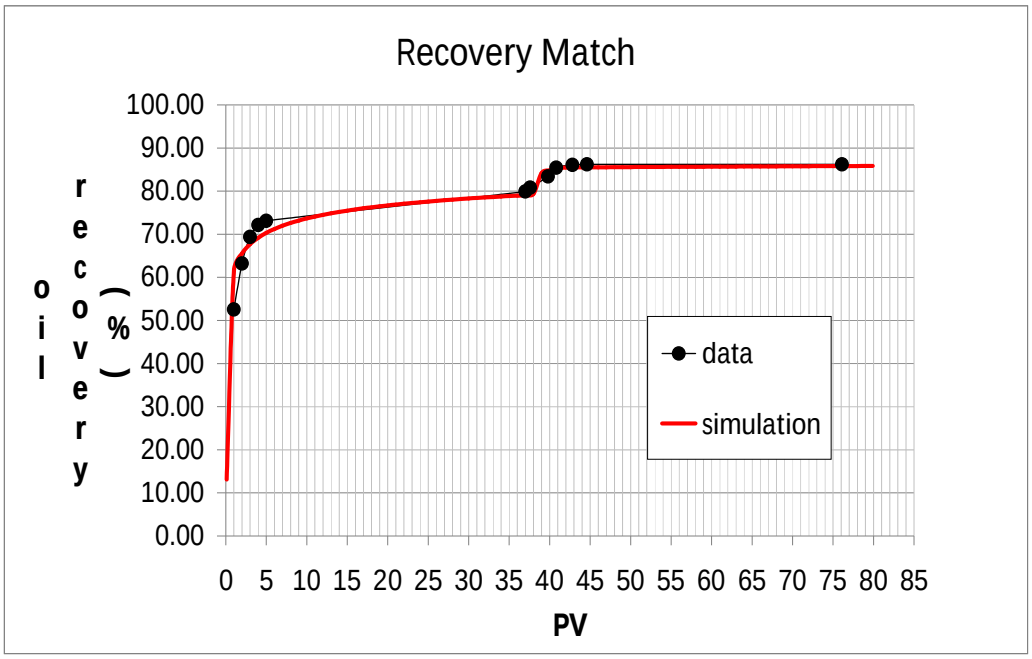

Figure 8-12– Match of recovery data from sandpack flooding with polymer solution

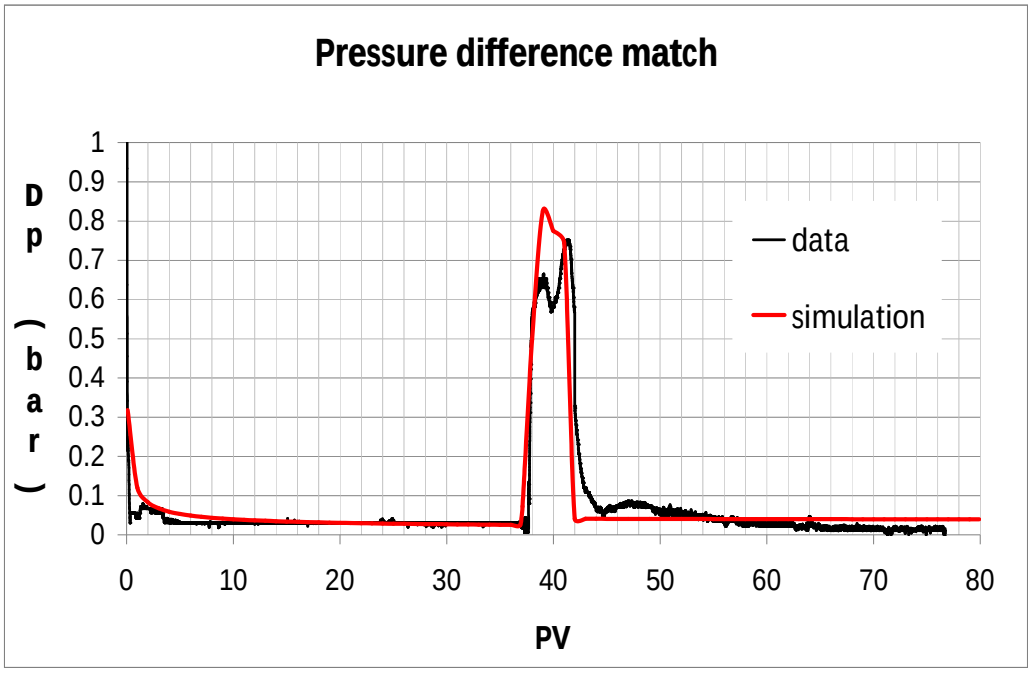

Figure 8-13 – Match of pressure data from sandpack flooding with polymer solution

8.4. Core flooding experiment

Below are listed the properties of the core used during the experiments:

RESERVOIR CORE PROPERTIES			
DIMENSIONS	Length Diameter Pore Volume Porosity	L(cm) D(cm) PV(ml) Φ(fraction)	5.23 3.8 14.9 0.263
PERMEABILITY	K	mD	209
INITAL SATURATIONS	Water Initial Residual water saturation Residual oil Saturation	S_{Wi} S_{Wr} S_{Or}	0.4 0.4 0.15

Table 8-4 – Properties of core used during experiments

Oil displacement has been performed at reservoir temperature, 77°C, in three steps:

1) Displacement with brine, with 1.7% NaCl concentration, for about 5.8 pore volumes;
2) Displacement with brine, with 1.7% NaCl concentration and 2500 ppm AN125 polymer. This step has been run for one PV;
3) Displacement with reservoir brine for other 2 PV's.

The flooding has been performed with a fixed injection rate of 0.06 ml/min, significantly less respect to the case with the sandpack.

The lapse in which polymer was injected is highlighted in the graph (Figure 8-15 and Figure 8-16).

8.5. Polymer core flooding matches

The results of the match with the core flooding are shown in Figure 8-17 and Figure 8-18.

It is possible to observe that the trend of the recovery curve is different compared to the case with the previous case with the sandpack. When the polymer injection begins, there is not a sudden increase in recovery, as it was observable in the other flux. There is only an increase in the slope of the recovery curve. This is probably due to the fact that polymer injection started when the oil recovery by waterflooding was not stabilized yet, but oil was still being produced. The experimental data about recovery, in fact, show that the recovery curve is not plan before the start of the polymer flux (Figure 8-15), but is still increasing.

In addition, the core's properties are less uniform and homogeneous than the sandpack's ones, since the core has been taken directly from the formation and it has not been prepared packing fine grained sands in laboratory. There can be different pore size distributions or presence of residual oil saturations. Because of the less pore size of the core, pore bridging is possible and, as a consequence, some channels can be sealed off and the flow can be diverted towards unswept channels (Ogunberu, Asghari, JCPT 2006, [19]). This effect, together with the permeability reduction, can aid the recovery from the sample.

Therefore, reproducing experimental data with a uniform model is more difficult respect to the case with the sandpack. This explains the small differences between the data and the simulation.

The Corey parameters which best fit the experimental data of both recovery and pressure experiments are shown in Table 8-5, while in Figure 8-14 the resulting curves are plotted.

The match with the polymer flooding was obtained simulating a shear rate of 40 s^{-1} and a R_{RF} of 3.5.

nw	3
no	4
Sor	0.15
kwr	0.25
kor	0.9

Table 8-5 - parameters from matches with core flooding

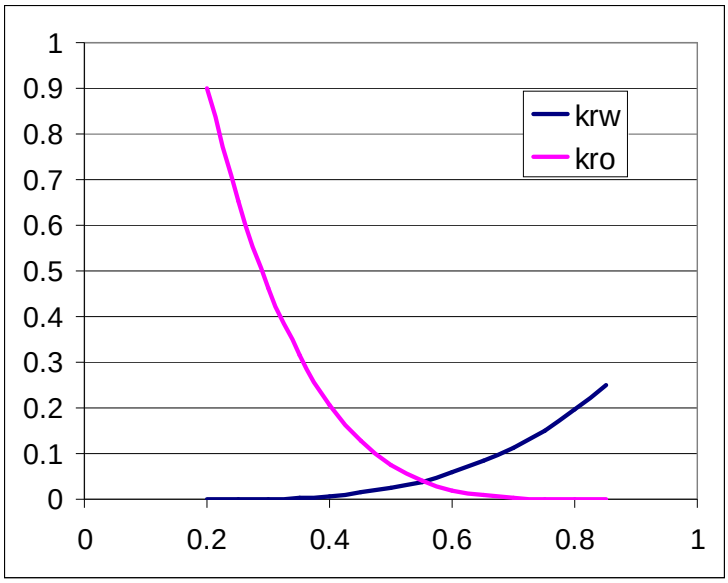

Figure 8-14 – relative-permeability curves resulting from core flooding matches

8.6. Effects of shear rate and adsorption

The value of adsorption which allows the better fit between the simulation and the experimental data is lower for the core compared to the sandpack. The adsorption for the core is about 200 μg per g of rock.

This effect can be explained by the fact that polymer adsorption is a function of the surface area in contact with the flooding fluid [28]. The grater the surface area per unit of bulk volume flooded, the greater the polymer loss. Therefore, the fine-grained sands of which a sandpack is composed adsorb much more polymer per unit of bulk volume than do the rock of a core (Omar, King Saud, SPE 11503, [29]).

The implementation of the shear rate simulation in the model is very important to represent correctly the experimental data, especially for the core flooding.

The bigger impact of shear effect upon the core is due to the fact that the loss of mobility control in a formation caused by mechanical degradation is more severe with lower formation permeability, typical of the core (Maeker, SPE 5101, [30]).

In Figure 8-19 is shown a comparison between two simulations, one of which implements the shear effect while the other doesn't. It is possible to note that neglecting the shear effect leads to a big error.

In Figure 8-20 is possible to observe the variation of brine viscosity inside the core, at the beginning of polymer flow, represented using the viewer Kraken.

In Figure 8-21 is possible to study the trend of viscosity linked to the shear rate variation of the fluid inside the core, at two different moments of the flooding.

At the time in which 6 pore volumes were fluxed, the injection of polymer had just began. It is possible to distingue the front of high viscosity fluid proceeding inside the core.

At 7 pore volumes injected, the polymer injection had just finished. The front of high-viscosity fluid is moving inside the core, followed by the low-viscosity brine, which is being injected after the polymer.

The shear rate effect makes the high-viscosity front not to be sheer. The viscosity of the polymer solution tends to decrease as the high viscosity solution proceeds inside the core.

Since the core is extracted directly from the reservoir, it is more representative of the reservoir rock properties. It can be deduced that the reservoir is largely composed by rock with a small permeability, and it will be important to consider the shear effect while doing the study upon the reservoir sector.

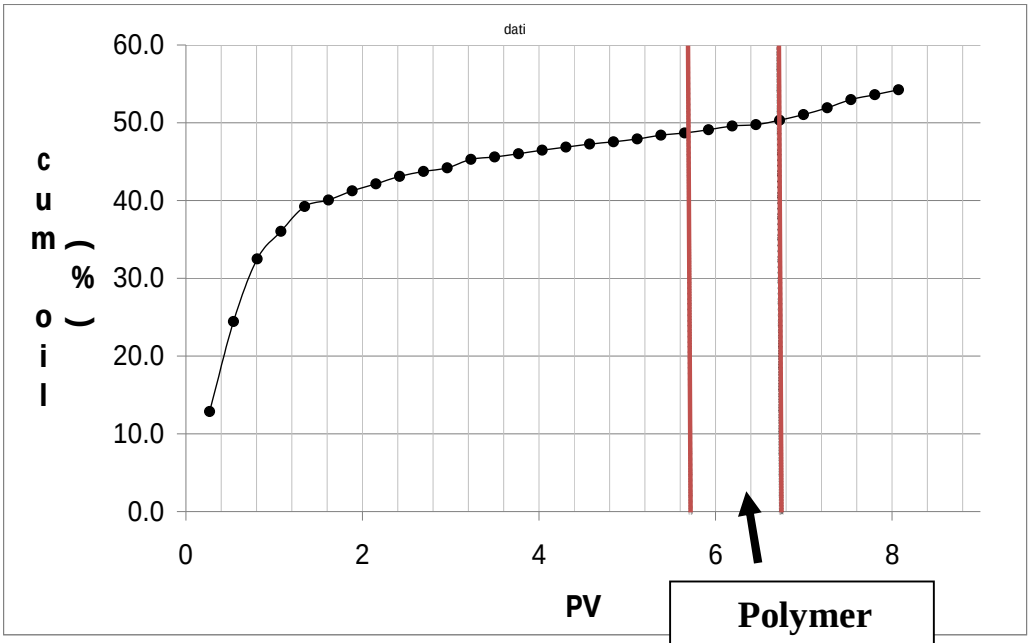

Figure 8-15 – Recovery data from core flooding

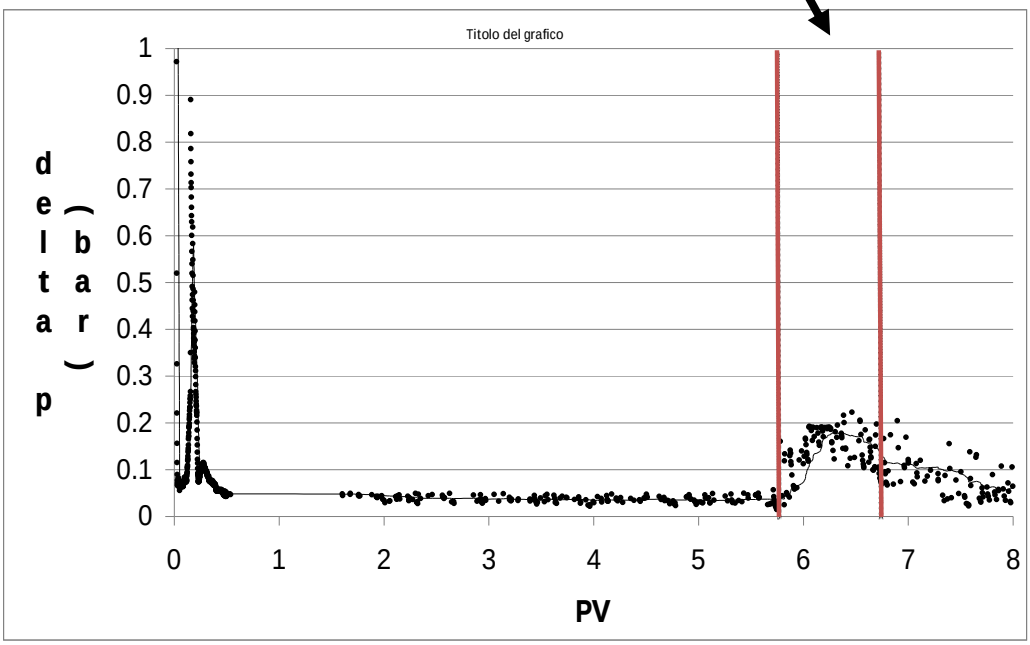

Figure 8-16 – Pressure data from core flooding

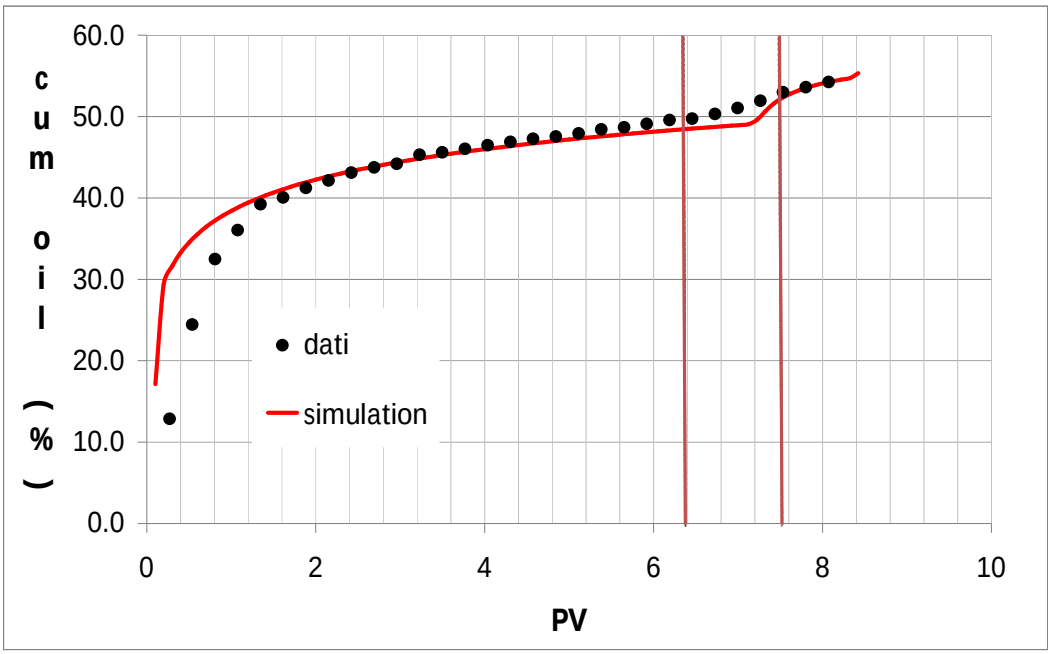

Figure 8-17– match of recovery data from core flooding with polymer solution

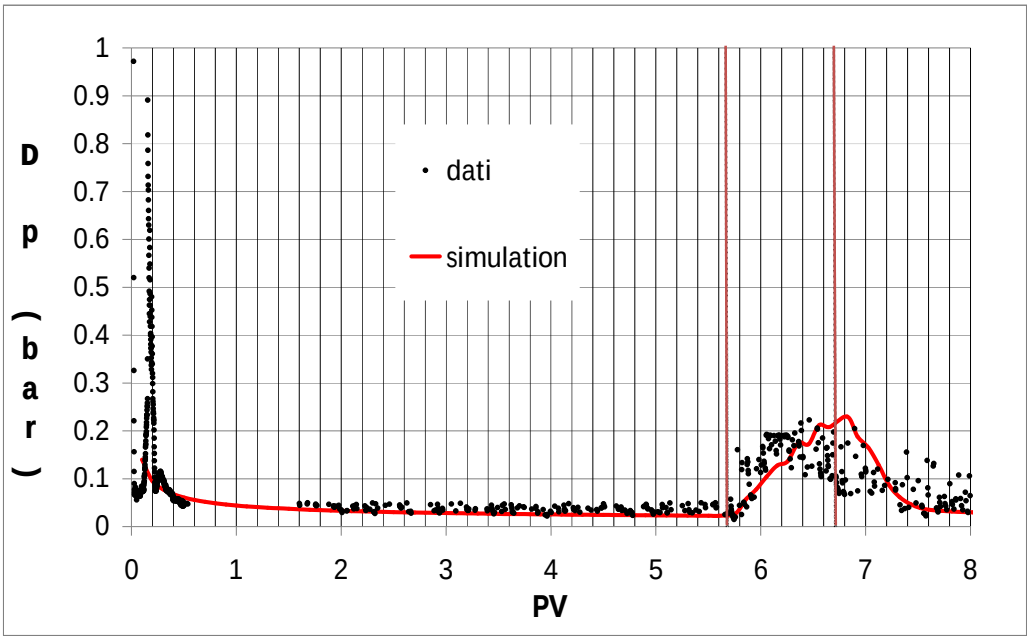

Figure 8-18 – match of pressure data from core flooding with polymer solution

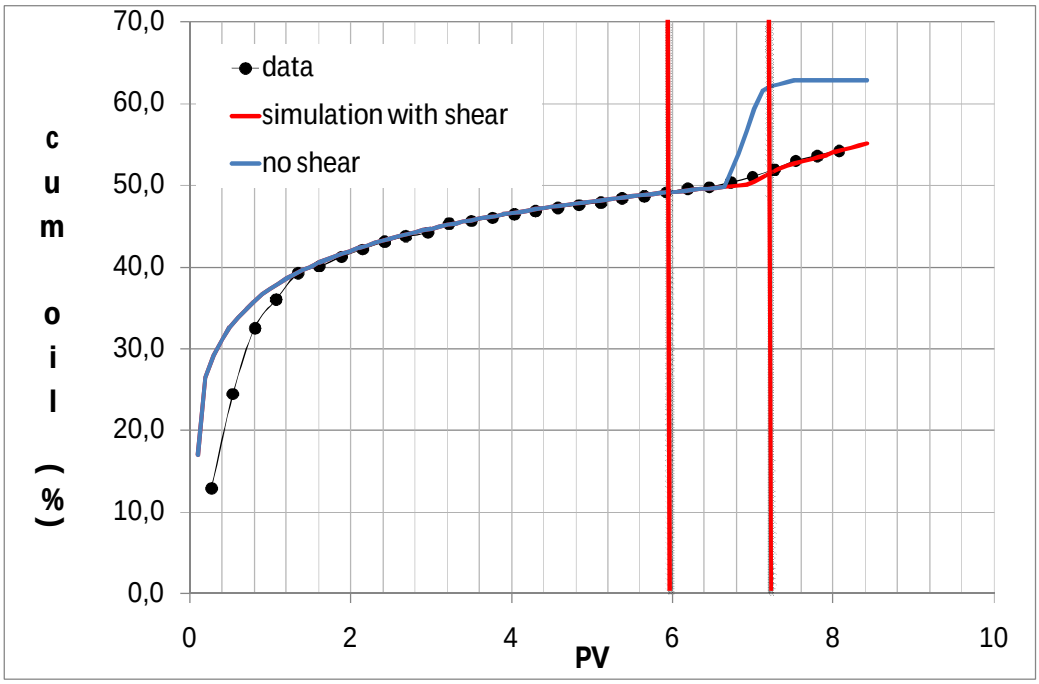

Figure 8-19 – Comparison between simulations implementing shear effect and not

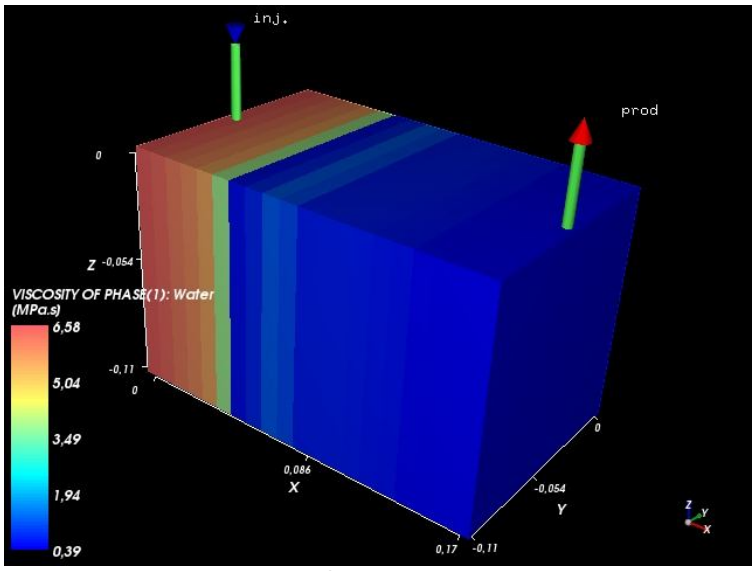

Figure 8-20 – representation of viscosity variation inside the core at the beginning of polymer flow

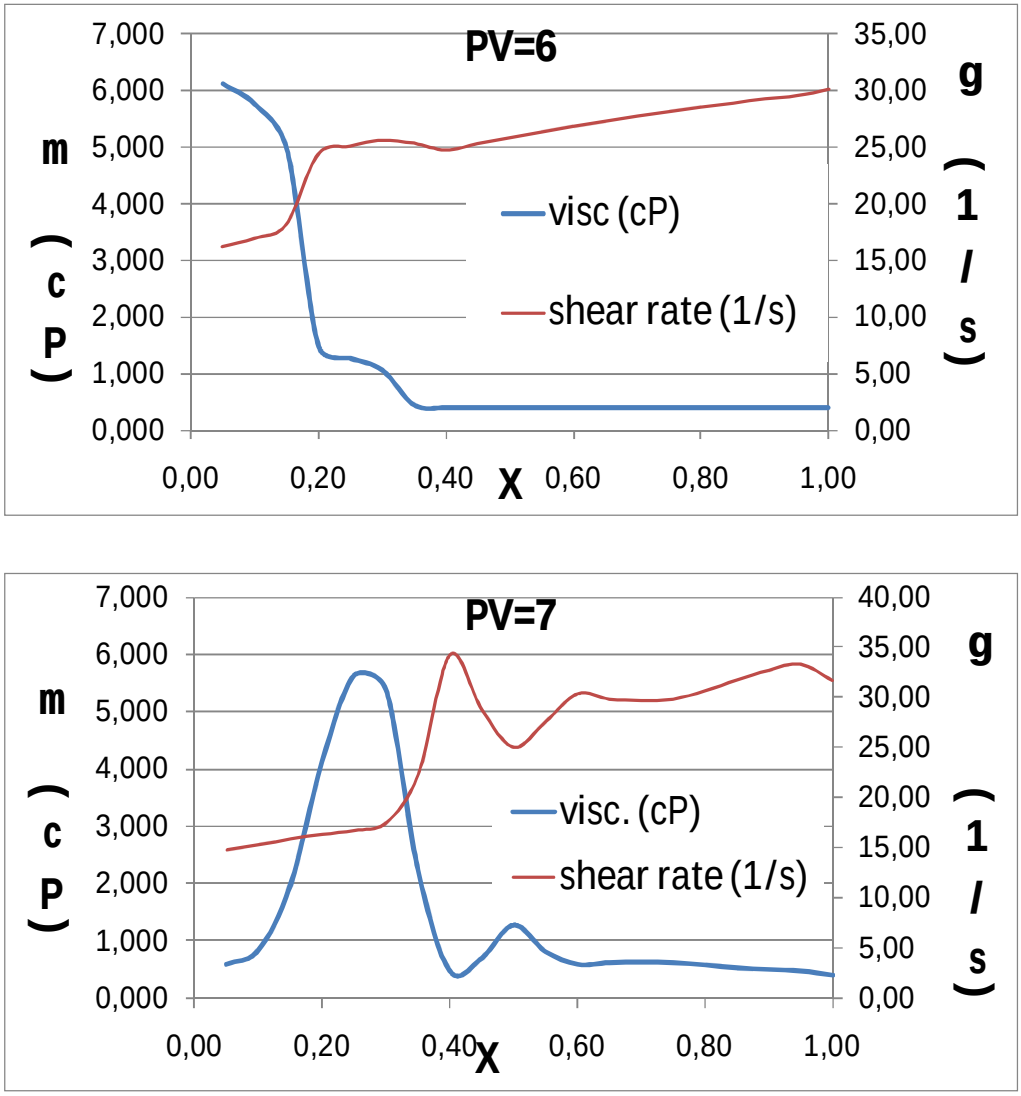

Figure 8-21 – viscosity and shear rate trend inside the core, at the begininning and and at the end of polymer injection

9. SIMULATION OF THE BEHAVIOR OF A RESERVOIR SECTOR

After identifying the most promising process, the screening methodology requires the preliminary prediction of reservoir performance.

The most common approach used to forecast future production profiles consists in detailed reservoir simulation. This approach requires specific data, such as historical production data and detailed simulation models. Data requirement can limit this application as a screening tool in situations in which few data are available.

To overcome these limitations, reservoir sector models are used.

The use of small sector models allows for a set of type curves to be quickly generated to cover the desired range of geological variables and development strategies. By varying the physical properties of the sector model to match those of the actual field, the curves are able to capture the expected impact of the technique studied on the flood performance.

9.1. Definition of a static model of reservoir rock

The most important phase of a reservoir study is probably the definition of a static model of the reservoir rock, given both the large number of activities involved, and its impact on the end results.

The production capacity of a reservoir depends on its geometrical/structural and petrophysical characteristics. The availability of a representative static model is therefore an essential condition for the subsequent dynamic modelling phase. A static reservoir study typically involves four main stages, carried out by experts in the various disciplines (Cosentino, 2001, [31]).

The first one is the structural modelling. It consists in reconstructing the geometrical and structural properties of the reservoir, by defining a map of its structural top and the set of faults running through it. This stage of the work is carried out by integrating interpretations of geophysical surveys with available well data.

The second is the stratigraphic modelling. In this phase a stratigraphic scheme is defined using well data, which form the basis for well-to-well correlations. The data used in this case typically consist of electrical, acoustic and radioactive logs recorded in the wells, and available cores, integrated where possible with information from specialist studies and production data.

Then there is the lithological modelling. Definition of a certain number of lithological types, also called basic facies, is performed in this phase for the reservoir in question. The facies can be considered the building ‘blocks’ of the

lithological reservoir model. They are aspects and characteristics of a rock unit, which allows distinguishing the rock from the units associated or adjacent. Sometimes they highlight the conditions of origin of the rock [32]. They are characterized on the basis of proper lithology, sedimentology and petrophysics. This classification into facies is a convenient way of representing the geological characteristics of a reservoir, especially for the purposes of subsequent three-dimensional modelling.

Finally a petrophysical modelling is carried out. It is a quantitative interpretation of well logs to determine some of the main petrophysical characteristics of the reservoir rock, such as porosity, water saturation, and permeability. Core data represent the essential basis for the calibration of interpretative processes.

The results of these different stages are integrated in a two or three-dimensional context, to build what we might call an integrated geological model of the reservoir. This one, on one hand, represents the reference frame for calculating the amount of hydrocarbons in place, and, on the other hand, forms the basis for the initialization of the dynamic model.

9.2. Field general information

The field studied is filled with heavy oil. The first main well was put on stream in 1992, and was the only well in this area for approximately 15 years, then following 12 additional wells were drilled for further development to increase oil production and recovery.

Detailed geological and dynamic modeling of this area was carried out in 2006, based on the data obtained from the only existing well at that time.

The formation is split into a lower and an upper member. The lower member is dominated by siliciclastic facies (clean sandstones), while the upper member is a mixed-sediment succession, where carbonate facies increase progressively upwards, until they become dominant.

The facies association observed on cores, the regional geological data and the image log report allow assuming that the formation deposited in a mixed carbonate/siliciclastic depositional system, fed by a fluvial system entering the basin from the south.

The system is thought to be influenced by a weak wave and tidal activity.

The characteristics of the siliciclastic finer sediments suggest the presence of a protected, possibly poorly oxygenated environment indicating a lagoonal-like character.

Using a geological model, incorporating the field data, the reservoir characterization was set up.

Five different facies, or rock types, were identified: carbonate, shale, shaly sand, silty sand, clean sand. The range or set of intervals of a rock reservoir

from which can be produced hydrocarbons in economic quantities is called “pay”. Carbonate and shale are not pay, while the sands are (Figure 9-2).

In general, all the tests show a very low well productivity index (less than 0.5 barrel/psi) and a quite good average permeability (around 200 mD).

The pressure measured at the depth of 5000 ft is around 2500 psi.

The main conclusions of the 2006 study suggested that water injection is the best development scenario for the area and recommended further work to evaluate the feasibility of polymer injection which turned out to be the most beneficial EOR.

9.3. Thermodynamic modeling

Both bottom-hole and surface oil samples were utilized to characterize the thermodynamic properties of oil.

The outcome of all PVT analysis shows that oil from Aghar-4 area is relatively heavy with an API gravity of 16. It is largely undersaturated due to extremely low bubble point pressure (36 psi).

Basic oil properties are the following:

Oil API density:	16 °API
Oil density at reservoir conditions:	58.6 lb/ft3 (938.7 kg/cm3)
Oil viscosity at reservoir conditions:	23 cP
Rs (flashed GOR):	7.2 scf/stb
Pb:	36 psi

The reservoir fluid is modelled as black oil, which means that the fluid composition is assumed to be constant.

The water properties were calculated by correlations as a function of pressure, temperature and salinity, based on a salinity value of 63400 ppm.

The values input in the model are:

Water density (Standard Conditions) = 64.8 lb/ft3

Water density (Reservoir Conditions) = 163.36 lb/ft3

$B_W = 1.023$

$C_W = 2.67E\text{-}6$ 1/psi

$\mu_W = 0.395$ cP.

9.4. Description of the reservoir sector considered

The facies distribution map for each layer was provided after sedimentological analysis. 71 zones were identified. The maps are drawn using the software Petrel. Each map honors both well data and conceptual sedimentological model (Figure 9-3).

The Facies Conceptual Model was used as a trend to drive the porosity and permeability distribution. Each facies has its own petrophysical characterization which was used to distribute petrophysical properties (Porosity, Permeability and Irreducible Water Saturation).

The dimensions of the grid relative to the field are summarized in the table below:

DIMENSIONS (number of cells in the three directions)	TOTAL NUMBER OF CELLS	ΔX (increment along x direction)	ΔY (increment along y direction)	ΔZ (increment along y direction)
151x68x407	$4.18*10^6$	≈164 ft	≈164 ft	≈1 ft

Table 9-1 – properties of the grid-model of the field

The layering was performed using a proportional method.

A detailed layering provides a better characterization of the properties such as porosity and permeability inside the 3D geological grid.

After the field modeling, the performance of the field has been tested by a limited sector model, to qualitatively evaluate the potential of the EOR method.

A sector containing a couple of wells was chosen (Figure 9-3). The wells were chosen because they showed a good hydraulic communication and a proper distance with the surrounding producers.

The number of layer was reduced from the original 407 to 71, to increase the speed of the simulations. 71 is the minimum number of layer which allows a good representation of reservoir properties. A smaller number of cells would have simplified too much the model, merging cells with too different properties.

The limited sector has the characteristics shown in Table 9-2.

DIMENSIONS (number of cells in the three directions)	TOTAL NUMBER OF CELLS	ΔX (increment along x direction)	ΔY (increment along y direction)	ΔZ (increment along y direction)
16x12x71	≈13632	≈80 ft	≈90 ft	≈3 ft

Table 9-2 – reservoir sector characteristics

The sector grid was defined using the simulator UtChem, by implementing corner-point geometry (Figure 9-1). The input of the program is made up with the coordinates of the corners of each cell.

The wells are open from layer 4 to layer 64.

In Figure 9-4 is possible to observe the reservoir sector modeled.

In Figure 9-5 the initial pressure distribution as modeled by UtChem is shown, while in Figure 9-6 is possible to observe the model map for absolute permeabilities.

Once the pressure at a particular depth is known, the model can compute the pressure distribution in the reservoir. Since the map of saturation is known, the pressure at different levels is computed by applying the hydrostatic gradient.

The pressure gradient expresses the reservoir fluid's increments in pressure in relation to a given increase in depth. It results from the force exerted by weight and is derived by multiplying the density of the reservoir fluid by the gravity acceleration.

The sector is considered as bounded: no flow is taken in consideration across the boundaries.

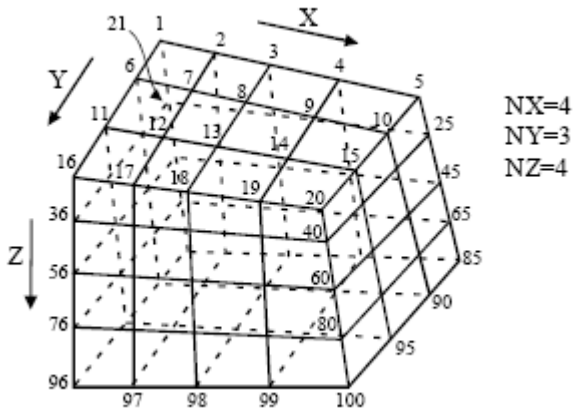

Figure 9-1 – example of corner-point geometry input in UtChem

0	Carbonate/Cemented		Not pay
1	Shale		Not pay
2	Shaly sand		Pay
3	Silty sand		Pay
4	Clean sand		Pay

Figure 9-2 – Types of facies identified in the field

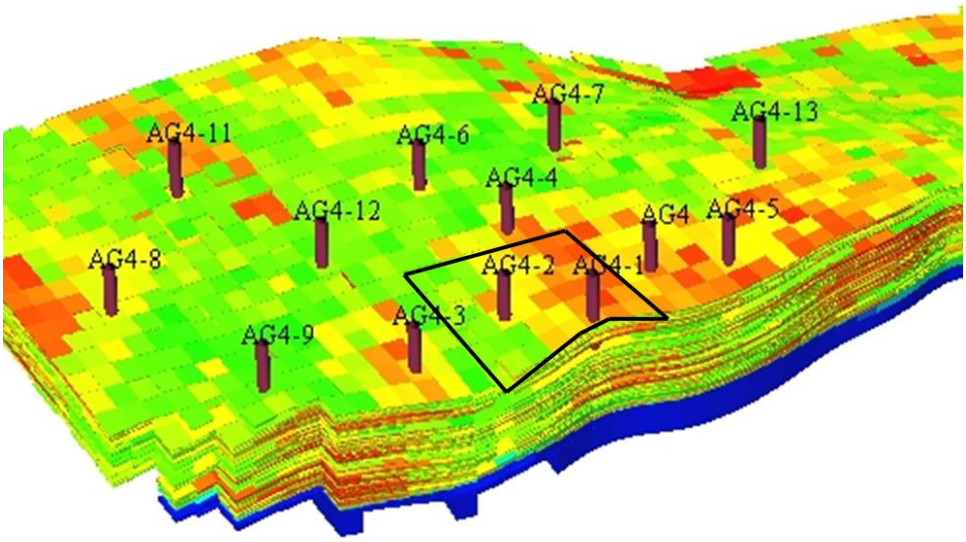

Figure 9-3 – map of the field, highlighting the reservoir sector considered

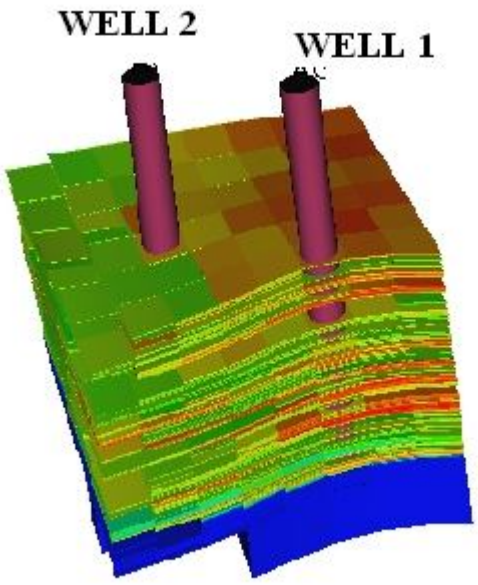

Figure 9-4 – model of the reservoir sector considered

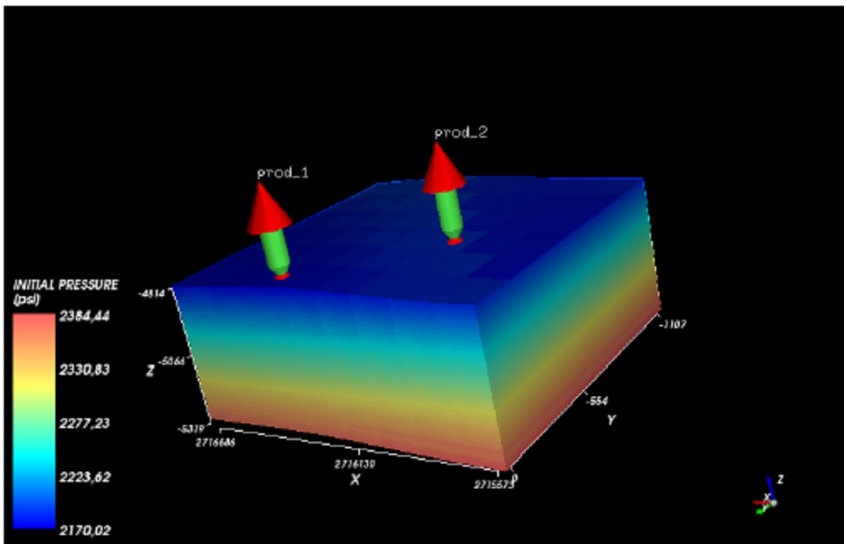

Figure 9-5 – visualization of the pressure distribution inside the reservoir sector

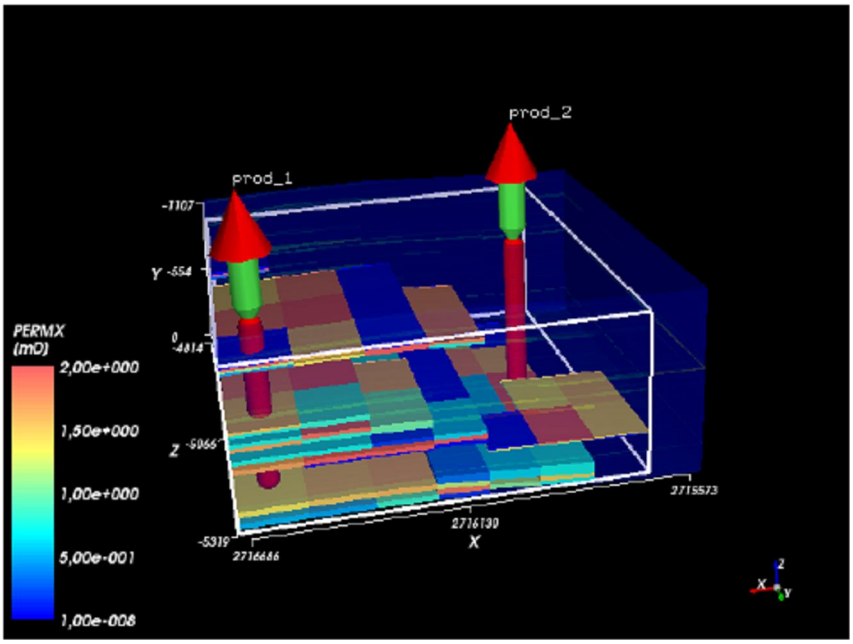

Figure 9-6 – map of permeability distribution

9.4.1.Map of relative permeabilities

To build the map of the rock properties, in particular for the relative permeabilities parameters, informations obtained from the laboratory experiments on core-flooding and sandpack flooding have been used.

In Table 9-4 and Table 9-3 the data found from flooding experiments and the following match are listed. The properties are slightly different from the sandpack and the core, probably due to the different absolute permeability of the two samples. The sandpack is characterized by a 1624 mD permeability, while the core has a 209 mD permeability.

Since the sector simulated is characterized a variable distribution of absolute permeability, the properties got from the sandpack flooding has been implemented in the high-absolute-permeability cells, while the properties got from core flooding has been used in low-absolute-permeability cells (Figure 9-6).

SANDPACK

nw	6
no	2.4
Sor	0.1
kwr	0.4
kor	0.9

Table 9-3

CORE

nw	3
no	4
Sor	0.15
kwr	0.25
kor	0.9

Table 9-4

9.5. Natural depletion simulation

In the sector considered two wells are present (Figure 9-4). In the first production phase, both wells were set up as producers, to make use of the energy within the system itself, which is the pressure already in the reservoir. The same condition has been set up in the simulations, to try to reproduce the same situation existing in reality.

Since the sector is completely bounded around its boundaries, the space available to hydrocarbons varies very little during production: in this situation, the reservoir performance is defined as being volumetric type. The main drive mechanism is the expansion of hydrocarbons contained in the reservoir, referred to as *natural depletion drive.*

The main consequence of the production of fluids from a field is a drop in the average reservoir pressure. The final recovery percentage depends on the initial pressure and the abandonment pressure (Verga, 2001, [33]).

The production wells have been set up to produce a fixed rate of liquid, corresponding to 60 barrels per day each.

The first noticeable effect of natural depletion simulation is the decrease of pressure with the passing of time, as shown in Figure 9-7.

In the simulation the depletion has been carried out for 700 days. In this way it was possible to represent the real development of the well, starting from the known value of initial average reservoir pressure to arrive to the current value of pressure in the sector.

The other curve shown in the graph is the recovery factor, which is the ratio between the volume of oil recovered and the volume of oil initially in the field (Equation 9-1).

$$RF = \frac{Volume\ \ of\ \ oil\ \ recoverd\ \ \left(Sm^3\right)}{Volume\ \ of\ \ oil\ \ initially\ \ in\ \ place\left(Sm^3\right)}$$

Equation 9-1 – recovery factor definition

Despite the production of liquid per day is fixed for each well, the cumulative recovery of oil is not a straight line, but the slope of the curve decrease during the time.

This effect is due to the increasing production of water. The water cut, which is the ratio between the rate of water produced and the rate of total liquid produced (Equation 9-2), is shown in Figure 9-8.

$$Water\ \ cut\ \ \left(WC\right) = \frac{rate\ \ of\ \ produced\ \ water}{rate\ \ of\ \ total\ \ liquid\ \ produced}$$

Equation 9-2 – water cut definition

The production of water in mainly due to the change in oil-water contact or profile as a result of drawdown pressures during production. This phenomenon is called "*water coning*", and occurs in vertical or slightly deviated wells and is affected by the characteristics of the fluids involved and the ratio of horizontal to vertical permeability. In this case the high viscosity of oil causes a mobility ratio favorable to water, and the value of vertical permeability is the same of horizontal permeability, so the water production from water coning is significant (Figure 9-9).

The trend of the watercut curve, for the well 2, presents a minimum. This is due to the fact that at the beginning the saturation of water in the sectors near the well decreases, because of the water production. The water saturation, in this production phase, approaches to the critical water saturation, so the water

relative permeability, and as a consequence the water mobility, decreases. After this initial step, other water arrives to the well, from the near cells. This effect increases again the water production.

The water-cut is different from the two wells, as can be inferred from the graph, and is greatly lower in the well n., respect to the well n.2.

This is due to the permeability distribution in the sector. The well n.1 is completed above a zone characterized by very low porosity and permeability, where the flow of fluids is hampered (Figure 9-10). This fact inhibits the water coning effect.

From the simulation results it is possible to observe the variation of the pressure at the wellbore conditions (Figure 9-11).

The solution of the diffusivity equation makes it possible to correlate the pressure's evolution in time p(rw,t), measured at the wellbore of radius rw, to the rate of oil produced qo_{ST} (valued at standard conditions), through the characteristics of the porous medium (permeability k, porosity ϕ; thickness h), the fluid properties (of viscosity μ and volume factor Bo of the oil), and the total compressibility of the system C_t. In measurement units of the International System (SI) such a solution is written:

$$p(r_w.t) = p_s(t) - \frac{q_{oST} \cdot B_o \cdot \mu}{a \cdot \pi \cdot k \cdot h} \cdot \left(\ln 2.25 \cdot \frac{A}{c_A r_w^2} \right)$$

Equation 9-3 – wellbore pressure, function of the production rate

Where $p_s(t)$ is the average pressure reached as a result of the production rate qo_{ST} in time t, A is the extension of the drainage area, and c_A is the Dietz factor, which is dependent on the shape of the drainage area and the position of the well within it.

When the pressure disturbance reaches the boundaries of the reservoir or the boundaries of the area that is drained by the well, the flow becomes pseudo-steady, and the variation of pressure in time becomes constant at any point in the system ($\partial p / \partial t = cons\tan t$) (Verga, 2001, [34]).

Wellbore pressures decrease at a higher rate respect to the average pressure of reservoir. This is because the pressure disturbance is first generated in the wellbore and then it propagates to the rest of the formation.

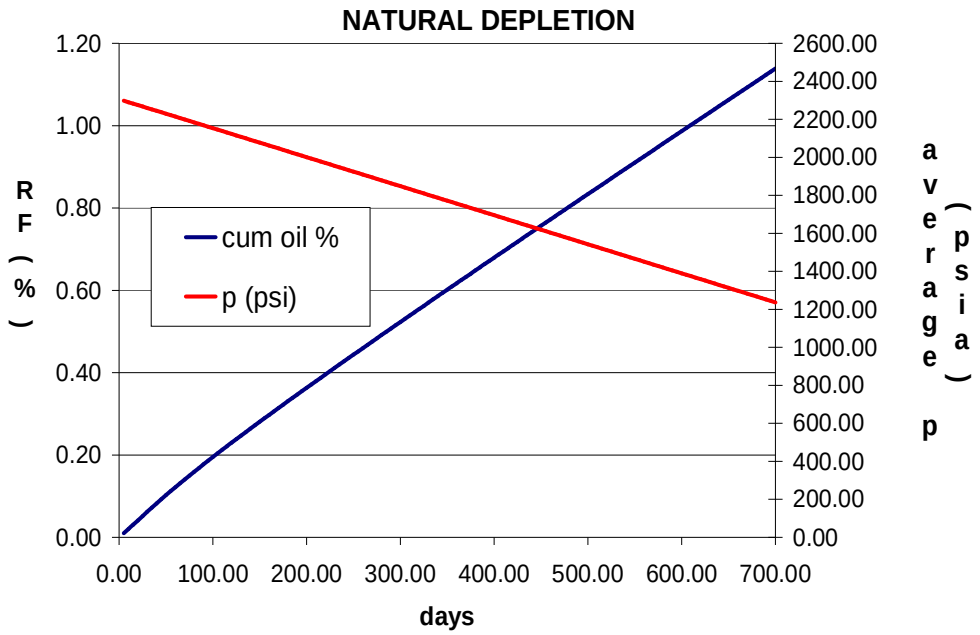

Figure 9-7 – average reservoir pressure and recovery of oil from a natural depletion simulation

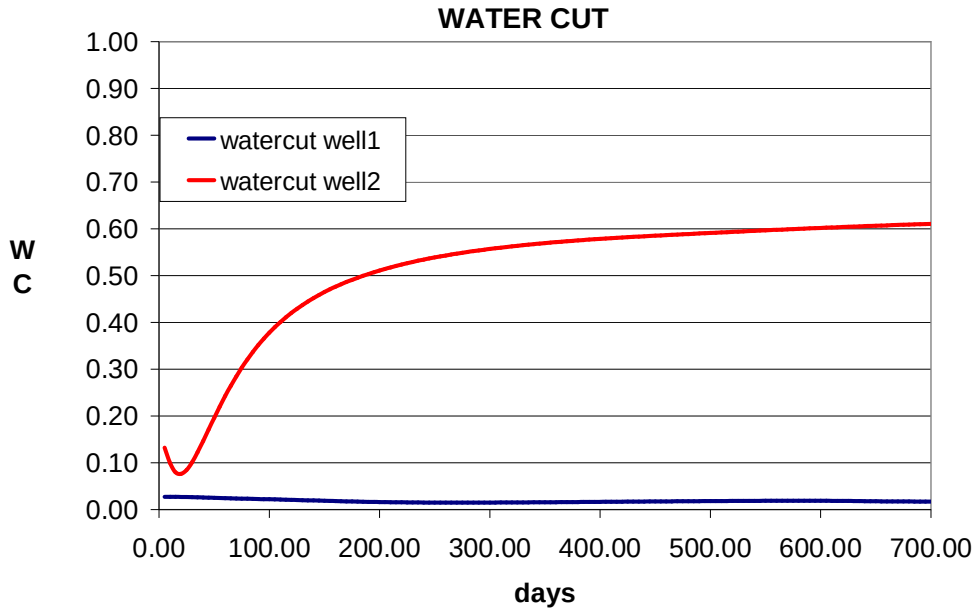

Figure 9-8 – watercut for each well

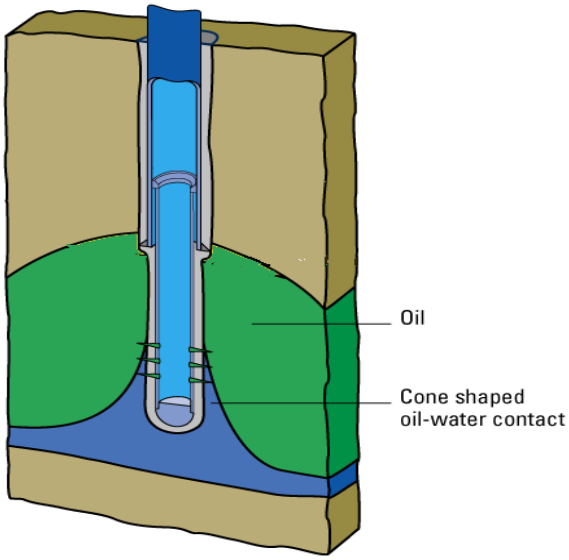

Figure 9-9 – water coning effect

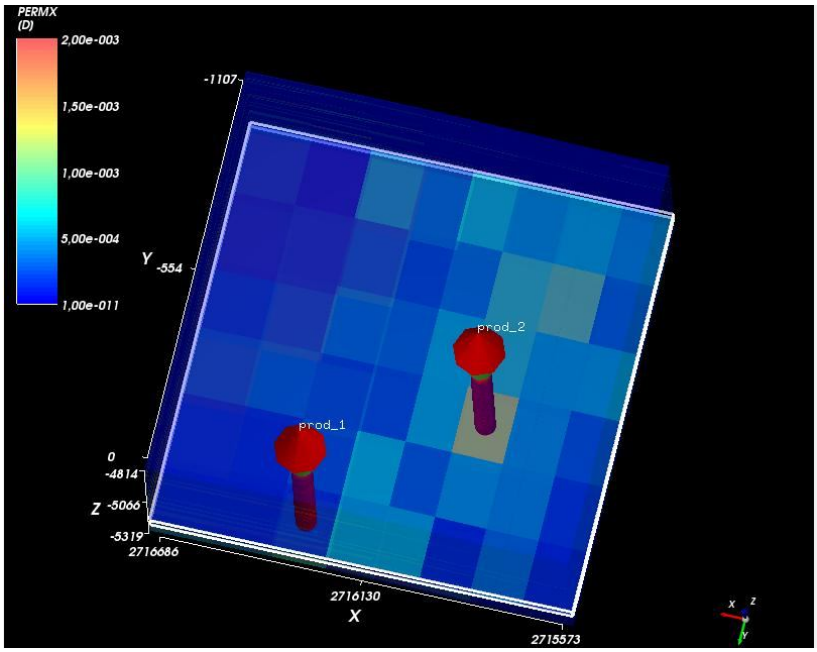

Figure 9-10 - Permeability distribution of the deepest layer, from which it is possible to note that the well n.1 is above a low-permeability area.

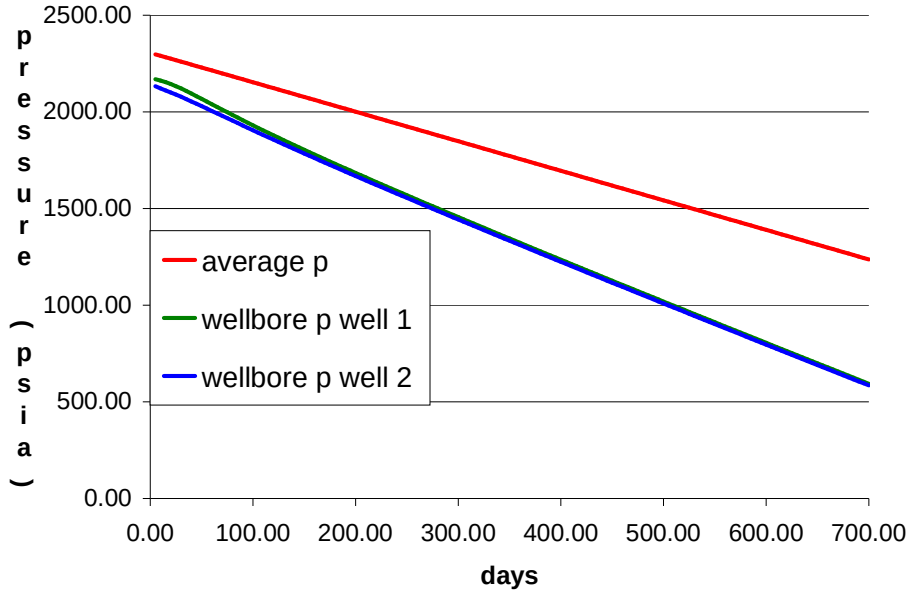

Figure 9-11 – wellbore pressures and average pressure trend

9.6. Waterflooding simulation

When the wellbore pressure reaches too low levels, it needs to be raised up, for mechanical reasons and to avoid the collapse of the well deep in the formation.

Waterflooding is the main method to raise the wellbore pressure of the wells and the average pressure of the reservoir, to supply energy necessary to the drive mechanism of recovery.

In the case studied a waterflooding was simulated, after 700 days of natural depletion. The water has been injected in well n.1. The rate of water injected is 300 bbls/day, three times the liquid produced by well n.2, and this injection has been carried for 300 days.

The results are shown in Figure 9-12 and Figure 9-13.

It is possible to notice that the waterflooding has successfully increased the reservoir pressure till a value near to the initial pressure.

Also the wellbore pressures of the two wells increased (Figure 9-13).

The wellbore pressure of the injector first suddenly increases, in the transient conditions. Then, when the pressure disturbance reaches the boundaries of the sector, the pressure trend reaches the steady conditions and the pressure increase becomes linear.

The wellbore pressure trend for the producer shows a delay, due to the time needed to the pressure disturbance to reach the producer, starting from the injector well.

Also the recovery increased, but the recovery curve is now characterized by a lower slope, which means a lower oil rate production. The total liquid flow rate is fixed, so the water produced increased, as it is possible to see from the watercut curve (Figure 9-14).

Waterflooding had a negative effect on displacement efficiency. Due to the high viscosity of oil, the mobility ratio was unfavorable and water tends to bypass oil, creating preferential channels, as it is possible to see from Figure 9-15, where the map of saturation of water for one layer during injection was plotted.

Pressure can't be raised to a value higher than the initial reservoir pressure, to avoid damages upon the formation.

So, when the initial value of pressure was reached, the water injection rate was decreased to 100 bbl/day, the same value of the liquid production rate (Figure 9-16).

Under these conditions the pressure remains constant, since the formation volume factor of the two liquid phases indeed have a similar value, and it is possible to observe a further increase in the watercut (Figure 9-17).

This is due to the fact that water has already its preferential channels, and plus the pressure drive is now decreased. It results in a further disadvantage for the flow of oil.

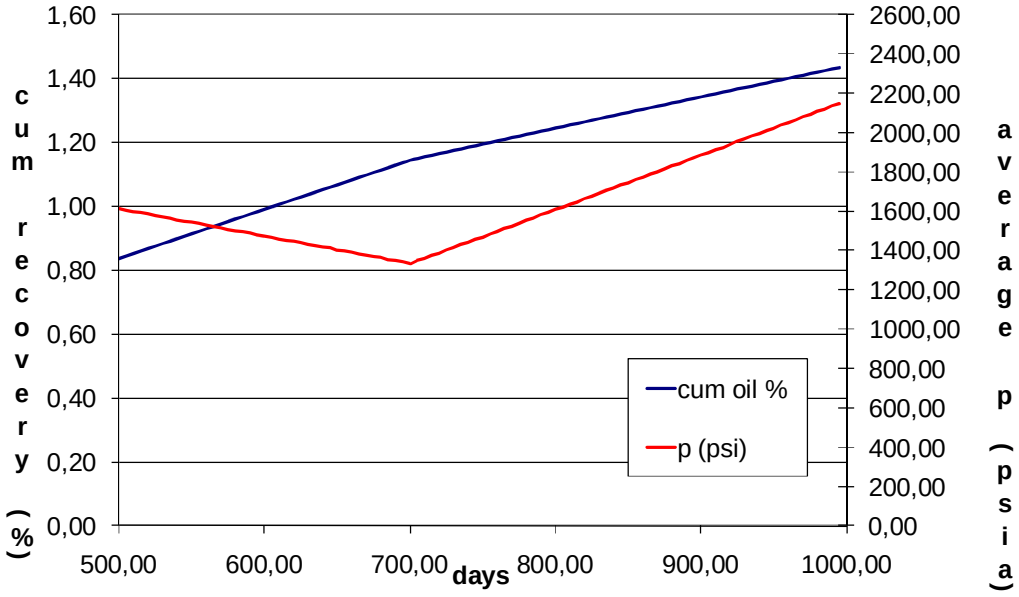

Figure 9-12 – results from water injection simulation

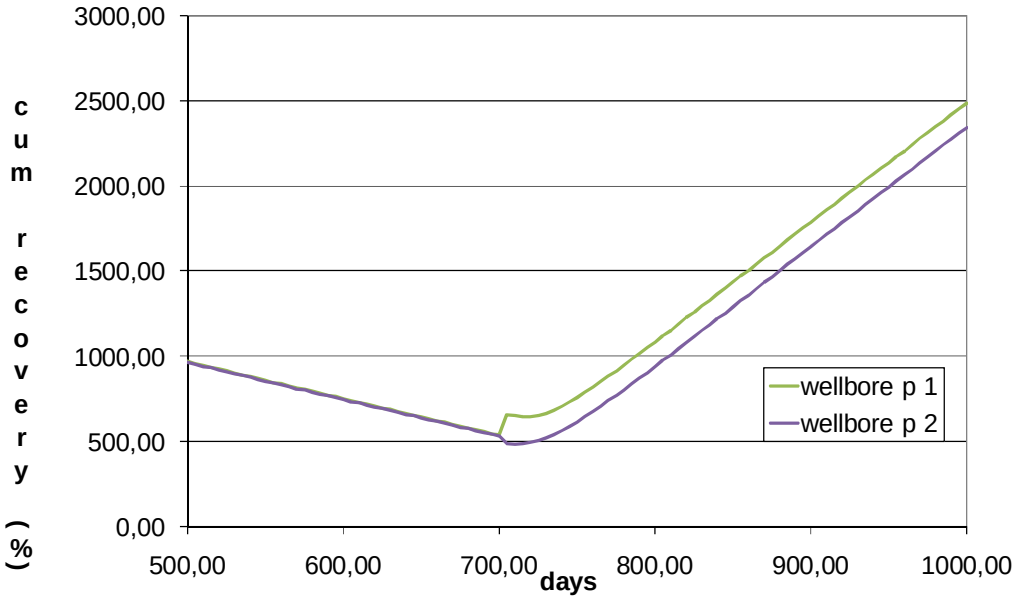

Figure 9-13 – wellbore pressure trends during water injection

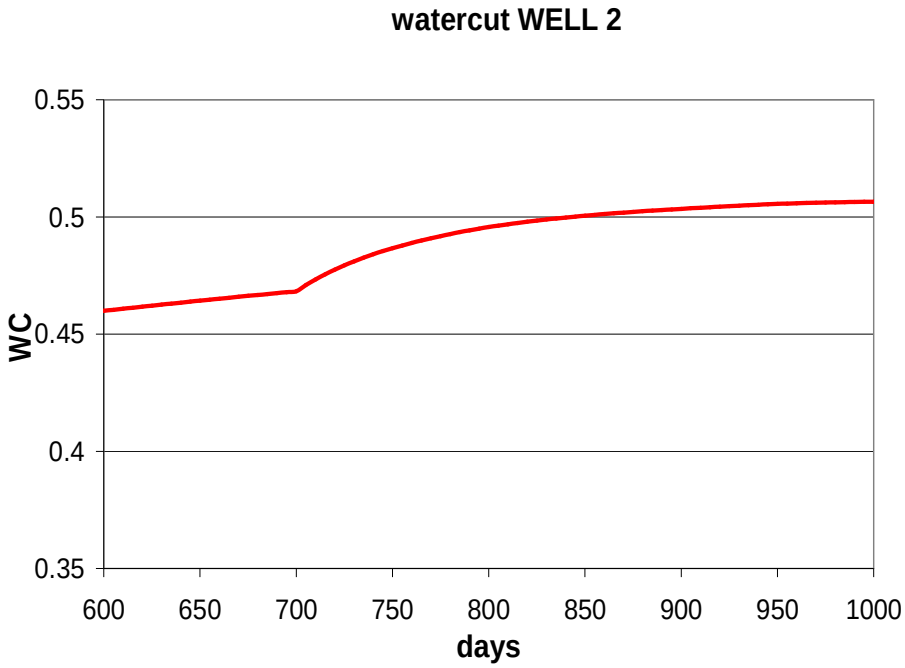

Figure 9-14 – watercut trend after water injection

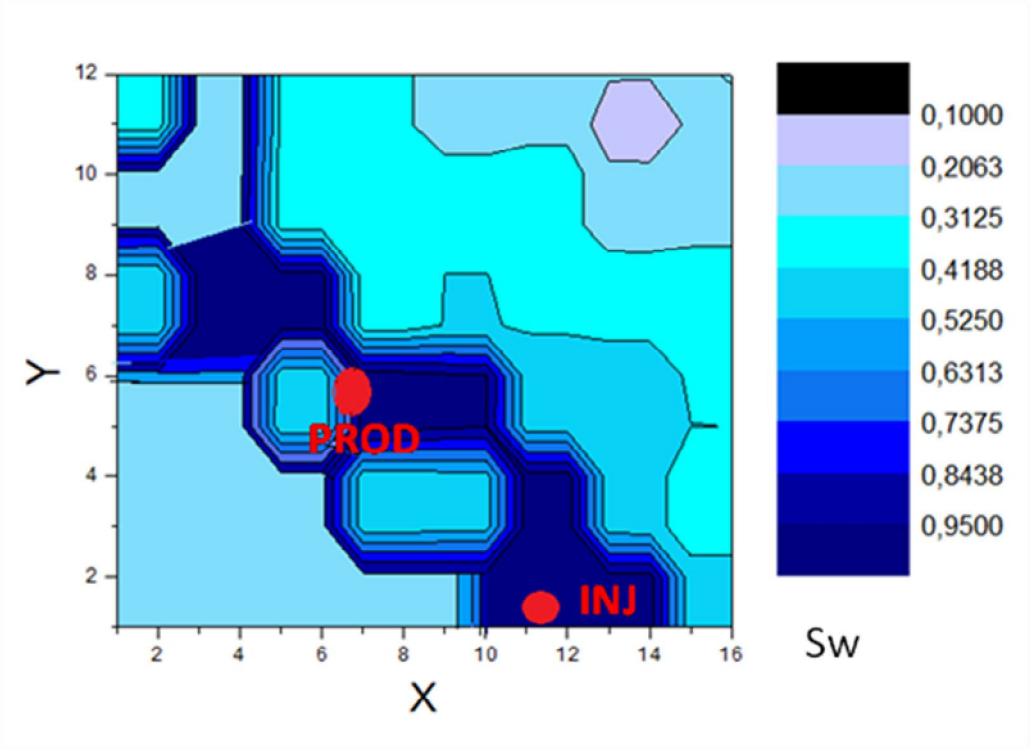

Figure 9-15 – map of water saturation in one layer during injection

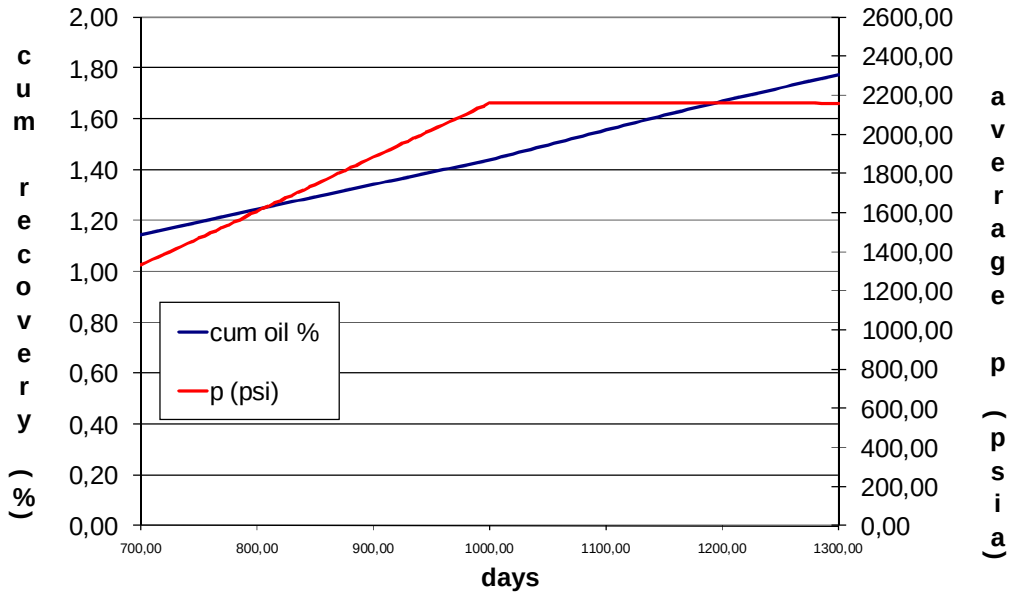

Figure 9-16 – results after continuing simulating wateflooding, injection the same rate produced

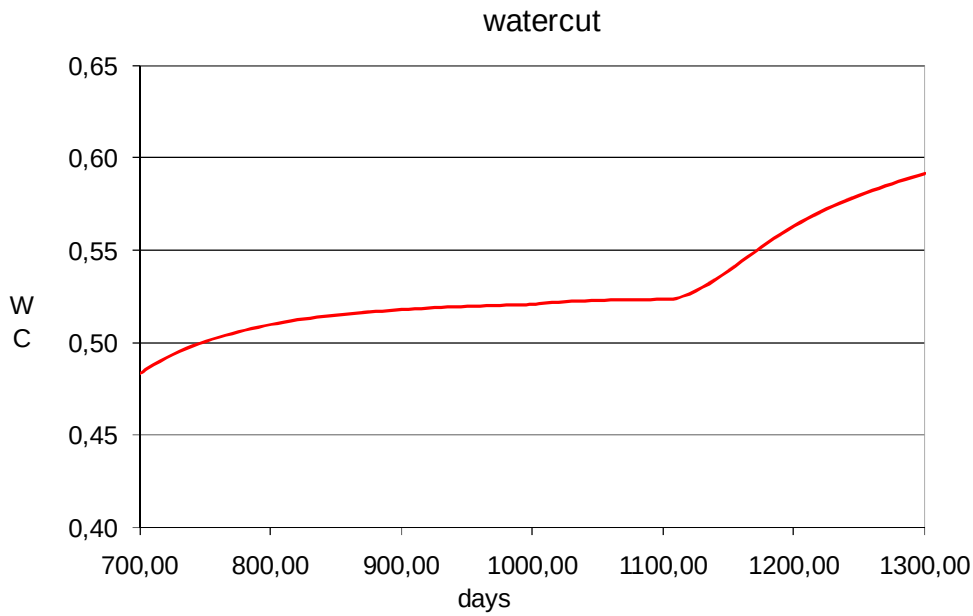

Figure 9-17 – watercut increase after having reduced the injection rate

9.7. Polymer flooding simulation

Two simulations have been conducted at this point. In the first a normal waterflooding is performed for additional two years. In the other simulation the flooding is conducted implementing a polymer injection.

Polymer concentration in the injected stream is set as 2500 ppm.

The two simulations were compared and the results are shown from page 111.

The increasing viscosity of the water injected inside the reservoir leads to a more favorable mobility ratio. This effect is visualized in Figure 9-18, were the viscosity distribution of the aqueous phase inside a reservoir layer is shown. The layer chosen to show the polymer spread is a high-permeability one, where the increased mobility of the solution shows its effects the best visibly. High viscosity brine spreads from the injection well, until it reaches the production well.

The increased areal efficiency determined by the higher viscosity is shown in Figure 9-19, Figure 9-20 and Figure 9-21.

In Figure 9-19 the water saturation distribution at 1300 days of simulation is shown. The existence of preferential channels in the flow of water from one well to the other can be noticed.

In Figure 9-20 the distribution is shown after 2500 days. In this case only the formation water has been injected, without any polymer.

In Figure 9-21 the distribution is shown at the same time step, 2500 days, but in this case the solution with polymer has been injected, starting from 1300 days.

In the case in which only water is injected preferential channels still exist. In the case in which polymer is injected and the water mobility is smaller, the area contacted by the aqueous solution is more uniformly distributed.

This result seems to confirm that polymer injection increases the areal sweep efficiency.

The production results of the two simulations were compared, and the comparison in the watercut results is shown in Figure 9-22.

In

Figure 9-23 the production rate of oil for the two cases is compared.

From the results it can be observed that adding polymer to the injected solution allows recovering more oil with the same amount of injected water.

Extending the simulation along the life of the field, after 24 years the scenario with polymer injection shows a production of oil the 38% greater respect to the scenario in which only water is injected (Figure 9-25).

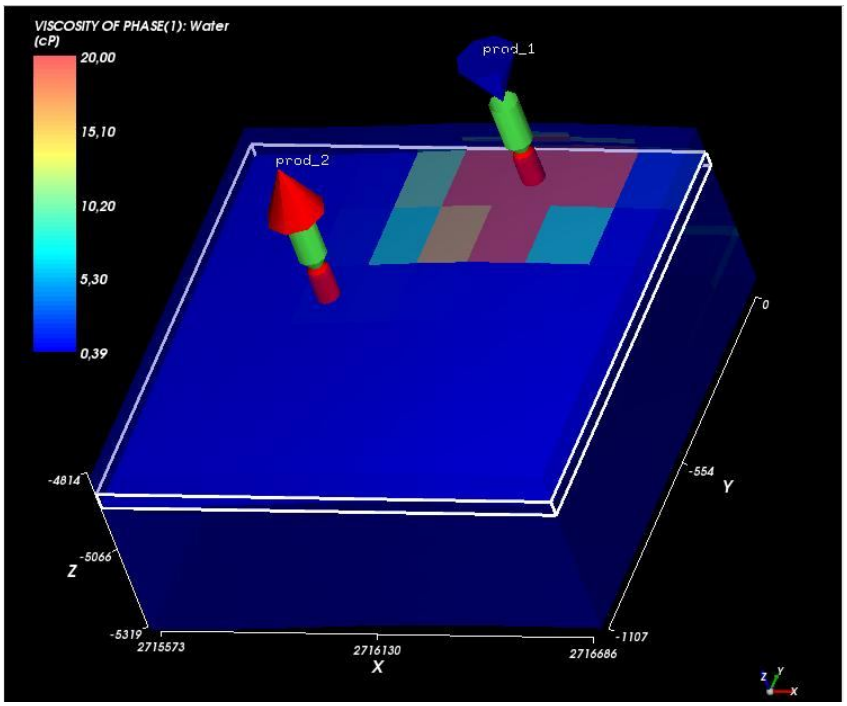

Figure 9-18 - spreading of the high-viscosity solution in a reservoir layer

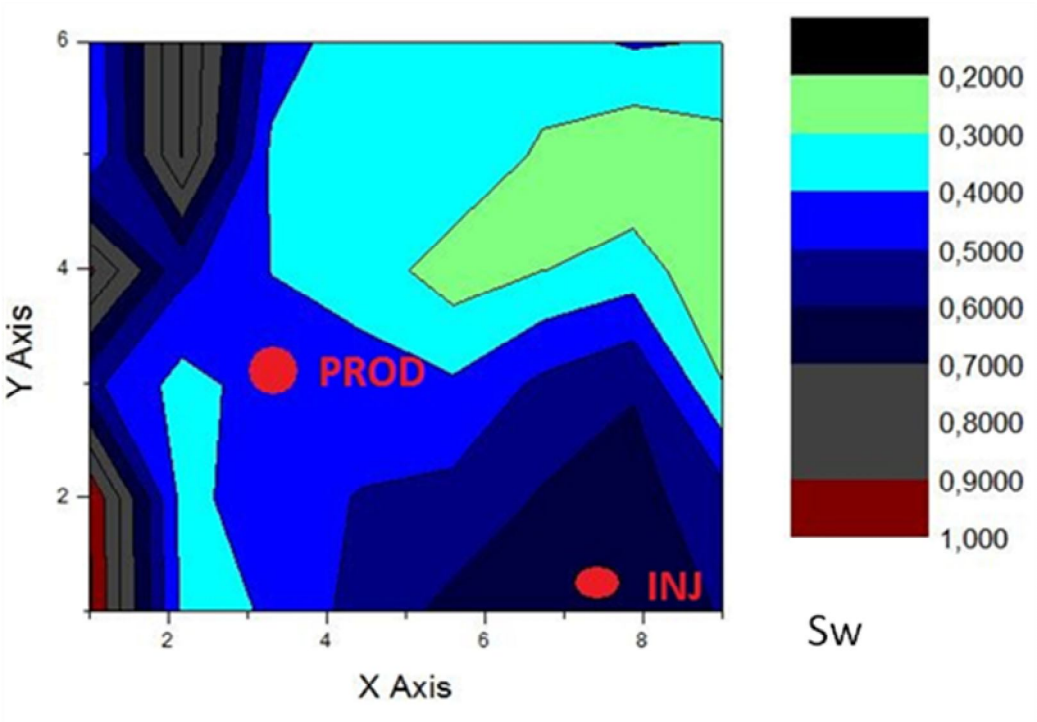

Figure 9-19 - water saturation distribution at 1300 days of simulation

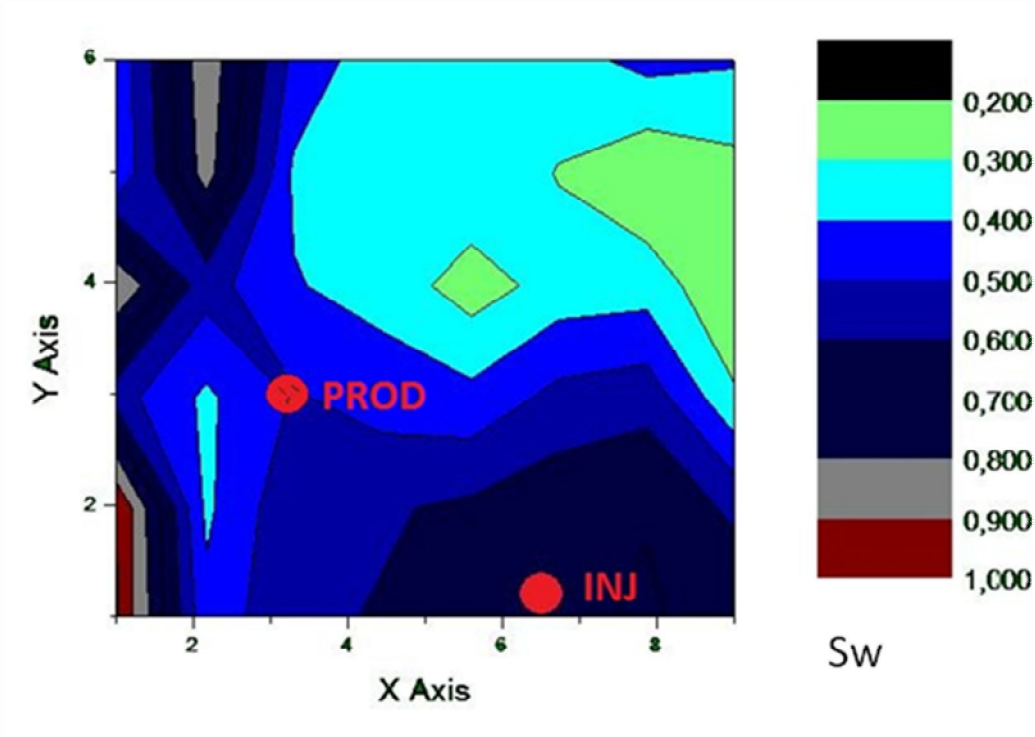

Figure 9-20 - water saturation distribution at 2500 days of simulation, injecting only water

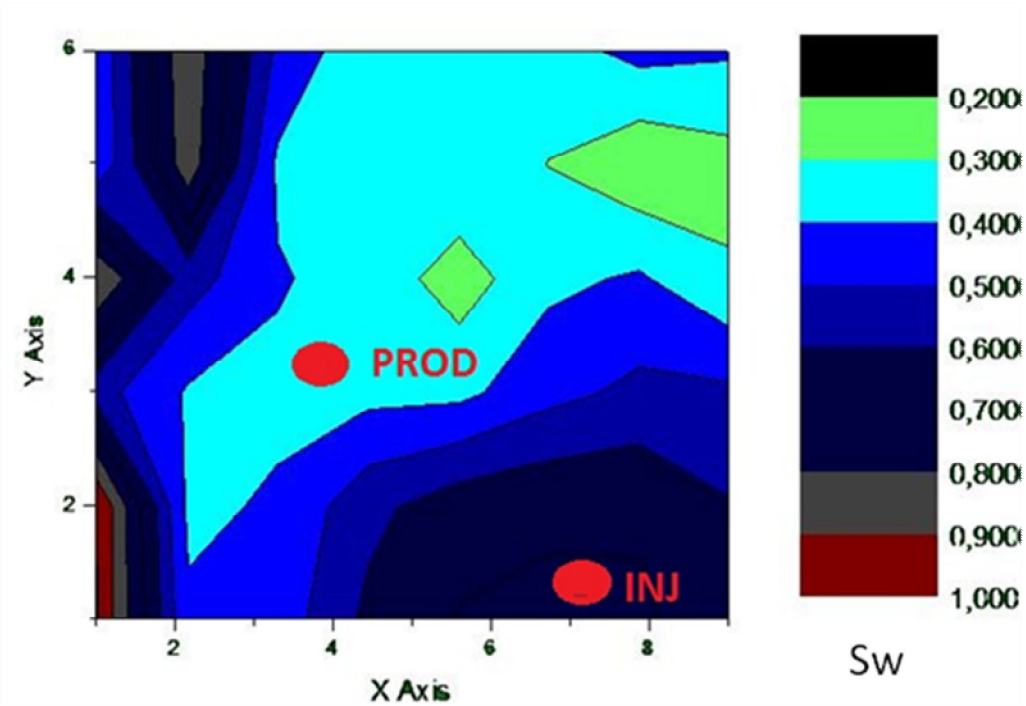

Figure 9-21 - water saturation distribution at 2500 days, injecting the solution with polymer. It is possible to note an increased areal efficiency

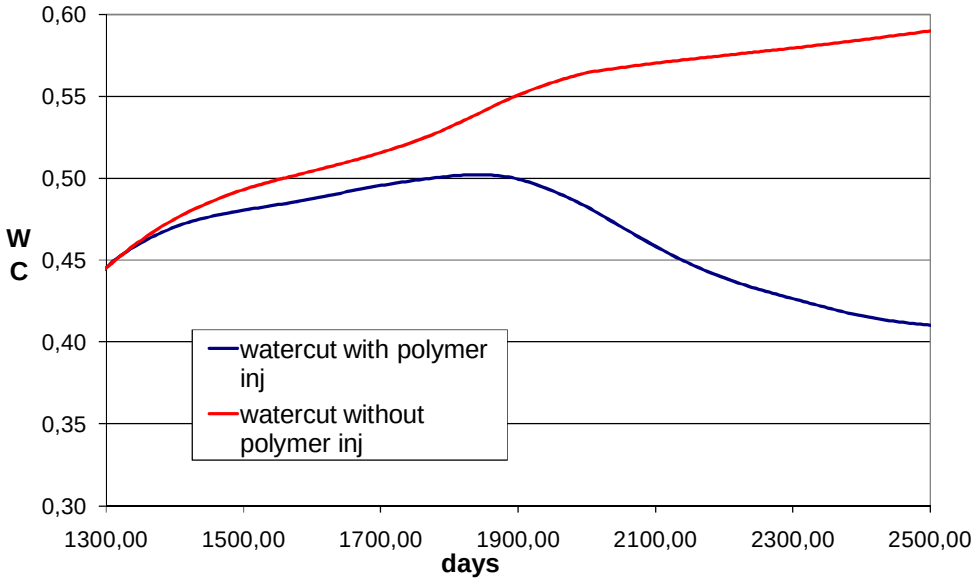

Figure 9-22 – watercut compared for the two simulations, with and without polymer injection

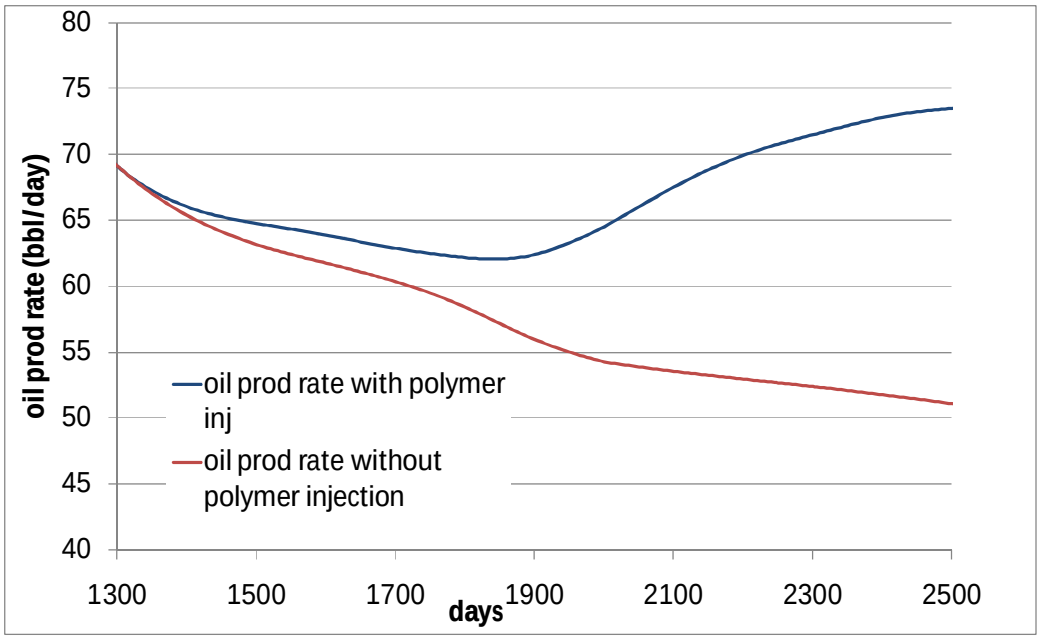

Figure 9-23 – comparison of the oil production rates for the two simulations, with and without polymer injection

9.8. Economics and optimization of injection time steps

The simulations were conducted to represent the trend for of watercut and production for several years. The results, up to 10000 days, are shown in Figure 9-24 and Figure 9-25.

Injecting polymer without interruptions for several years is not the only solution to increase recovery. Since the polymer has a cost estimated around 2 $/kg, the bigger income deriving from the increase in oil production can be balanced by the cost of the polymer to inject. Injecting for a period, then stop and subsequently restart injecting could be more convenient from an economic point of view.

Several configurations of injection time steps were put on comparison.

First the polymer injection was stopped earlier in time and the simulation continued injecting only water. Proceeding with the simulations, injection of polymer was stopped later and later. First at 2000 days of production (which means 700 days of injection) then, in the next scenarios, after 3000 days and then after 5000 (Figure 9-26, Figure 9-27, Figure 9-28). In the graphs the oil production rate of these situations is compared with the ones in the two extreme scenarios: only water injection and only polymer injection for the entire simulation time.

The periods in which polymer was injected are highlighted in the graphs.

The area highlighted in red represents the incremental production of oil due to the polymer injection.

Afterwards new configurations were compared, injecting, stopping and then injecting again the polymer solution along the simulation time.

Polymer was first stopped after 2000 days, and then re-injected from 3000 to 4000 days (Figure 9-29). Another trial was made stopping the polymer at 3000 days, then re-injecting it from 6000 to 7000 days (Figure 9-30). The last trial simulates a first stop at 2000 days, then a reinjection from 3000 to 4000 days, and then another reinjection from 6000 to 7000 days (Figure 9-31).

An economic comparison between the different configurations was made. There is a fixed initial investment (capex), which is the cost of the mixing and polymer-injecting facility. It is estimated to be around 1,500,000 $. The opex, the expense per year, is represented by the cost of the polymer to inject. It can be computed, since the polymer concentration in aqueous phase and the injection rate of the solution are known (120 bbl/day injected, with 2500 ppm polymer concentration, equals to 278 kg of polymer injected every day).

The incremental production due to the polymer has been computed, and the price of oil was set equal to 70 $/bbl. So it is possible to compute the cash flow for each year of production. The cash flow needs to be updated to the present value, using the net present value equation:

$$NPV = \frac{NV_n}{(1+r)^n}$$

Equation 9-4 – net present value equation

NV_n is the net value of the cash flow after n years from the beginning of the investment. r is the discount rate, set up to 10%.

With these conditions, the solution which has the highest net present value is the third discussed, in which the solution with polymer is injected until 5000 days, 14 years of simulation.

After this result another simulation was performed. This time the polymer was injected until 5000 days, but with a smaller concentration, 1500 ppm instead of 2500 ppm. The less the polymer, the less is the viscosity of the solution in the reservoir, and the higher the mobility ratio. As a consequence the recovery decreases, but this effect can be balanced by a decrease in the opex costs, due to the smaller amount of polymer to inject (Figure 9-31).

From the results of the economic comparison, it results that injecting the solution with polymer until 5000 days with a 1500 ppm polymer concentration is the most convenient choice (Figure 9-33). This choice is economic until the oil price keeps higher than 48 $/bbl.

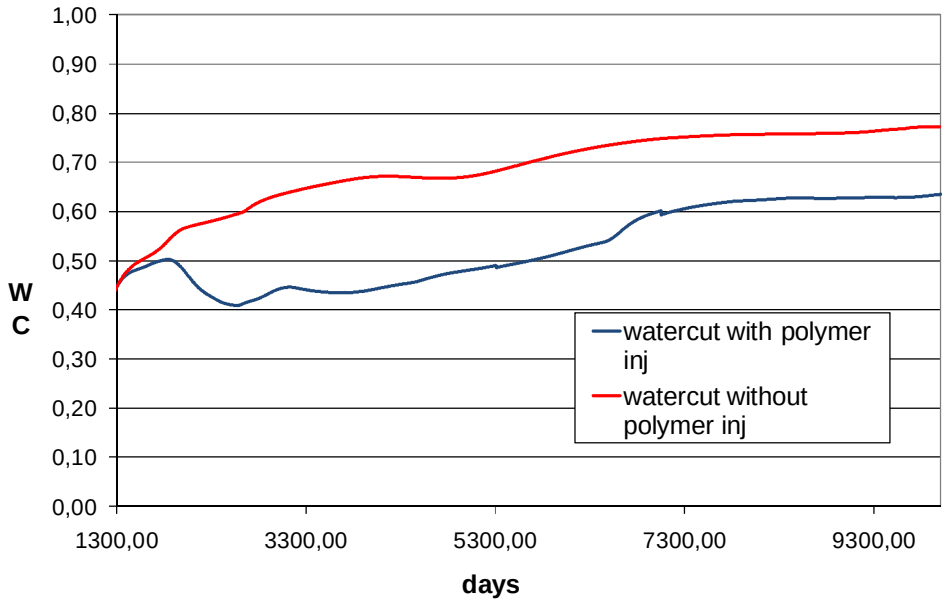

Figure 9-24 – comparison of watercuts until 10000 days

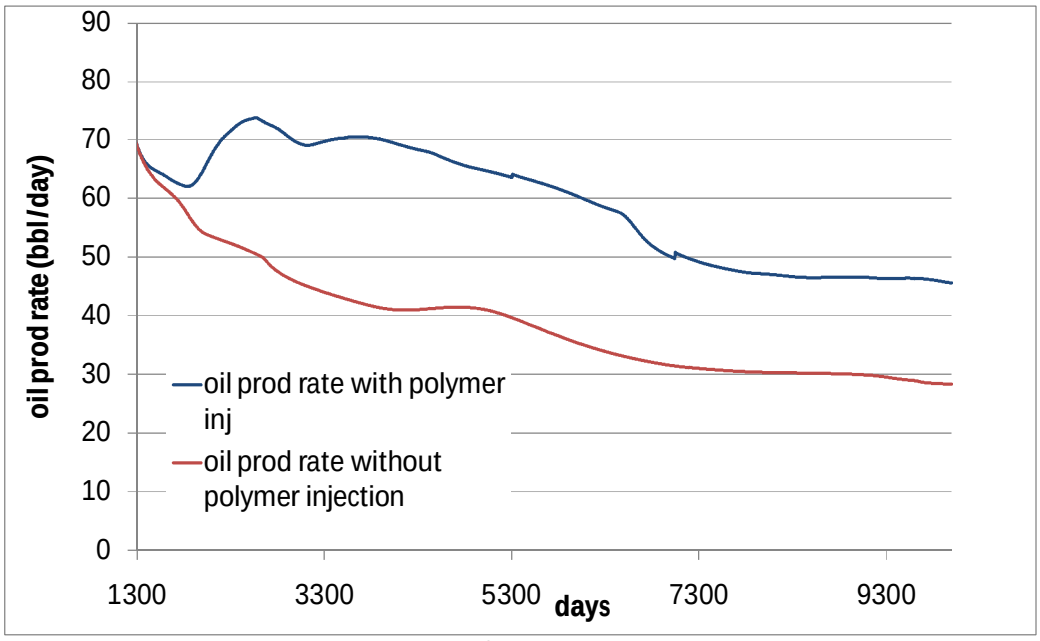

Figure 9-25 – comparison of production rates until 10000 days

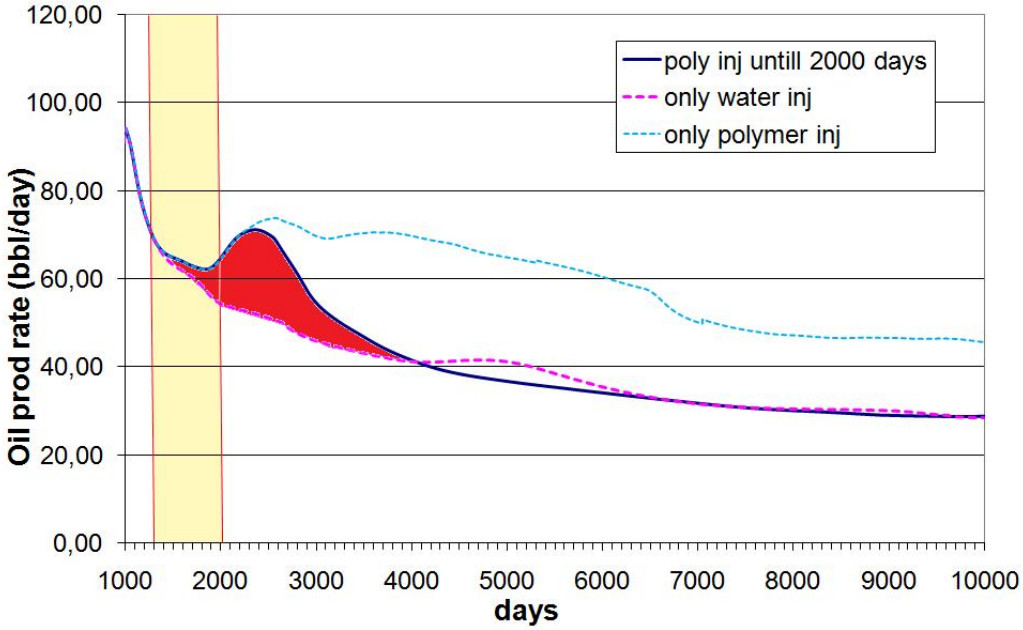

Figure 9-26 – watercut injecting polymer only until 2000 days of production

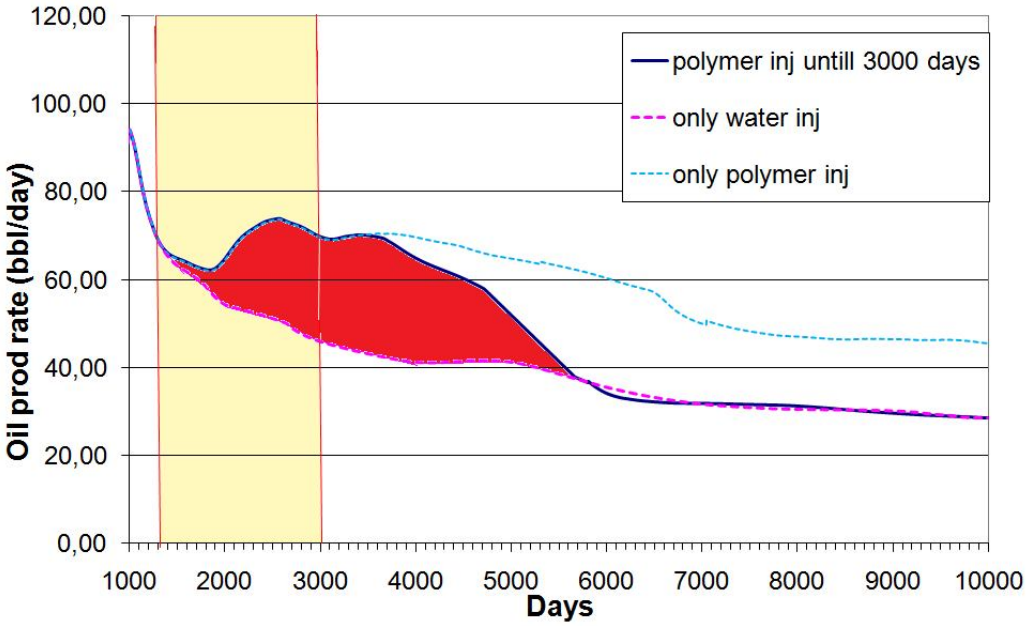

Figure 9-27 – injecting polymer until 3000 days

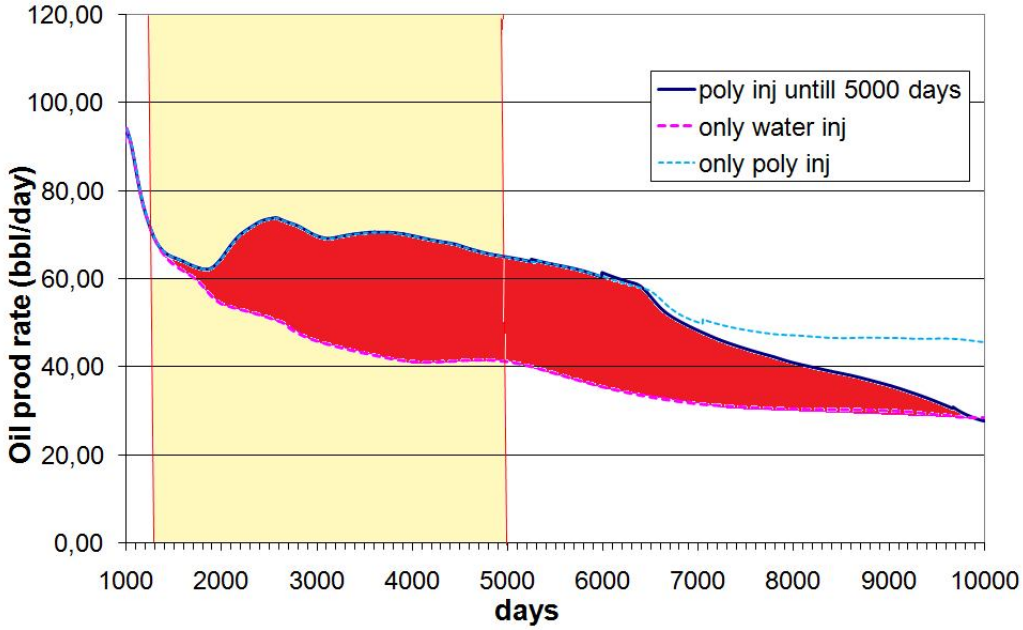

Figure 9-28 – injecting polymer until 5000 days

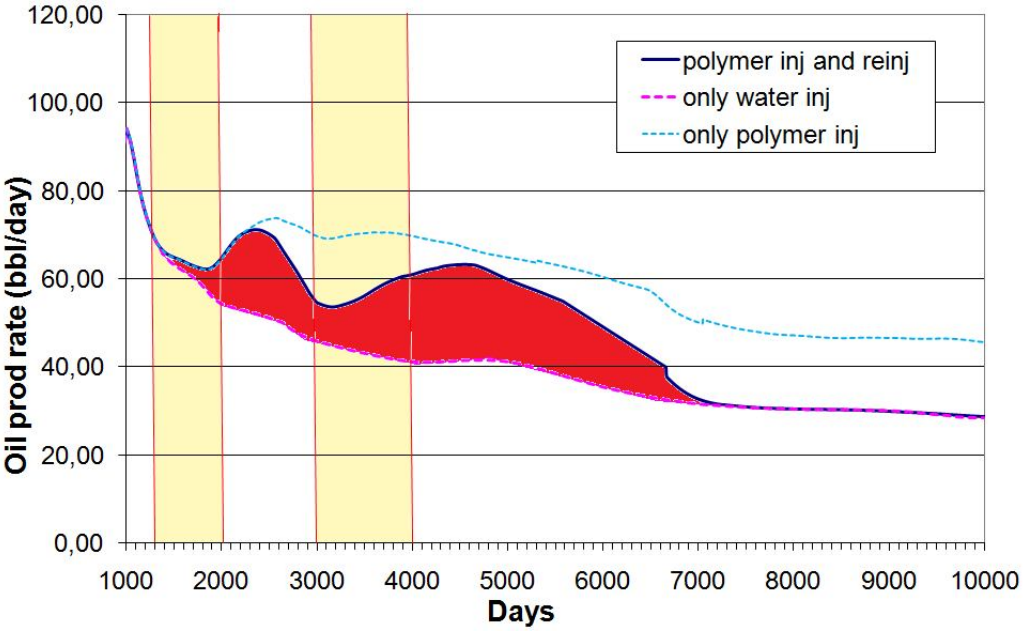

Figure 9-29 – injecting polymer until 2000 days and then from 3000 to 4000. The polymer injection times are highlited

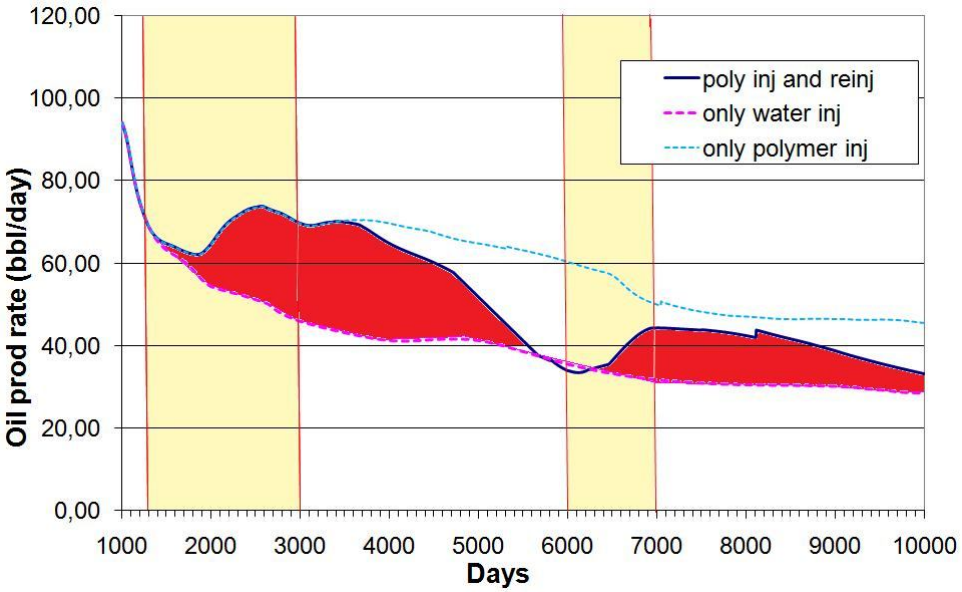

Figure 9-30 - injecting polymer until 3000 days and then from 6000 to 7000

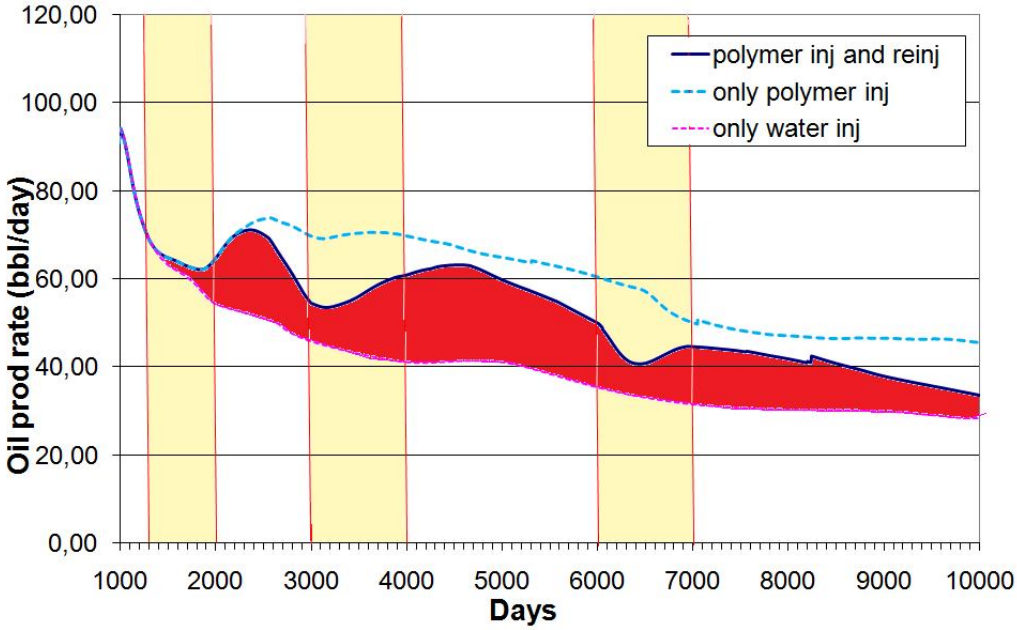

Figure 9-31 – injecting until 2000 days, then from 3000 to 4000 days, then from 6000 to 7000.

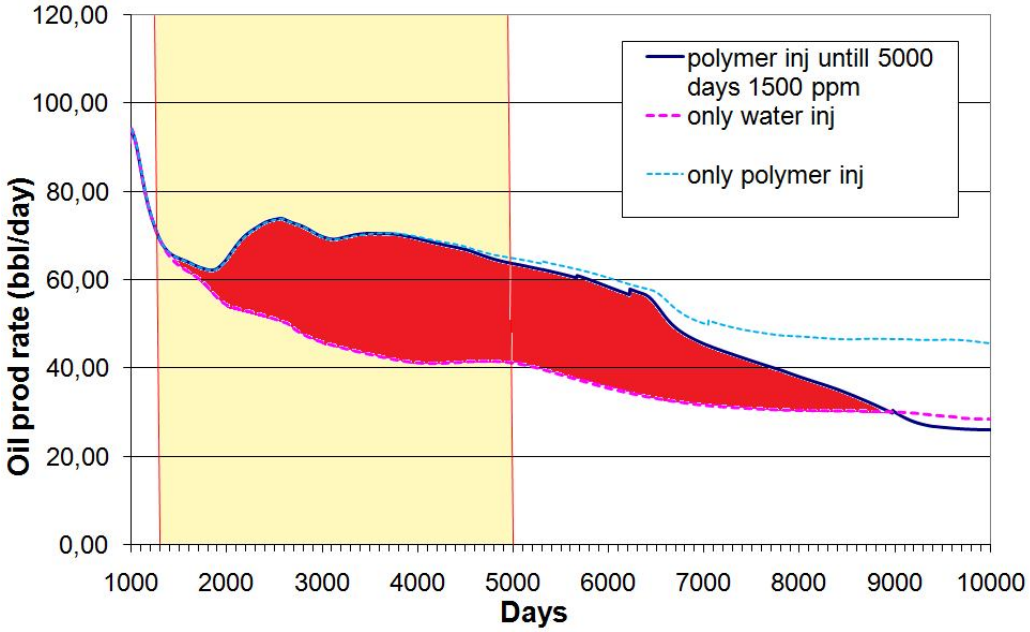

Figure 9-32 – injecting until 5000 days, with a 1500 ppm polymer solution

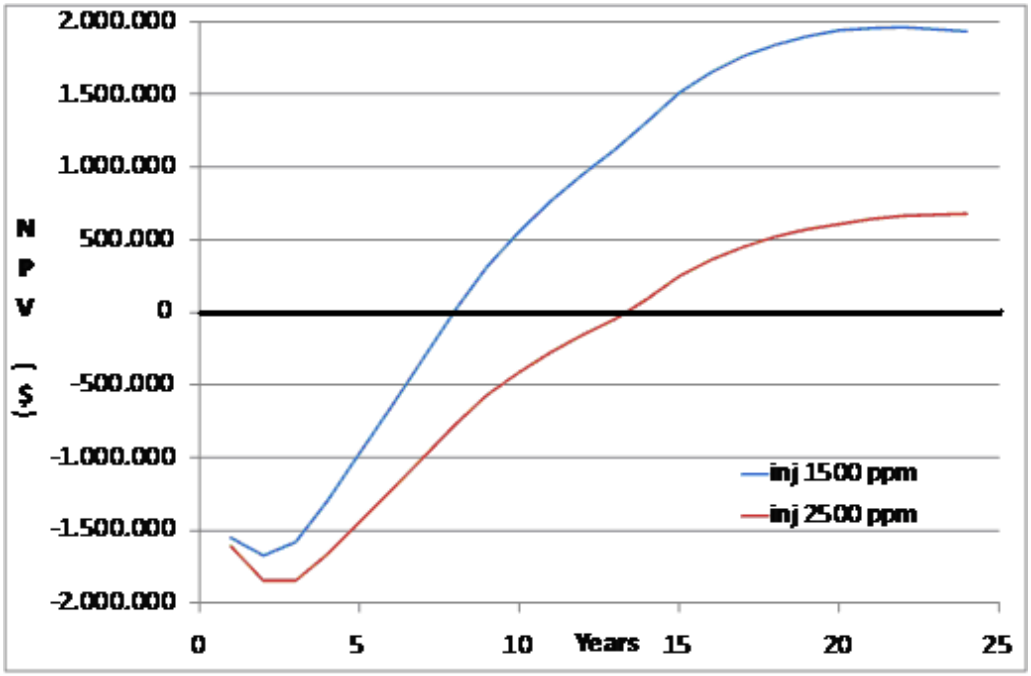

Figure 9-33 - Trend of net present value for two polymer concentration of solution injected

10. OTHER ASPECTS ABOUT POLYMER BEHAVIOR

10.1. Shear thickening behavior of the polymer

One important characteristic of a HPAM, or similar polymer, solution flowing in porous media is that, while it is shear thinning at low-to-intermediate flow velocity, beyond a certain flow velocity, or effective shear rate, it can show a shear thickening (also called dilatant, pseudodilatant and viscoelastic) behavior.

The resistance factor increases with increased flux for high velocities.

The main reason for the high apparent viscosity is that, as the polymer molecules flow through series of pore bodies and pore throats in reservoir rock, the flow field elongation and contraction occurs. If the flow velocity is too high, the polymer molecules do not have sufficient relaxation time to stretch and re-coil, adjusting to the flow. The resultant elastic strain can cause an apparent high viscosity. HPAM with a higher molecular weight (MW) tends to exhibit a more shear-thickening behavior than a lower-MW one.

In particular the resistance factor, residual resistance factor and polymer retention can increase dramatically as the permeability decreases below a critical value (Seright, Tianguang, Wavrik, Balaban, 2010, [36]).

A new model was studied, to try to represent the trend of viscosity including the shear thickening behavior:

$$\mu_{app} = \mu_W + \left(\mu_p^0 - \mu_w\right) \cdot \left[1 + \left(\lambda \cdot \gamma_{eff}\right)^2\right]^{(n-1)/2} + \mu_{\max} \cdot \left[1 - \exp\left(-\left(\lambda_2 \cdot \tau_r \cdot \gamma_{eff}\right)^{n2-1}\right)\right]$$

Equation 10-1 – apparent viscosity including shear thickening effects at high velocities

Where:

μ_W is the water viscosity

μ_p^0 is the viscosity of solution at zero shear rate

$\mu_{\max}$ is the shear thickening plateau viscosity

γ_{eff} is the effective shear rate

λ, λ_2, τ_r, n_1, n_2 are constants typical of the polymer used.

A representation of this model, compared to the shear-thinning-only one, is represented in Figure 10-1.

The shear thickening behavior at high fluxes can lead to added improvement in oil recovery, since it can help to displace the still mobile but hard-to-displace oil, which is near the residual oil condition, faster. It can also displace the

bypassed oil in small-scale heterogeneities more effectively (Delshad, Magbagbeola, 2010 [37]).

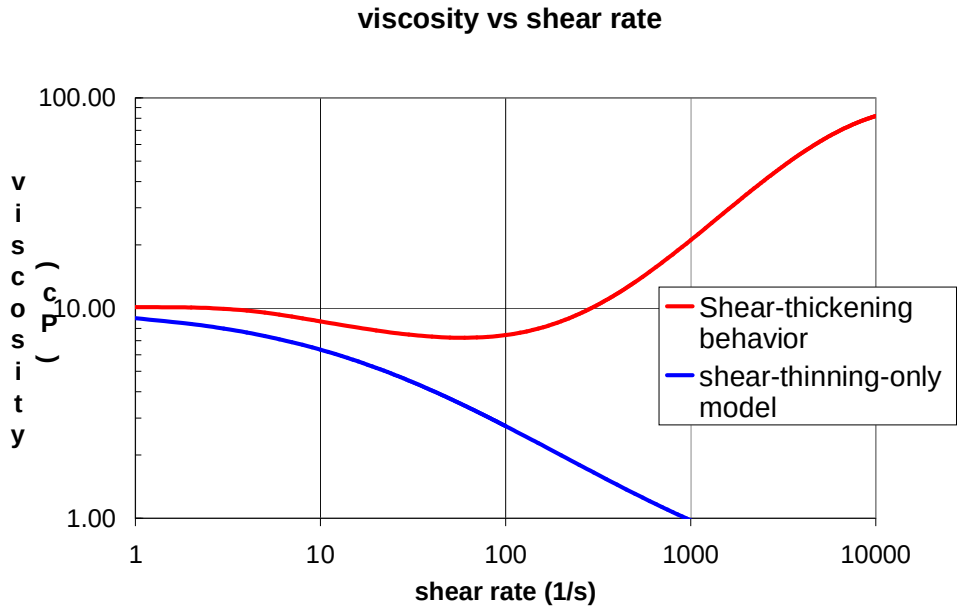

Figure 10-1 – comparison of the shear thickening model and shear thinning model for polymer viscosity

In the reservoir rock the velocities are almost always low, so the shear thickening behavior is seldom observed.

However, when the polymer solution first leaves the wellbore and enters the porous rock, the velocities are higher, and the shear thickening behavior can appear.

Most chemical flooding simulators does not include this effect in the simulations, and this can lead to:

- An overly optimistic prediction of polymer injectivity if wells are not fractured;
- An incorrect prediction that fractures in the formation will not be open during polymer injection.

To prevent this from happening, more studies about polymer rheology in porous media are needed.

10.2. Face plugging

Face plugging is a type of damage in which foreign particles injected during normal well operations block the near-wellbore formation, reducing well productivity.

Polymer plugging is partly a mechanical filtration process which is governed by the total throughput per cross-sectional area open to flow and by the sizes of the polymer molecules and the pore throats. At the same time, the composition of the reservoir rock and the polymer-rock interaction can influence polymer plugging significantly (Treiber and Young, SPE 14948, [38]).

Polymer plugging depends upon several factors, like volume injected per cross-sectional area, which determines an increase in polymer plugging at high values. Also low rock permeability contributes to increase plugging.

The greater is the hydrodynamic size of polymer molecule the higher is the pore plugging.

Both pore plugging and shear thickening behavior of polymer solution are difficult to determine through laboratory experiments and simulation matches. They have to be studied through field injectivity tests.

They consist first in injecting tracers, to determine the connectivity and diffusivity characteristics of the formation sector to study. Subsequently a pilot test is performed injecting polymer solution, to see the response of the reservoir and check the influence of the effect not considered in the previous studies.

11. CONCLUSIONS

With the increasing demand for energy for the development of world economies, the increasing of oil prices and the dropping of reserves, the interest for EOR techniques increased. Several studies have been conducted for method which could help maintaining the oil extraction rates at a high level, and EOR techniques are now a mature technology.

In this work the possibilities of the application of a chemical EOR upon a real oil reservoir in North Africa have been considered.

First a preliminary screening phase, considering the main characteristics of the reservoir, to detect the most promising EOR method has been performed, and it was found that the injection of a polymer solution of brine into the reservoir was the most promising technology.

The characteristics of several polymers and their behavior under different conditions have been studied. Considering the conditions of pH and temperature, and the high salinity of the reservoir water, the AN-125 polymer, produced by SNF-Floerger, was chosen. It is a co-polymer with acrylamide, acrylate and 2-acrylamid-2-methylpropane sulfonate moieties.

Then the exact properties of the reservoir rock needed to be found, so an approach based on laboratory studies on reservoir samples and matches through numerical simulations was carried on. The model implemented by the simulator was found to be accurate in reproducing the experimental data obtained for floodings.

The waterflooding upon reservoir cores and the matches to represent the behavior observed lead to the determination of the relative permeabilities and of the water-oil displacement behavior of the rock forming the reservoir.

Then the study focused upon a sector of the field. First simulations have been conducted to represent the behavior of the field during its life up to now, through history-match computations.

Then the polymer injection was simulated, to find out what changes this technique could have on the reservoir behavior.

The results confirmed what was expected according to the technical literature (Lake, 1989 [17]; Wyatt, Pitts, 2008 [13]), showing a decreasing in water production from the wells and an increasing in the oil production rate.

An economic study was then performed, to optimize the amount of polymer to be injected and the time steps in which implementing the polymer injection into the field. After having evaluated the capex and the opex of the project, the cash flow for each year was computed and then updated to the present, to find the most competitive solution.

Polymer flooding confirms to be a useful and promising method to improve oil recovery from this field and improve the net gain, in particular if the oil price keeps itself on the present value.

New developments of the research on this technique are expected in the future. In particular the polymer possible shear thickening behavior at very high shear rates and the face plugging effect need to be investigated through field injectivity tests.

12. APPENDIX A: VISUALIZATIONS FROM SECTOR SIMULATIONS

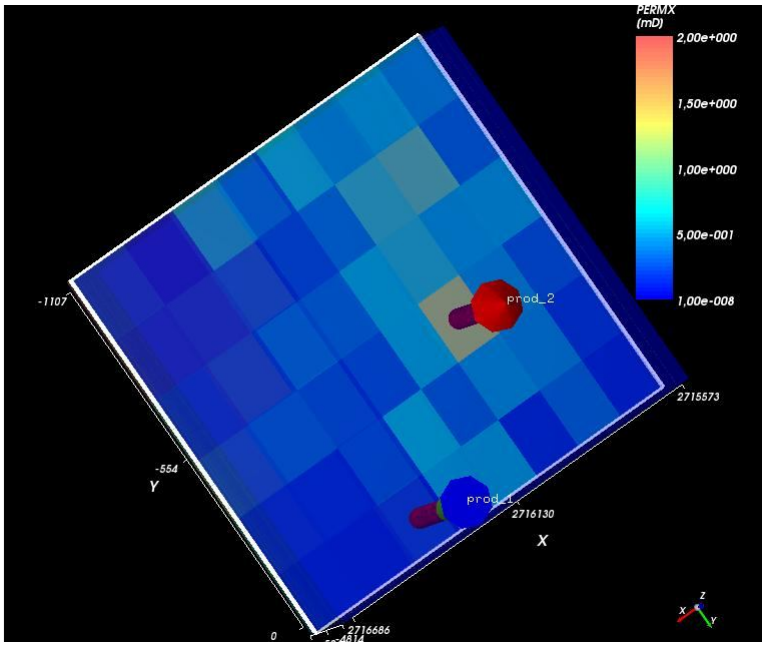

Figure 12-1 – permeability distribution in layer 64

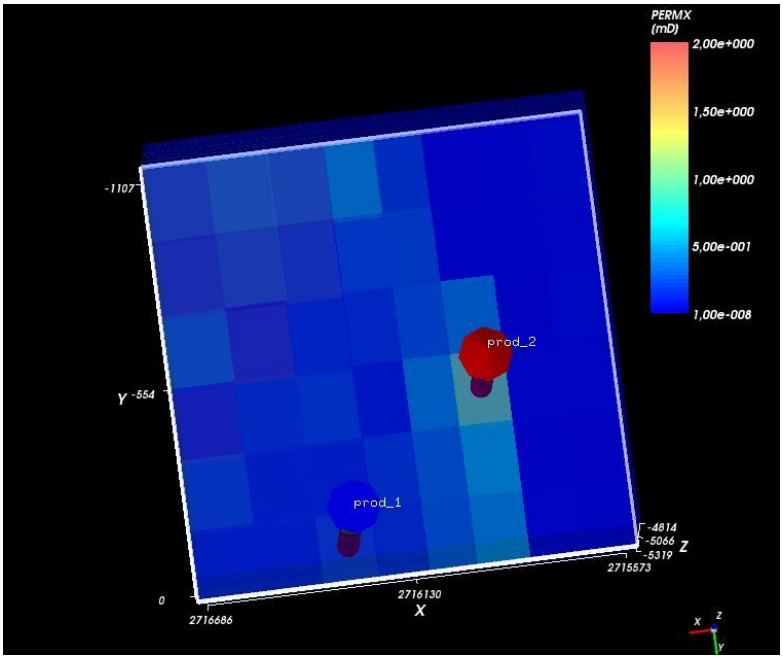

Figure 12-2 – permeability distribution in layer 65

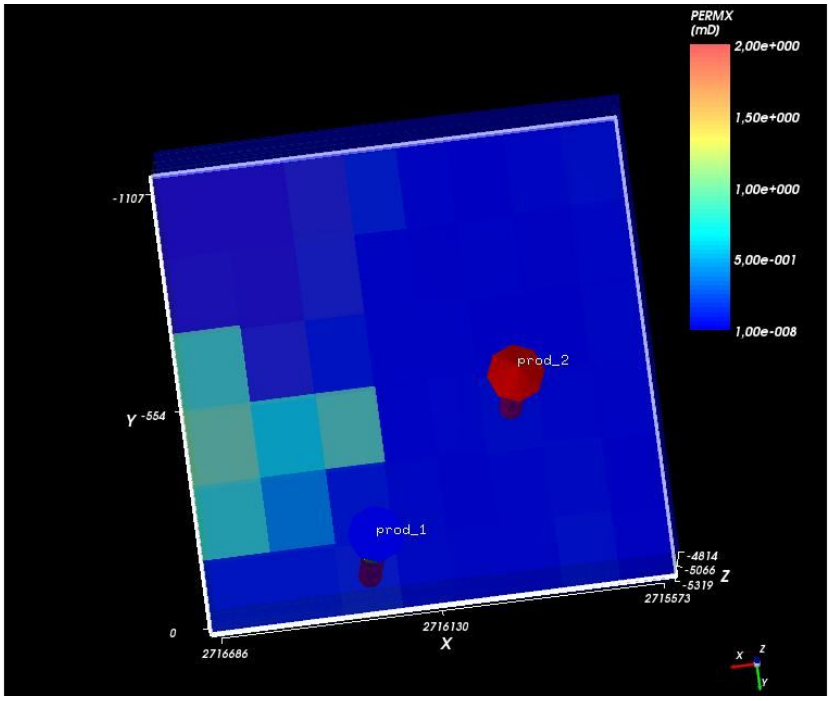

Figure 12-3 – permeability distribution in layer 66

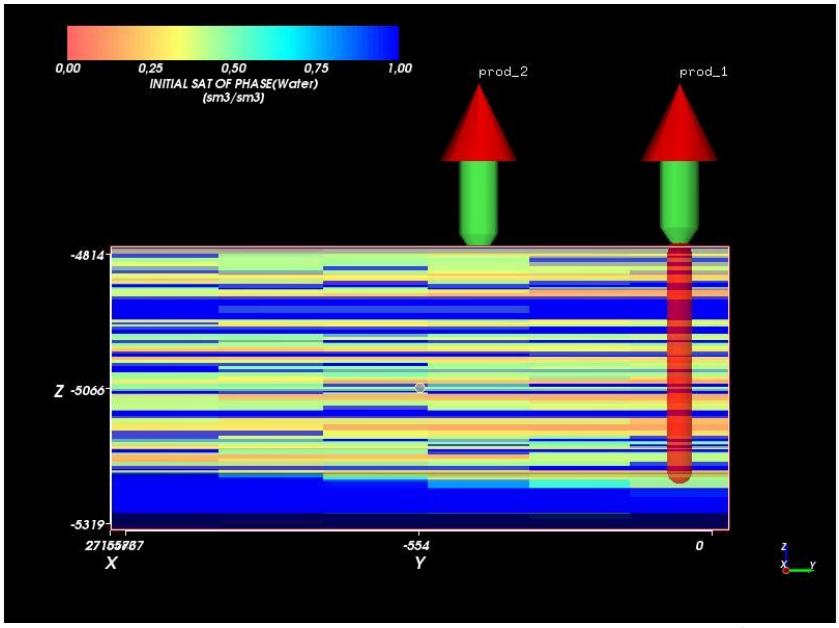

Figure 12-4 – water saturation in the sector. It is possible to observe the aquifer layer in the bottom of the reservoir

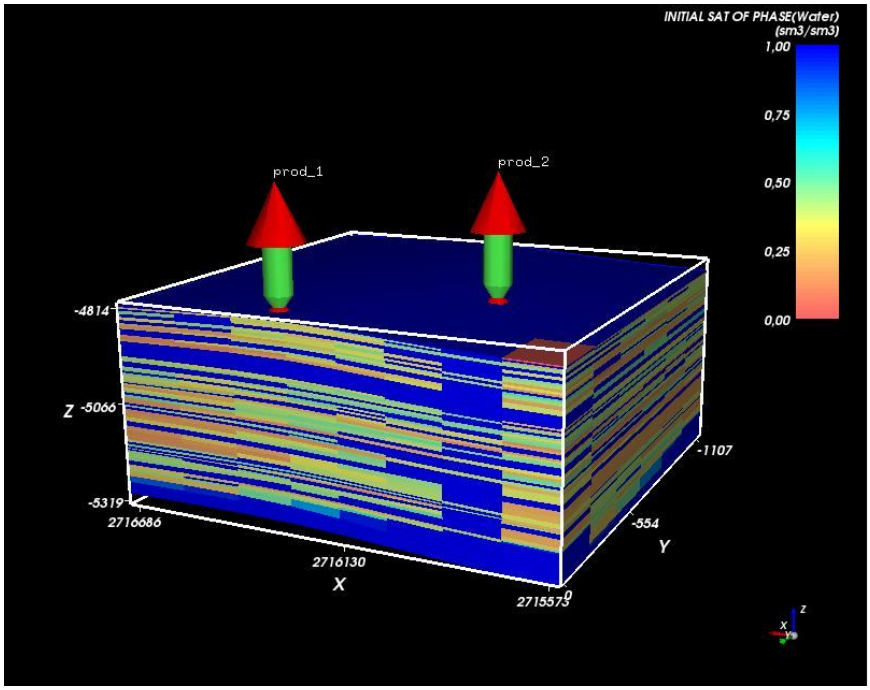

Figure 12-5 – water saturation inside the sector

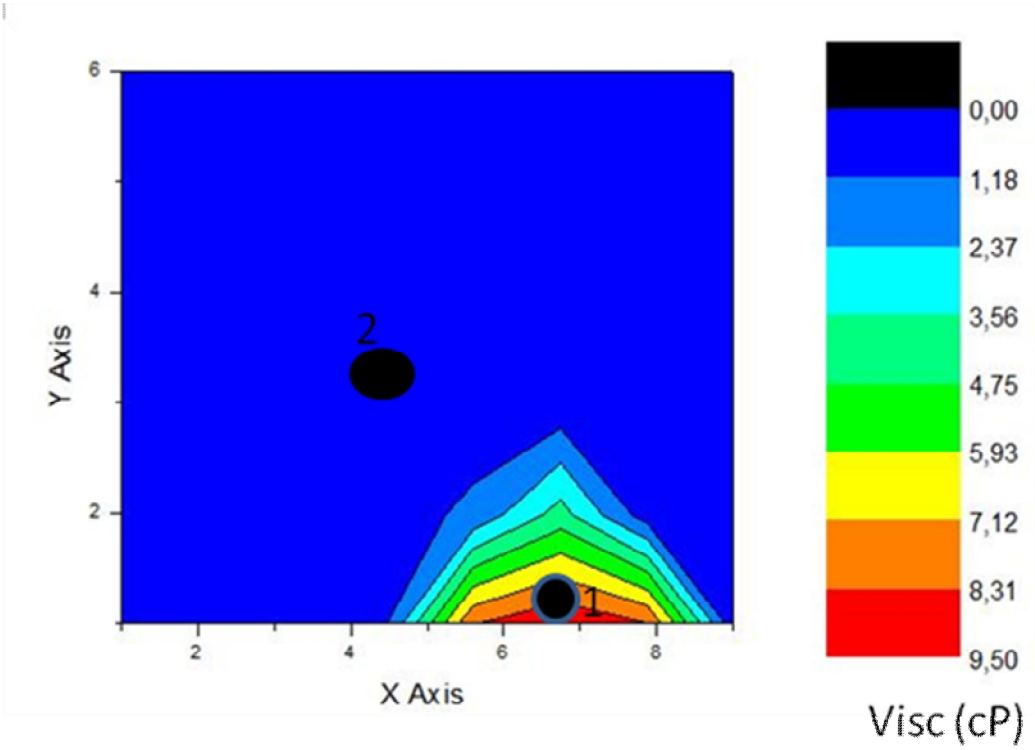

Figure 12-6 – Viscosity of water after 700 days of polymer injection

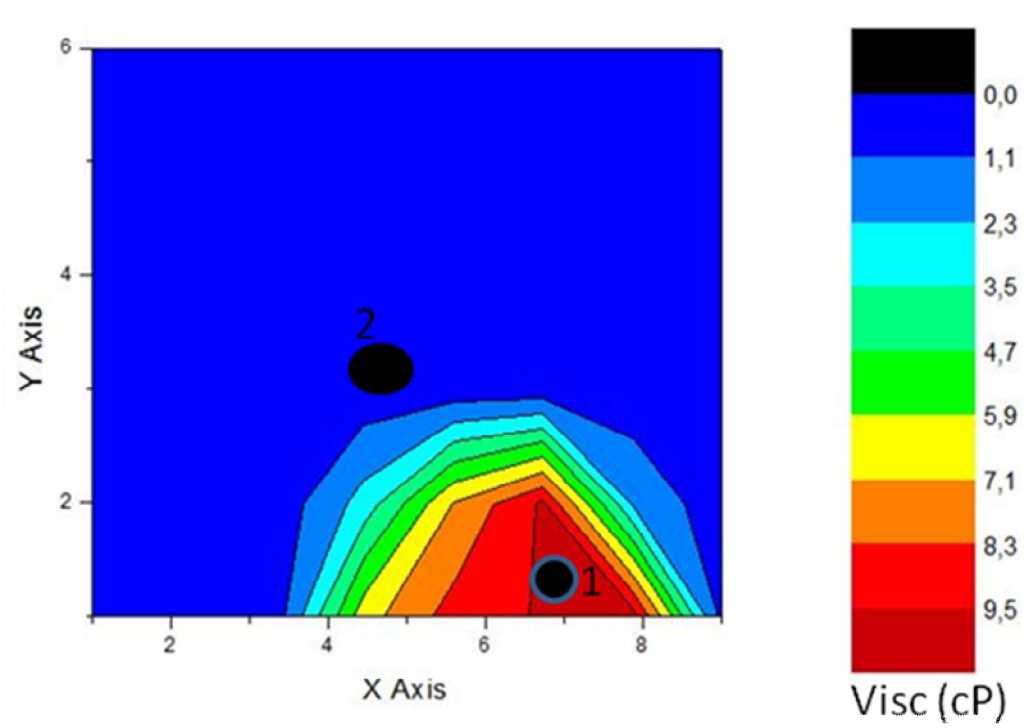

Figure 12-7 viscosity after 1200 days of polymer injection

13. APPENDIX B: UTCHEM INPUT FILE

```
CC*****************************************************************
CC                                                                 *
CC    BRIEF DESCRIPTION OF DATA SET : UTCHEM (VERSION 9.0)         *
CC                                                                 *
CC*****************************************************************
CC                                                                 *
CC                                                        *        *
CC                                                                 *
CC                                                                 *
CC  DIMENSIONS (FT): 3 ft           PROCESS : water   FLOODING     *
CC  THICKNESS (FT) : 0.433 ft       COORDINATES : CARTESIAN        *
CC  POROSITY :  0.26                VERTICAL WELL                  *
CC  GRID BLOCKS : 100 X 1 X 1                                      *
CC  DATE :  06/16/2000                                             *
CC                                                                 *
CC*****************************************************************
CC
CC*****************************************************************
CC
CC
CC
CC*****************************************************************
CC
CC
*----RUN NUMBER
waterflooding
CC
CC
*----TITLE
 EX13 : 1-d waterflooding without initial gas satutration USING
  using utchem 9.0
 corey's model
CC
CC SIMULATION FLAGS
*---- IMODE IMES IDISPC ICWM ICAP IREACT ibio ICOORD ITREAC ITC igas  ieng
       1    1    3      0    0     0      0    1     0     0    0     0
CC
CC No.OF GRIDBLOCKS, FLAG SPECIFIES CONS. OR VAR. GRID, unit(0:english)
*----NX    NY  NZ  IDXYZ iunit
     20   1   1   0      1
CC
CC  grid size in X, y , and z  direction, in m:
*----dx1        dy1   dz1
    0.002615  0.0329  0.0329
CC
CC TOTAL NO. OF COMPONENTS, NO. OF TRACERS, NO. OF GEL COMPONENTS
*----N   no  NTW NTA  ngc NG NOTH
     8    0   0   0    0   0  0
cc
cc
*--- spname
water
oil
surf.(no)
polymer
anion
cation
alcohol(no)
gas (no)
CC
CC FLAG INDICATING IF THE COMPONENT IS INCLUDED IN CALCULATIONS OR NOT
*----ICF(KC) FOR KC=1,N
     1  1  0  1 1 1 0 0
CC
CC*****************************************************************
CC                                                                 *
CC    OUTPUT OPTIONS                                               *
CC                                                                 *
```

```
CC*********************************************************************
CC
CC
CC FLAG FOR PV OR DAYS
*----ICUMTM ISTOP  IOUTGMS
       1        1    2
CC
CC FLAG INDICATING IF THE PROFILE OF KCTH COMPONENT SHOULD BE WRITTEN
*----IPRFLG(KC),KC=1,N
     1  1  0 1 0 0 0 0
CC
CC FLAG FOR PRES,SAT.,TOTAL CONC.,BIO CONC.,CAP.,GEL, ALKALINE PROFILES
*----IPPRES IPSAT IPCTOT IPBIO IPCAP IPGEL IPALK iptemp  ipobs
      1      1      0      0      0     0    0      0       0
CC
CC FLAG FOR WRITING SEVERAL PROPERTIES
*----ICKL IVIS IPER ICNM  icse IFOAM IHYST INONEQ
      0     1    1    0    0    0    0       0
CC
CC FLAG FOR WRITING SEVERAL PROPERTIES TO PROF
*----IADS  IVEL IRKF IPHSE
      1     0    1    0
CC
CC*********************************************************************
CC                                                                     *
CC    RESERVOIR PROPERTIES                                             *
CC                                                                     *
CC*********************************************************************
CC
CC
CC MAX. SIMULATION TIME ( DAYS)
*---- TMAX
       8.5
CC
CC ROCK COMPRESSIBILITY (1/PSI), STAND. PRESSURE(PSIA)
*----COMPR         PSTAND
      0.0           551.58
CC
CC FLAGS INDICATING CONSTANT OR VARIABLE POROSITY, X,Y,AND Z PERMEABILITY
*----IPOR1 IPERMX IPERMY IPERMZ  imod
       0      1     0      0      0
CC
CC CONSTANT POROSITY
*----PORC1
    0.263
CC
CC  constant x perm. in md
*----PERMX
     209.
CC
CC CONSTANT Y-PERMEABILITY (MILIDARCY)
*----PERMy
      209.
CC
CC kv = kx
*----PERMZ(1)
     209.
CC
CC FLAG FOR CONSTANT OR VARIABLE DEPTH, PRESSURE, WATER SATURATION
*----IDEPTH  IPRESS  ISWI  ICWI
      0        0       0    -1
CC
CC CONSTANT DEPTH (FT)
*----D111
      0.0
CC
CC INITIAL PRESSURE (kPa)
*----PINIT
      101.325
CC
CC INITIAL WATER SATURATION
*----SWI
    0.4
CC
```

```
CC CONSTANT CHLORIDE AND CALCIUM CONCENTRATIONS (MEQ/ML)
*----C50       C60
     1.8        0.1
CC
CC*************************************************************************
CC                                                                        *
CC    PHYSICAL PROPERTY DATA                                              *
CC                                                                        *
CC*************************************************************************
CC
CC
CC OIL CONC. AT PLAIT POINT FOR TYPE II(+)AND TYPE II(-), CMC
*---- C2PLC   C2PRC  EPSME      ihand
      0.       1.0     .0001      0
cc
cc flag indicating type of phase behavior parameters
*---- ifghbn
        0
CC  SLOPE AND INTERCEPT OF BINODAL CURVE AT ZERO, OPT., AND 2XOPT SALINITY
CC FOR ALCOHOL 1
*----HBNS70 HBNC70 HBNS71 HBNC71 HBNS72 HBNC72
     0.1    .1006   .191   0.0267    .363    0.1006
CC  SLOPE AND INTERCEPT OF BINODAL CURVE AT ZERO, OPT., AND 2XOPT SALINITY
CC FOR ALCOHOL 2
*----HBNS80 HBNC80 HBNS81 HBNC81 HBNS82 HBNC82
     0.     0.     0.     0.     0.     0.
CC
CC LOWER AND UPPER EFFECTIVE SALINITY FOR ALCOHOL 1 AND ALCOHOL 2
*----CSEL7  CSEU7  CSEL8  CSEU8
     0.0198 0.0231   0.     0.
CC
CC THE CSE SLOPE PARAMETER FOR CALCIUM AND ALCOHOL 1 AND ALCOHOL 2
*----BETA6  BETA7  BETA8
     1.0     -2.    0.
CC
CC FLAG FOR ALCOHOL PART. MODEL AND PARTITION COEFFICIENTS
*----IALC  OPSK7O  OPSK7S  OPSK8O  OPSK8S
     0     0.      0.      0.      0.
CC
CC NO. OF ITERATIONS, AND TOLERANCE (for two alcolhol system)
*----NALMAX   EPSALC
     20        0.0001
CC
CC ALCOHOL 1 PARTITIONING PARAMETERS IF IALC=1
*----AKWC7   AKWS7  AKM7  AK7     PT7
     4.671   1.79   48.   35.31   .222
CC
CC ALCOHOL 2 PARTITIONING PARAMETERS IF IALC=1
*----AKWC8   AKWS8  AKM8  AK8     PT8
     0.      0.     0.    0.      0.
cc
cc
*---- ift
      0
CC
CC INTERFACIAL TENSION PARAMETERS
*----G11  G12     G13   G21      G22      G23
     13.  -14.8   .007  13.0  -14.5  0.010
CC
CC LOG10 OF OIL/WATER INTERFACIAL TENSION
*----XIFTW
     1.3
CC
CC FLAG FOR OIL SOLUBILITY IN WATER
*---- IMASS  icor
       0      0
CC
CC CAPILLARY DESATURATION PARAMETERS FOR PHASE 1, 2, AND 3
*----itrap  T11    T22     T33
      1      1.   1.      0.
CC
CC FLAG FOR REL. PERM. CURVES
*----iperm
     0
```

```
CC
CC CONSTANT RES. SATURATION OF PHASES 1,2,AND 3 AT LOW CAPILLARY NO.
*----ISRW IPRW IEW
     0    0     0
CC
CC CONSTANT RES. SATURATION OF PHASES 1,2,AND 3 AT LOW CAPILLARY NO.
*----S1RWC  S2RWC  S3RWC
     .4    .140      .2
CC
CC ENDPOINT REL. PERM. OF PHASES 1,2,AND 3 AT LOW CAPILLARY NO.
*----P1RW  P2RW  P3RW
     0.21   0.9    1.000
CC
CC REL. PERM. EXPONENT OF PHASES 1,2,AND 3 AT LOW CAPILLARY NO.
*----E1W  E2W  E3W
     3.    4.    2.85
CC
CC  PARAMETERS FOR HIGH CAPILLARY NUMBER
*----S1RC S2RC S3RC
      0.39  0.135   0.
CC
CC
*----P1RC P2RC P3RC
      0.19   0.9   1.
CC
CC
*----E13C E23C E31C
     2.3   3.5    1.
CC
CC WATER AND OIL VISCOSITY , RESERVOIR TEMPERATURE
*----VIS1   VIS2     TEMPV
     0.395    64      77
CC
CC VISCOSITY PARAMETERS
*----ALPHA1 ALPHA2  ALPHA3  ALPHA4  ALPHA5
     0.     0.      .00      .0     0.
CC
CC PARAMETERS TO CALCULATE POLYMER VISCOSITY AT ZERO SHEAR RATE
*----AP1     AP2     AP3
     30.    150.   230.
CC
CC PARAMETER TO COMPUTE CSEP,MIN. CSEP, AND SLOPE OF LOG VIS. VS. LOG CSEP
*----BETAP CSE1  SSLOPE
     10.     .01   -0.17
CC
CC PARAMETER FOR SHEAR RATE DEPENDENCE OF POLYMER VISCOSITY
*----GAMMAC  GAMHF  POWN
     14.      20.    9.3
CC
CC FLAG FOR POLYMER PARTITIONING, PERM. REDUCTION PARAMETERS
*----IPOLYM EPHI3 EPHI4 BRK    CRK
     0      1.    1.    0.8  1.3
CC
CC SPECIFIC WEIGHT FOR COMPONENTS 1,2,3,7,AND 8 , AND GRAVITY FLAG
*----DEN1  DEN2     DEN23  DEN3      DEN7    DEN8      IDEN
    1.07   0.925   0.29194  .4980   .346  0.001623    2
cc
cc ft3 or res. bbls
*---- istb
       0
CC
CC COMPRESSIBILITY FOR VOL. OCCUPYING COMPONENTS 1,2,3,7,AND 8
*----COMPC(1)  COMPC(2)  COMPC(3)  COMPC(7)  COMPC(8)
     0.0       6.96e-6       0.        0.        0.0
CC
CC CONSTANT OR VARIABLE CAPILLARY PRESSURE CURVES, FLAG FOR OIL OR WATER WET
*---- ICPC   IEPC   IOW
      0       0      0
CC
CC CAPILLARY PRESSURE PARAMETERS,CPC
*----CPC
     0.
CC
CC CAPILLARY PRESSURE PARAMETERS,EPC
```

```
*---- EPC
      0.
CC
CC MOLECULAR DIFFUSIVITY OF KCTH COMPONENT IN PHASE 1 (D(KC),KC=1,N)
*D(1) D(2) D(3) D(4) D(5) D(6) D(7) D(8)
 0.   0.   0.   0.   0.   0.   0.   0.
CC
CC MOLECULAR DIFFUSIVITY OF KCTH COMPONENT IN PHASE 2 (D(KC),KC=1,N)
*D(1) D(2) D(3) D(4) D(5) D(6) D(7) D(8)
 0.   0.   0.   0.   0.   0.   0.   0.
Cc
CC MOLECULAR DIFFUSIVITY OF KCTH COMPONENT IN PHASE 3 (D(KC),KC=1,N)
*D(1) D(2) D(3) D(4) D(5) D(6) D(7) D(8)
 0.   0.   0.   0.   0.   0.   0.   0.
CC
CC LONGITUDINAL AND TRANSVERSE DISPERSIVITY OF PHASE 1 (feet)
*----ALPHAL(1)     ALPHAT(1)
      0.0          0.0
CC
CC LONGITUDINAL AND TRANSVERSE DISPERSIVITY OF PHASE 2
*----ALPHAL(2)     ALPHAT(2)
      0.0          0.0
CC
CC LONGITUDINAL AND TRANSVERSE DISPERSIVITY OF PHASE 3
*----ALPHAL(3)     ALPHAT(3)
     0.0           0.0
cc
cc flag to specify organic adsorption calculation
*----iadso
      0
CC
CC SURFACTANT AND POLYMER ADSORPTION PARAMETERS
*----AD31  AD32  B3D    AD41   AD42  B4D  iadk, iads1, fads refk
     1.0    0.5  1000.  5.      5.    100.  0    0       0  209
CC
CC PARAMETERS FOR CATION EXCHANGE OF CLAY AND SURFACTANT
*----QV     XKC   XKS  EQW
     0.0    0.0   0.0   1.
CC
CC*************************************************************************
CC                                                                        *
CC 3.5    WELL DATA: repeat ENTIRE section for rate changes etc.          *
CC                                                                        *
CC*************************************************************************
CC
CC
CC  FLAG FOR BOUNDARIES
*---- IBOUND  IZONE
        0     0
CC
CC TOTAL NO. OF WELLS, WELL RADIUS MODEL FLAG
*----NWELL  IRO  ITSTEP  nwrel
      2     2     0       2
CC injector, rate controlled:
CC WELL LOCATIONS, FLAG FOR SPECIFYING WELL TYPE, WELL RADIUS, SKIN
*----IDW  IW   JW   IFLAG    RW     SWELL  IDIR  KFIRST  KLAST IPRF
     1    1    1     1     0.3048     0.     3      1      1      0
CC
CC NAME OF THE WELL
*---- WELNAM
  inj.
CC
CC MAX. AND MIN. ALLOWABLE BOTTOMHOLE PRESSURE AND RATE
*----ICHECK  PWFMIN   PWFMAX  QTMIN   QTMAX
      0      0.0     40000.   0.0     500.
CC producer, pressure controlled:
CC WELL LOCATIONS, FLAG FOR SPECIFYING WELL TYPE, WELL RADIUS, SKIN
*----IDW  IW   JW   IFLAG    RW     SWELL  IDIR  KFIRST  KLAST  IPRF
     2    20    1     2   0.3048     0.   3      1     1       0
CC
CC NAME OF THE WELL
*---- WELNAM
    prod.
Cc
```

```
CC MAX. AND MIN. ALLOWABLE BOTTOMHOLE PRESSURE AND RATE
*----ICHECK PWFMIN   PWFMAX  QTMIN   QTMAX
      0     0.0     40000.   0.0     10000.
CC inj.
CC INJ. RATE AND INJ. COMP. FOR RATE CONS. WELLS FOR EACH PHASE (L=1,3)
*----QI(M,L)  C(M,KC,L),
  1   0.0000864     1.0  0.  0. 0. 2. 0.1 0. 0.
  1   0.           0.0  0.  0. 0. 0. 0. 0. 0.
  1   0.           0.0  0.  0. 0. 0. 0. 0. 0.
CC
CC
*----id   pwf(kPa)
     2    101.325
CC
CC CUM. IN.pro:maps. pro:well   .sum      .his1     .conc   restart
*----TINJ    CUMPR1   CUMHI1    WRHPV     WRPRF   RSTC
     5.65         0.1     0.1      0.1       0.1     50
CC
CC FOR IMES=3 ,THE INI. TIME STEP,CONC. TOLERANCE,MIN. AND MAX. TIME STEP
     DCLIM   cnMAX   cnMIN
     0.00005
cc
cc
*--- ibmod
     0
CC
CC IRO, ITIME, NEW FLAGS FOR ALL THE WELLS
*---- IRO ITSTEP IFLAG
       2   0     1 2
CC
CC NUMBER OF WELLS CHANGES IN LOCATION OR SKIN OR PWF
*----NWEL1
      0
CC
CC NUMBER OF WELLS WITH RATE CHANGES, ID
*----NWEL2   ID
     1        1
CC
CC ID,INJ. RATE AND INJ. COMP. FOR RATE CONS. WELLS FOR EACH PHASE (L=1,3)
*----QI(M,L)  C(M,KC,L),
  1   0.0000864     1.    0.  0. 0.25  2. 0.1 0. 0.
  1   0.           0.0  0.  0. 0. 0. 0. 0. 0.
  1   0.           0.0  0.  0. 0. 0. 0. 0. 0.
CC
CC CUM. INJ. TIME , AND INTERVALS (PV) FOR WRITING TO OUTPUT FILES
*----TINJ    CUMPR1  CUMHI1   WRHPV     WRPRF   RSTC
     6.72     0.1     0.1      0.1     0.1    50
CC
CC FOR IMES=2 ,THE INI. TIME STEP,CONC. TOLERANCE,MAX.,MIN. TIME STEPS
*----DT     DCLIM   cnMAX   cnMIN
     0.00005
cc
cc
*--- ibmod
     0
CC
CC IRO, ITIME, NEW FLAGS FOR ALL THE WELLS
*---- IRO ITSTEP IFLAG
       2   0     1 2
CC
CC NUMBER OF WELLS CHANGES IN LOCATION OR SKIN OR PWF
*----NWEL1
      0
CC
CC NUMBER OF WELLS WITH RATE CHANGES, ID
*----NWEL2   ID
     1        1
CC
CC ID,INJ. RATE AND INJ. COMP. FOR RATE CONS. WELLS FOR EACH PHASE (L=1,3)
*----QI(M,L)  C(M,KC,L),
  1   0.0000864    1.   0.  0. 0. 2.  0.1  0. 0.
  1   0.           0.0  0.  0. 0. 0. 0. 0. 0.
  1   0.           0.0  0.  0. 0. 0. 0. 0. 0.
CC
```

```
CC CUM. INJ. TIME , AND INTERVALS (PV) FOR WRITING TO OUTPUT FILES
*----TINJ    CUMPR1  CUMHI1   WRHPV     WRPRF   RSTC
      8.5          0.1     0.1      0.1     0.1    50
CC
CC FOR IMES=2 ,THE INI. TIME STEP,CONC. TOLERANCE,MAX.,MIN. TIME STEPS
*----DT      DCLIM   cnMAX   cnMIN
     0.00005
```

14. APPENDIX C: ECONOMIC COMPUTATIONS

INIEZIONE DA 1300 A 5000 GIORNI 1500 PPM

YEAR	YEARLY PROD WI [STB]	YEARLY PROD POLY [STB]	INCREMENTAL PROD DUE TO POLY [STB]	OIL PRICE [US$/STB]	INCOME [US$]
1	26,150	26,555	405	70	28336.78255
2	22,278	23,160	881	70	61702.26327
3	19,941	23,852	3,910	70	273729.4429
4	18,965	26,403	7,438	70	520637.0531
5	17,708	26,403	8,695	70	608645.5069
6	16,506	25,369	8,863	70	620392.1105
7	15,792	25,652	9,860	70	690198.1702
8	15,191	25,515	10,324	70	722689.9636
9	15,002	24,888	9,886	70	692022.7811
10	15,109	24,174	9,065	70	634576.9658
11	15,066	23,642	8,575	70	600266.0335
12	14,496	22,711	8,216	70	575094.8945
13	13,688	22,097	8,409	70	588619.6364
14	12,905	21,179	8,275	70	579228.3927
15	12,254	20,344	8,090	70	566271.8487
16	11,773	17,650	5,877	70	411406.0189
17	11,452	16,409	4,957	70	346981.3527
18	11,256	15,183	3,927	70	274909.3615
19	11,139	14,235	3,096	70	216752.3433
20	11,079	13,267	2,188	70	153133.9549
21	11,038	12,197	1,159	70	81127.488
22	10,969	11,116	148	70	10333.85018

YEAR	CAPEX	YEARLY POLYMER WEIGHT [LB]	OPEX [US$]	CASH FLOW [US$]	NPV [US $]
					10%
1	**1,500,000**	67,297	84,122	-1,555,785	-1,555,785
2	0	153,522	191,903	-130,200	-118,364
3	0	132,492	165,615	108,115	89,351
4	0	134,332	167,915	352,722	265,005
5	0	134,332	167,915	440,731	301,025
6	0	134,332	167,915	452,477	280,953
7	0	134,332	167,915	522,283	294,815
8	0	134,332	167,915	554,775	284,687
9	0	134,332	167,915	524,108	244,500
10	0	134,332	167,915	466,662	197,910
11	0	134,332	167,915	432,351	166,690
12	0	134,332	167,915	407,180	142,714
13	0	134,332	167,915	420,705	134,050
14	0	93,848	117,310	461,918	133,801
15	0	0	0	566,272	149,117
16	0	0	0	411,406	98,487
17	0	0	0	346,981	75,513
18	0	0	0	274,909	54,389
19	0	0	0	216,752	38,985
20	0	0	0	153,134	25,039
21	0	0	0	81,127	12,059
22	0	0	0	10,334	1,396
				TOT NPV [US $]	1,301,528

15. NOMENCLATURE

a_k	Polymer adsorption parameter
a_{K1}	Polymer adsorption parameter, (L2)0.5
a_{K2}	Polymer adsorption parameter, (L2)0.5(eq/L3)-1
b_k	Polymer adsorption parameter, L3/wt% of polymer
A	Area perpendicular to flow direction
AA	Acrylate moieties on polymer chain
AM	Acrylamide moieties on polymer chain
AMPS	2-acrylamid-2-methylpropane sulfonate monomer
B_O	Oil Formation Volume Factor
Bg	Gas Formation Volume factor
$C \equiv Ct$	Total compressibility
C_{11}	Water concentration in aqueous phase
C_{51}	Anion concentration in aqueous phase
C_{61}	Calcium concentration in aqueous phase
$Cf \equiv C_R$	Compressibility of the rock formation
C_{pol}	Polymer concentration in aqueous phase
$C_{pol-ads}$	Adsorbed concentration of polymer
CPC	Parameter for Corey's capillary pressure model
C_{SE}	Effective salinity for phase behavior and adsorption, eq/L^3
C_W	Water compressibility
$\hat{C}_k$	Adsorbed concentration of species k
$\tilde{C}_k$	Overall concentration of species k in the mobile and stationary phases, L3/L3 PV
C_{kl}	Concentration of species k in phase l
$D \equiv h$	Depth
$\tilde{D}_{kl}$	Diffusion coefficient of species k in phase l
$e_O \equiv n_O$	Corey exponent for oil relative permeability in Corey's model
$e_W \equiv n_W$	Corey exponent for water relative permeability in Corey's model

E_A	Areal sweep efficiency
E_V	Vertical sweep efficiency
E_D	Microscopic displacement efficiency
EOR	Enhanced Oil Recovery
EPC	Exponent for Corey's capillary pressure model
HCPV	Hydrocarbon Pore Volume
HPAM	Hydrolyzed PolyAcrylAmide
k	Permeability
k_{rl}^0	Endpoint relative permeabilità of phase l
kr_{FL}	Relative permeability of fluid FL
kr_j	Relative permeability of component j
k_x	Absolute permeabilità along x direction
k_y	Absolute permeabilità along y direction
$kv \equiv k_z$	Absolute permeability along vertical direction
M	Mobility ratio
M'	End-point mobility ratio
MOV	Moveable oil volume
NPV	Net Present value
NV	Net value
N	Volume of oil in place in standard conditions
N_c	Capillary number
N_P	Cumulative oil production volume in standard conditions
$OOIP$	Oil originally in place
$PV \equiv V_P$	Total pore volume
p	Pressure
ps	Average reservoir pressure
Pb	Bubble point pressure
P_C	Capillary pressure
P_L	Pressure at the left side of the core
p_O	Oil phase pressure
p_W	Water phase pressure
Q_k	Source/sink termo for species k, L3/t
q	Flow rate

qo_{ST}	Production rate
r	Discount Rate
r_1	Principal radius of curvature where the pressure at oil-water interface is p_O
r_2	Principal radius of curvature where the pressure at oi-water interface is p_W
r_{Kl}	Reaction rate for species k in phase l, $mL^{-3}t^{-1}$
r_W	Wellbore radius
RF	Recovery Factor
R_L	Factor for vertical communication
R_F	Resistance Factor
R_k	Permeability reduction factor
R_{RF}	Residual resistance factor
Rs	Solution gas-oil ratio
S_{nj}	Normalized saturation of phase j, in the Coreys model for relative permeabilities
S_O	Saturation of oil phase
SOi	Initial oil phase saturation
S_{OR}	Residual oil saturation
S_W	Saturation of aqueous phase
S_{Wi}	Initial satuation of aqueous phase
S_{WC}	Critical aqueous phase saturation
$STOIIP$	Volume of oil originally in place in standard conditions
t	Time
TXli+1/2	Transmissibility of phase l in block i
THF	Tetrahydrofurane
u	Flow velocity
V_t	Total volume of reservoir
WC	Water cut
W_e	Aquifer influence volume in standard conditions
W_i	Water injected volume in standard conditions
W_P	Water produced in standard conditions
x	Coordinate along flow direction

15.1. Greek symbols

β_P	Input parameter in the UtChem model for the computetion of effective salinity
γ_O	Oil specific weight
γ_w	Water specific weight
$\dot{\gamma}$	Shear rate
Φ	Porosity
λ_W	Water mobility
λ_O	Oil mobility
λ_{aq}^I	End-point mobility of aqueous phase
μ	Viscosity
μ_{aq}	Viscosity of aqueous phase
μ_w	Viscosity of water as component
$\mu_P^0 \equiv \mu_{aq}^I$	Viscosity of polymer solution for a certain polymer concentration at zero shear rate
μ_{aq}^∞	Viscosity of a polymer solution at very high shear rates
$[\mu]$	Intrinsic viscosity
υ	Kinematic viscosity
ρ_O	Oil viscosity in reservoir conditions
ρ_{OS}	Oil viscosity in standard conditions
ρ_{gS}	Gas viscosity in standard conditions
σ	Interfacial tension between phases
Ω_P	Hydrodynamic radium of a molecule

15.2. Subscripts

1	Relative to initial conditions
2	Relative to final conditions
FL	Fluid considered
i	Block of the grid considered
k	Species considered
l	phase considered
N	Total number of blocks
O	Relative to oil
R	Residual

t	time considered
W	relative to water

15.3. Superscripts

nCV	Total numer of components
np	Total number of phases
→	Vector
•	Indicates a rate

16. Bibliography

[1] *World Energy Outlook 2009. Executive Summary*. **IEA, International Energy Agency**

[2] *Quantification of the Viscoelastic Behaviour of High Molecular Weight Polymers used for Chemical Enhanced Oil Recovery.* **Olowaseun Adedeji Magbagbeola** –. Thesis, University of Texas, Austin, 2008

[3] *Ingegneria dei Giacimenti e Trasporto degli Idrocarburi,* pp. 2-21, **Romagnoli, Raffaele**. Torino : adk/Elarts, 2009.

[4] *Fundamentals of Reservoir Engineering.* **Dake, L.P.**, pp. 343-348 s.l. : Elsevier, 2008.

[5] *Fundamentals of Reservoir Engineering.* **Dake, L.P.**, pp. 45-52 s.l. : Elsevier, 2008.

[6] *Ingegneria dei Giacimenti e Trasporto degli Idrocarburi,* pp. 125-132, **Romagnoli, Raffaele**. Torino : adk/Elarts, 2009.

[7] *Reservoir Recovery tecniques.* **Kleppe, Jon.**. Norwegian University of Science and Tecnology. [Online] 2009. http://www.ipt.ntnu.no/~kleppe/TPG4150/index.html.

[8] *Fundamentals of Reservoir Engineering.* **Dake, L.P.**, pp. 73-80 s.l. : Elsevier, 2008.

[9] *Fundamentals of Reservoir Engineering.* **Dake, L.P.**, pp. 103-110 s.l. : Elsevier, 2008.

[10] *Ingegneria dei Giacimenti e Trasporto degli Idrocarburi,* pp. 176-181, **Romagnoli, Raffaele**. Torino : adk/Elarts, 2009.

[11] *Introduction to Enhanced Oil recovery Methods.* **Barrufet, Maria Antonieta**. PETE 609 - Module 2 2001.

[12] *Enhanced Oil recovery.* **Lake, Larry W.** pp. 1 -6 New Jersey : Prentice-Hall, 1989.

[13] Economics of Field Proven Chemical Flooding **Wyatt, Pitts, Surkalo, Surtek**. 2008.

[14] *Improved Waterflooding Processes.* **Barrufet, Maria Antonieta**. PETE 609 - Module 6 2001.

[15] *Devopment of Improved Hydorcarbon Recovery Screening Methodologies.* **Dickson, Dios, Wylie, SPE 129768.**

[16] *EOR: The New Frontier in the Malay Basin Development.* **Selamat, Teletzke, Patel, Darman, Suaimi -** IPTC 12085, International Petroleu Technology Conference, Kuala Lampur, 2008

[17] *Enhanced Oil recovery.* **Lake, Larry W.** pp. 314 - 331 New Jersey : Prentice-Hall, 1989.

[18] *Selection and Screening of Polymers for Enhanced Oil Recovery.* **Levitt, Pope**, university of Austin Texas. (SPE 223845, 2008).

[19] *Water permeability reduction under flow-induced polymer adsorption.* **Ogunberu, Asghari**, JCPT 05/11/06

[20] *Limiting conditions for the use of Hydrolyzed Polyacrylamides in brines containing divalent ions.* **Zaitoun and Ptie**, 1983 –SPE 11785

[21] *Modified synthetic polymers for high salinity and high temperature,* from **CIPR, Centre for Integrated Petroleum Research**

[22] *Simulation of Chemical Flood Enhanced Oil Recovery Processes.* **Anderson, Glen Allen.** University of Texas at Austin : s.n., 2006.

[23] *Heavy oil best practice for sampling, oil characterization and IOR-EOR studies.* **Parasiliti, Arlotto.**

[24] *Reservoir simulation.* **Kleppe, Jon.** Norwegian University of Science and Tecnology. [Online] 2010.

[25] *Recent Advantages in Improved Oil Recovery Methods for North Sea Sandstone Reservoirs.* **Svein M. Skjaeveland and Jon Kleppe**, SPOR Monograph (pp. 172-173)

[26] *A Fully Implicit, Parallel, Compositional, Chemical Flooding Simulator.* **C. Han, M. Delshad, K. Sepehrnoori, G.A. Pope, SPE, University of Texas at Austin**

[27] *UTCHEM 10, Technical Documentation.* Reservoir Engineering Research Program Center for Petroleum and Geosystems Engineering. **The University of Texas at Austin**

[28] *Analysis of factors influencing mobility and adsorption in the flow of polymer solution through porous media.* **Hirasaki and Pope**, SPEJ 14(4): 337-346, 1974

[29] *Effects of polymer adsorption on mobility ratio.* **Omar, King Saud**, SPE 11503

[30] *Shear degradation of partially hydrolyzed polyacrylamide solutions.* **Maeker**, SPE 5101

[31] "*Encyclopaedia of hydrocarbons*", pp. 553-574, "Static Reservoir study". **Luca Cosentino**

[32] *Shlumberger oilfield glossary, http://www.glossary.oilfield.slb.com*

[33] "*Encyclopaedia of hydrocarbons*", pp. 509-526, "Drive Mechanisms and Displacement Processes". **Francesca Verga**

[34] "*Encyclopaedia of hydrocarbons*", pp. 527-552, "Well Testing". **Francesca Verga**

[35] *Polymer flood application to improve heavy oil recovery at east Bodo.* **Wassmuth, Arnold, Green, Cameron** – (JCPT, feb 2009)

[36] *New insights into polymer rheology in porous media.* **Seright, Tianguang Fan, Wavrik, New Mexico Petroleum research center, Rosangela de Carvalho Balaban, Universitade federal do Rio Grande do Norte**, SPE 12900, 2010

[37] *Mechanistic interpretation and utilization of viscoelastic behaviour of polymer solutions for improved polymer flood efficiency.* **Delshad, Hoon Kim, Magbagbeola, Huh, Pope, Tarahhom**, SPE 113620, 2008

[38] *The Nature of Polymer Plugging and a Wellbore Treatment To Minimize It.* **L.E. Treiber, Amoco Production Co, S.H. Yang, Exxon Production Research Co.** SPE 14948